

COMPREHENSIVE METABOLOMICS OF PEANUT ALLERGY

**COMPREHENSIVE METABOLOMICS ANALYSIS OF PEANUT ALLERGY
AND PEANUT-INDUCED ANAPHYLAXIS**

By

KENNETH ROSS CHALCRAFT, M.Sc. B.Sc.

**A Thesis Submitted to the School of Graduate Studies
In Partial Fulfillment of the Requirements for the Degree
Of Doctor of Philosophy**

McMaster University

©Copyright by Kenneth Chalcraft, January 2013

Doctor of Philosophy (2013)
(Chemistry)

McMaster University
Hamilton, Ontario

TITLE: **Comprehensive metabolomics analysis of peanut allergy and peanut induced anaphylaxis**

AUTHOR: **Kenneth Ross Chalcraft, M.Sc. (McMaster University), B.Sc. (Brandon University)**

SUPERVISOR: **Professor Brian E. McCarry**

NUMBER OF PAGES: **xix, 205**

Abstract

The work in this thesis encompasses (a) the development of a robust analytical method suitable for the comprehensive analysis of polar and non-polar metabolites in a single analysis and (b) the application of this method to the study of the metabolites involved in peanut allergy. During the course of this work the methods for the analysis of large metabolite data sets evolved significantly and the approaches used in this work evolved in parallel to the literature. This work constitutes the first comprehensive metabolomic investigation of an allergy response.

Hypersensitivity or allergy to peanuts is an increasingly problematic health concern around the world involving approximately 1-2% of children in North America. There are no useful clinical biomarkers for this allergy. Comprehensive metabolomics holds vast potential for the discovery of metabolites and metabolite pathways that may be involved during the development of peanut allergy and during peanut-induced anaphylaxis. The comprehensive study of metabolites involved in peanut allergy presented a significant challenge since no single analytical technique is capable of analysis of all metabolites within a single analytical run.

The thesis begins with development of a tandem column liquid chromatography-electrospray ionization-mass spectrometry method which allowed the separation and analysis of both polar and non-polar metabolites in a single analysis. This tandem column technique was also shown to significantly reduce the amount of ion suppression

observed compared to the ion suppression observed when using either column independently.

This methodology was applied to the comprehensive metabolomics analysis of blood serum samples obtained from mice which were (a) being sensitized to peanuts and (b) undergoing anaphylaxis. This analysis discovered a profound impact on metabolites involved with purine metabolism, resulting in an elevation of uric acid levels. This discovery led to further investigations which confirmed that uric acid is essential for peanut sensitization in mice. This discovery was only possible due to the use of a comprehensive metabolomics approach.

The analytical methodology was then applied to the study of metabolomic changes in sensitized mice as they experienced peanut-induced anaphylaxis. A number of metabolomic changes including taurine level elevation were correlated with peanut-induced anaphylaxis. Finally, a serendipitous opportunity arose to analyze blood serum samples from peanut allergic children that had undergone an oral peanut challenge. The comprehensive metabolomic study of these samples revealed massive changes in their serum metabolomes as a result of peanut exposure. A number of lipids and lysophospho-lipids were shown to have increased dramatically and may represent novel biomarker candidates for peanut-induced anaphylaxis in humans.

In summary, this thesis had demonstrated that comprehensive metabolomic analyses can be successfully applied to complex syndromes such as peanut allergy and yield useful mechanistic and clinical insights to this disorder.

Acknowledgements

During the past 4 ½ years I have been blessed with the opportunity to work with a great number of people who have given me immeasurable amounts of support and without whom this thesis would not be possible. Firstly, I would like to thank Dr. Brian McCarry for not only passing on his great wealth of knowledge but for believing in me in my moments of doubt. I will forever be in your debt. Secondly, I would also like to thank my friends and fellow McCarry students, Sujan Fernando, Roger Luckham, Fan Fei, David Bowman, Paul Hodgson, Vi Dang, Yemi Sofowote and Catherine Amoateng who have made my time here so memorable. Next I would like to thank our collaborators Dr. Manel Jordana and Joshua Kong. It has been a genuine pleasure to work with you both. I also need to thank my committee members Dr. Murray Potter and Dr. Philip Britz-McKibbin as well as Dr. Inga Kirreva, Dr. Kirk Green and Dr. Steven Kornic for all of their assistance and advice over the years.

Finally, I need to express my gratitude to my parents David and Betty and to my wife Amber for their unconditional love and support. Without you there is no way I would have had the strength to see this work through and I thank god every day for having you in my life.

Table of Contents

Abstract.....	iii
Acknowledgement	vi
Table of Contents	vii
List of Figures	xii
List of Tables	xvi
List of Abbreviations	xvii
Declaration of Academic Achievement and Contributions	xix
Chapter 1: Introduction to Metabolomics and Analytical Strategies for Comprehensive Metabolomic Analysis	1
<i>1.1. Metabolomics and the Metabolome.....</i>	<i>2</i>
<i>1.2 Challenges in Comprehensive Metabolomics.....</i>	<i>4</i>
<i>1.3. Comprehensive Metabolomics as a Tool for Discovery of Biomarkers.....</i>	<i>6</i>
<i>1.4. Sampling Considerations and Workflow for Comprehensive Metabolomics</i>	<i>7</i>
<i>1.5. Analytical Methods for Comprehensive Metabolomic Analysis</i>	<i>9</i>
<i>1.6. Fundamentals of Mass Spectrometry</i>	<i>11</i>
<i>1.7. Electrospray Ionization for MS Analysis</i>	<i>13</i>
<i>1.8. Mass Analyzers for Mass Spectrometry</i>	<i>17</i>
<i>1.9. Chemical Separation Prior to ESI-MS</i>	<i>18</i>
<i>1.10. Allergy Mechanisms</i>	<i>24</i>
<i>1.11. Anaphylaxis Mediators</i>	<i>28</i>
<i>1.12 Thesis Objectives</i>	<i>29</i>

Chapter 2. Methods and Materials	31
2.1. <i>Equipment and Chemicals</i>	31
2.1.1. <i>LC-ESI-TOF-MS instrumentation</i>	31
2.1.2. <i>Other Instrumentation</i>	32
2.2. <i>Liquid Chromatography Mobile Phases and Extraction Solvents</i>	32
2.3. <i>Chemical Standards</i>	33
2.4. <i>LC Gradients and MS Parameters</i>	33
2.5. <i>MS/MS Spectra Acquisition Parameters</i>	35
2.6. <i>Tandem Column Configuration</i>	35
2.7. <i>Post Column Addition Experiments – Ion Suppression Determination</i>	36
2.8. <i>Data Alignment, Preprocessing, and Data Extraction</i>	36
2.9. <i>Criteria for Metabolite Identification</i>	37
2.10. <i>Statistical Analyses</i>	38
2.11. <i>Peanut Sensitization Protocol and Intraperitoneal Challenge</i>	38
2.12. <i>Blood Sample Collection, Preparation, and Extraction</i>	39
Chapter 3. LC-MS Method Development	41
3.1. <i>Method Development Considerations and Challenges</i>	41
3.2. <i>Results</i>	45
3.2.1. <i>Initial Screening of LC Columns & Determination of Orthogonality</i>	45
3.2.2. <i>Determination of Ion Suppression Observed with Blood Serum Extract</i>	49
3.2.3. <i>Evaluation of Retention Properties of Single Columns Compared to Columns Operated in Tandem</i>	53
3.2.4. <i>Total Feature Retention</i>	56
3.2.5. <i>Reproducibility</i>	57

3.2.6. <i>Comparison of Blood Serum vs. Blood Plasma</i>	58
3.3. <i>Discussion</i>	59
3.3.1. <i>Ion Suppression Reduction</i>	59
3.3.2. <i>Tandem Column Retention Characteristics and Total Feature Detection</i>	60
3.3.3. <i>Column Order, Gradient Type, and Other Considerations</i>	60
3.4. <i>Conclusions</i>	63
Chapter 4. Metabolomic Analysis of Mice Undergoing Sensitization to Peanuts	65
4.1. <i>Introduction</i>	65
4.1.1. <i>Development of Peanut Hypersensitivity</i>	66
4.1.2. <i>Research Objectives</i>	67
4.2. <i>Experimental Design</i>	69
4.3. <i>Results</i>	71
4.3.1. <i>Metabolomic Profiles of Naïve Mice Compared to Sensitized Mice</i>	71
4.3.2. <i>Sensitized Mice Compared to Mice Treated with Peanut Only</i>	76
4.3.3. <i>Time-Course Analysis of Mice Undergoing Sensitization</i>	79
4.4. <i>Discussion</i>	85
4.4.1. <i>Metabolite Profiles Reveal Significant Differences in Serum Metabolome</i>	85
4.4.2. <i>Alteration of Purine Levels in Fully Sensitized Mice</i>	86
4.4.3. <i>Uric Acid as an Adjuvant for the Induction of Peanut Hypersensitivity</i>	89
4.4.4. <i>Effect of Cholera Toxin on Levels of Uric Acid and Other Purines</i>	92
4.5. <i>Conclusions</i>	93

Chapter 5. Metabolomic Screening of Peanut-Induced Anaphylaxis	95
5.1. Introduction	95
5.1.1. Introduction-The Health Problem	95
5.1.2. Research Objectives	98
5.2. Experimental Design	100
5.2.1. First Challenge Experiment	101
5.2.2. Second Challenge Experiment	103
5.3 Results	104
5.3.1 Clinical Measurement of PIA Severity-First Experiment	104
5.3.2. Global Metabolite Profiling of Mice First Experiment	105
5.3.3. Comparison of Metabolomic Profiles of Mice During PIA Found in the First Challenge Experiment	107
5.3.4. Global Metabolite Profiling of Mice - Second Experiment	108
5.3.5. Comparison of Metabolomic Profiles of Mice During PIA Found in the Second Challenge Experiment	116
5.3.6. Identification of Statistically Significant Metabolite Features in the Second Challenge Experiment	121
5.4 Discussion	124
5.4.1. Global Metabolite Profile in Mice Reflects Clinical Measurements and Observations	124
5.4.2. Immediate Metabolite Changes in Mice Reflective of Early Stage PIA	124
5.4.3. Late Stage PIA Metabolic Changes	127
5.4.4. Special Challenges to Screening for PIA Mediators	128
5.5. Conclusions	130
Chapter 6. Comprehensive Metabolomics of Pediatric Blood Serum Samples from Peanut Allergic Patients	131
6.1. Introduction	131

6.2. Results	134
6.3. Discussion	145
6.3.1. Differentiation of Pre-Challenge Metabolome from Post-Challenge Metabolome	145
6.4. Conclusions	150
Chapter 7. Conclusions and Future Directions	152
7.1. Conclusions	152
7.2. Future Directions	156
Section 8. References.....	159
Appendix 1. Appendix 1. Listing of Chemical Standards Used for Method Development	167
Appendix 2. XCMS and CAMERA Operational Parameters	184
Appendix 3. Metabolites Exhibiting statistically significant changes 20 minutes post challenge and beyond in serum from the second challenge experiment	185

List of Figures

<i>Figure 1.1. Overview of systems biology</i>	1
<i>Figure 1.2. Number of publications containing “metabolomics” as a key word</i>	3
<i>Figure 1.3. Typical workflow for comprehensive metabolomics analysis</i>	9
<i>Figure 1.4. Summary of strengths and weaknesses of common analytical methods used for comprehensive metabolomics</i>	11
<i>Figure 1.5. Applicability of commonly used ionization types for comprehensive metabolomics</i>	12
<i>Figure 1.6. Ionization models for electrospray mass spectrometry</i>	15
<i>Figure 1.7. Common mass analyzer types and characteristics</i>	18
<i>Figure 1.8. Formation and partition of water enriched pseudo stationary phase in HILIC chromatography</i>	22
<i>Figure 1.9. Standard “type B” silica and modified “type C” silica used in aqueous normal phase chromatography</i>	23
<i>Figure 1.10. Chemical structures of select anaphylaxis mediators and biomarkers</i>	26
<i>Figure 1.11. Common lymphocyte-Ig mechanisms which trigger anaphylaxis</i>	27
<i>Figure 2.1. Instrumental setup for the tandem column configuration in liquid chromatography-mass spectrometry experiments</i>	36
<i>Figure 2.2 Treatment schedule for the sensitization of mice to peanut protein</i>	39
<i>Equation 3.1. Pearson product-moment correlation coefficient</i>	46
<i>Figure 3.1. Pair-wise comparison of relative retention of 100 metabolite standards</i>	48
<i>Figure 3.2. Mass chromatogram scaled by retention factor (k') of the $[M+H]^+$ ion of L-phenylalanine-d_8 added post column</i>	50

<i>Figure 3.3. Mass chromatogram scaled by retention time of the [M+H]⁺ ion of L-phenylalanine-d₈ added post column</i>	<i>51</i>
<i>Figure 3.4. Regions of ion suppression observed in chromatograms by post column addition.</i>	<i>53</i>
<i>Figure 3.5. Retention of a variety of polar metabolites on the ZIC column RP-amide column and ZIC-amide combination.</i>	<i>55</i>
<i>Figure 4.1. Summary of three experiments performed for the metabolomic analysis of mice undergoing sensitization to peanuts</i>	<i>69</i>
<i>Figure 4.2. Bleeding schedule for metabolomic study of mice undergoing sensitization with peanut and cholera toxin.....</i>	<i>71</i>
<i>Figure 4.3. OPLS-DA analysis of blood serum metabolome comparing naïve mice to sensitized mice.</i>	<i>73</i>
<i>Figure 4.4. OPLS-DA analysis of blood serum metabolome comparing mice treated with peanut extract only to fully sensitized mice.</i>	<i>77</i>
<i>Figure 4.5. OPLS-DA analysis of blood serum metabolome after two weeks of treatment.</i>	<i>80</i>
<i>Figure 4.6. OPLS-DA analysis of blood serum metabolome after four weeks of treatment.</i>	<i>81</i>
<i>Figure 4.7. OPLS-DA analysis of blood serum metabolome after six weeks of treatment</i>	<i>83</i>
<i>Figure 4.8. OPLS-DA analysis of blood serum metabolome comparing mice treated with peanut extract only, with CT only, Naïve mice, and fully sensitized mice</i>	<i>83</i>
<i>Figure 4.9. Observed impact on purine metabolism due to treatment with peanut and cholera toxin.</i>	<i>87</i>
<i>Figure 4.10. Relative levels of purines involved in uric acid production after 6 weeks of treatment from the third sensitization experiment</i>	<i>87</i>
<i>Figure 4.11. Relative levels of uric acid comparing sensitized mice treated with peanut and cholera toxin to peanut treated mice only</i>	<i>88</i>
<i>Figure 4.12 Observed clinical responses in mice treated with peanut extract and uric acid compared to non-sensitive mice and mice treated with peanut and cholera toxin.</i>	<i>90</i>

<i>Figure 4.13. Clinical observations of mice treated with peanut, cholera toxin and uricase compared to naïve and sensitized mice after intraperitoneal challenge</i>	92
<i>Figure 5.1. Types of time-based metabolomic comparisons</i>	101
<i>Figure 5.2. Sampling schedule for bleeding and sacrifice after intraperitoneal challenge of mice with peanut extract for first and second challenge experiments</i>	102
<i>Figure 5.3. Core body temperature and hematocrit levels of mice undergoing peanut-induced anaphylaxis as a function of time- first challenge experiment.</i>	105
<i>Figure 5.4. OPLS-DA score plot of metabolomic features found in the first peanut-challenge experiment.</i>	106
<i>Figure 5.5. Core body temperature and hematocrit levels of mice undergoing peanut-induced anaphylaxis as a function of time- second challenge experiment.</i>	111
<i>Figure 5.6. OPLS-DA score plot of metabolomic features from second challenge experiment.</i>	112
<i>Figure 5.7. OPLS-DA score plot of metabolomic features in non-sensitized mice from second challenge experiment.</i>	114
<i>Figure 5.8. OPLS-DA separation of treated and control mice by post-challenge time.....</i>	115
<i>Figure 5.9. Volcano plots of metabolite features at various stages of the second peanut-induced anaphylaxis experiment.</i>	118
<i>Figure 5.10. Plot of 3500 metabolite features observed in all samples plotted by retention time (0-10 minutes) versus m/z ratio.</i>	119
<i>Figure 5.11. Plot of 3500 metabolite features observed in all samples plotted by retention time (20-40 minutes) versus m/z ratio.</i>	120
<i>Figure 5.12. Positive mode MS/MS spectra of methylhistamine</i>	122
<i>Figure 6.1. Principal component analysis (PCA) score plot of blood serum samples from nine children with known peanut allergy.</i>	135
<i>Figure 6.2. Orthogonal partial least squares-discriminate analysis (OPLS-DA) score plot of blood serum samples from children with known peanut allergy.</i>	136

<i>Figure 6.3. Plot of fold change (post-challenge vs. pre-challenge) as a function of mass-to-charge ratio</i>	140
<i>Figure 6.4. Plot of fold change (post-challenge vs. pre-challenge) for metabolite features found to be significant as a function of the mass-to-charge ratio</i>	141
<i>Figure 6.5. Volcano plot of metabolomic features observed in human challenge samples</i>	142
<i>Figure 6.6. Chromatographic profile of metabolomic features found in at least five subjects plotted as retention time versus m/z ratio</i>	143
<i>Figure 6.7. Averaged mass spectra of lyso lipid mass region in chromatograms over 2-5 minutes</i>	147
<i>Figure 6.8. MS/MS spectra of lyso-phosphatidylcholine(18:0)</i>	147
<i>Figure 6.9. Positive ionization mass spectra of eight lyso-phospholipids</i>	148

List of Tables

<i>Table 2.1. LC columns investigated and column details</i>	32
<i>Table 3.1. Pearson correlation coefficients between HILIC, AqNP and RP columns</i>	47
<i>Table 3.2. Summary of regions of ion suppression</i>	52
<i>Table 3.3. Numbers of mass spectral features detected in a pooled mouse serum sample following analysis on various LC columns and column pairings</i>	56
<i>Table 4.1. Fifteen Metabolites exhibiting statistically significant fold changes comparing naïve and sensitized mice in the first pilot experiment</i>	75
<i>Table 4.2. List of twenty-five metabolites exhibiting statistically significant fold changes comparing sensitized versus mice treated only with peanut extract</i>	78
<i>Table 4.3. Nineteen metabolites exhibited significant differences from the third sensitization experiment</i>	84
<i>Table 5.1 Metabolites of sensitized mice found to be changing 1 minute post challenge in the first challenge experiment</i>	109
<i>Table 5.2. Twenty-eight metabolites exhibiting significant fold changes comparing naïve and sensitized mice 40 minutes post-challenge</i>	109
<i>Table 5.3. Total sum of features with significant fold changes and p values</i>	116
<i>Table 5.4. Fifty-one Metabolites found to be significantly altered in early stage PIA</i>	123
<i>Table 6.1. Metabolites observed to change in serum samples obtained from children with peanut allergies after an oral peanut challenge</i>	137
<i>Table 6.2. Numbers of metabolite features which showed significant changes arranged in one of three groups according to their m/z range</i>	144
<i>Table 6.3. Numbers of metabolite features which showed significant changes arranged by fold change</i>	144

List of Abbreviations

2D-LC: Two-Dimensional Liquid Chromatography
ANOVA: Analysis of Variance
AP: Aminopropyl
APCI: Atmospheric Pressure Chemical Ionization
AqNP: Aqueous Normal Phase
C18: octadecyl
CE: Capillary Electrophoresis
CID: Collision-Induced Dissociation
CT: Cholera Toxin
DAMP: Danger Associated Molecular Pattern
EDTA: Ethylenediaminetetracetic acid
EI: Electron Impact
ESI: Electrospray Ionization
EtOH: Ethanol
FC: Fold Change
FT-ICR: Fourier Transform Ion Cyclotron Resonance
FWHM: Full Width Half Maximum
GC: Gas Chromatography
HILIC: Hydrophilic Interaction Chromatography
HPLC: High Performance Liquid Chromatography
i.p.: Intraperitoneal
Ig: Immunoglobulin
IL: Interleukin
k': Capacity Factor
LC: Liquid Chromatography
LT: Leukotriene
lysoPC: Lysophosphatidylcholine
lysoPE: Lysophosphatidylethanolamine
m/z: Mass-to-Charge Ratio
MeOH: Methanol
MS: Mass Spectrometry
MS/MS: Tandem Mass Spectrometry
MSⁿ: Multi-Stage Mass Spectrometry
NMR: Nuclear Magnetic Resonance
OPLS-DA: Orthogonal Partial Least Squares-Discriminate Analysis
PAF: Platelet Activating Factor
PC: Phosphatidylcholine

PCA: Principal Component Analysis
PE: phosphatidylethanolamine
PFP: Pentafluorophenyl
PIA: Peanut Induced Anaphylaxis
PN: Peanut
QTOF: Quadrupole-Time-of-Flight
r: Pearson Coefficient
RP: Reversed Phase
RRF: Relative Response Factor
SiIH: Silica Hydride
Th1: T Helper Cell type 1
Th2: T Helper Cell type 2
TOF: Time-of-Flight
UA: Uric Acid
UPLC: Ultra Performance Liquid Chromatography
XB-C18: Cross-Bridge octadecyl
ZIC: Zwitterionic Sulfonyletaine

Declaration of Academic Achievement and Contributions

All animal handling/treatment procedures, clinical measurements of anaphylaxis and immunology experiments described in Chapters 4 and 5 were performed by Joshua Kong a graduate student under the supervision of Dr. Manel Jordana research group; Dept. of Pathology and Molecular Medicine McMaster University. Animal blood samples were processed by both the author and by Joshua Kong.

Human samples analyzed as described in Chapter 6 were collected as part of an on-going Allergen study led by Dr. Susan Wasserman, Dept. of Medicine, McMaster University; human serum samples were extracted by Joshua Kong.

All other work presented in this thesis was performed by the author.

Chapter 1. Introduction to Metabolomics and Analytical Strategies for Comprehensive Metabolomic Analysis

1.1 Metabolomics and the Metabolome

Systems biology is the holistic study of all biological components and functions. The small organic molecules or metabolites found in living organisms represent the furthest downstream expression of biochemical activity, reflecting the total contributions of genomic, transcriptomic, and proteomic activities in the organism along with nutritional and environmental factors¹. (Figure 1.1). The information represented by metabolite levels holds vast potential for researchers to describe the true chemical state of an organelle or an organism. One of the very first general metabolite profiling experiments reported was by Pauling et al. in 1971 where the organic chemical species found in human urine and breath vapor were measured for the first time using packed column gas chromatography². In this study hundreds of substances were detected. This study marked the beginning of what is now known as metabolome profiling or more commonly, metabolomics.

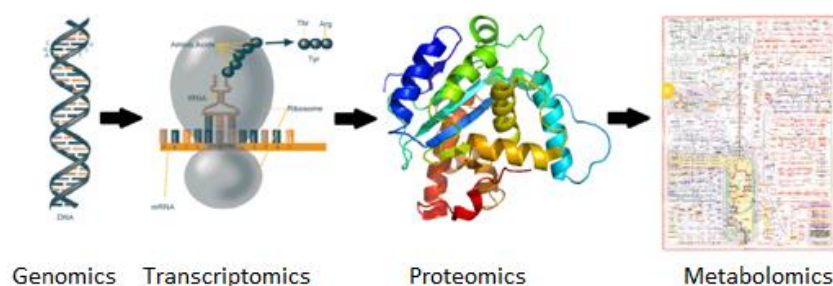


Figure 1.1. Overview of systems biology showing relationships between Genomics, Transcriptomics, Proteomics, and Metabolomics

The first use of the term “metabolome” is credited to Oliver et al. in 1998 who defined the metabolome as “the qualitative and quantitative collection of all low molecular weight molecules present in a cell that are participants in general metabolic reactions and that are required for the normal function of a cell”³. Shortly after Oliver’s paper, Nicholson et al. introduced an approach to studying the metabolome which they dubbed metabonomics and defined as “the quantitative measurement of the dynamic multiparametric metabolic response of living systems to pathophysiological stimuli or genetic modification”⁴. While the definition does not specifically mention the means of how the metabolome should be measured, Nicholson specifically states in this work that it is a nuclear magnetic resonance (NMR) based approach.

In 2001 Fiehn defined “metabolomics” as the “comprehensive analysis of all metabolites in a biological system in which the low molecular weight species are both identified and quantified”⁵. This definition now is currently used for “comprehensive metabolomics” to differentiate it from “Targeted metabolomics” where only a few metabolites are quantified. In the years since Nicholson and Fiehn introduced these respective terms, metabonomics and metabolomics have been used interchangeably although metabolomics has become the more common of the two terms and because of this precedence, “metabolomics” will be used throughout this thesis.

Unlike other “-omics” studies, metabolomics is capable of providing real-time information as to the health and general state of an organism due to both *in vivo* and *ex*

vivo stresses. Since metabolite levels can change very quickly, this aspect has made it especially attractive to researchers in health sciences, environmental toxicology, and systems biology⁶; this is reflected in the rapid growth of the field over the past decade.

Figure 1.2 charts the total number of publications since 2000 from searches of the terms “Liquid Chromatography AND metabolomics”, “Gas Chromatography AND metabolomics”, “Capillary Electrophoresis AND metabolomics” and “NMR AND metabolomics” using the search engine Web of Science.

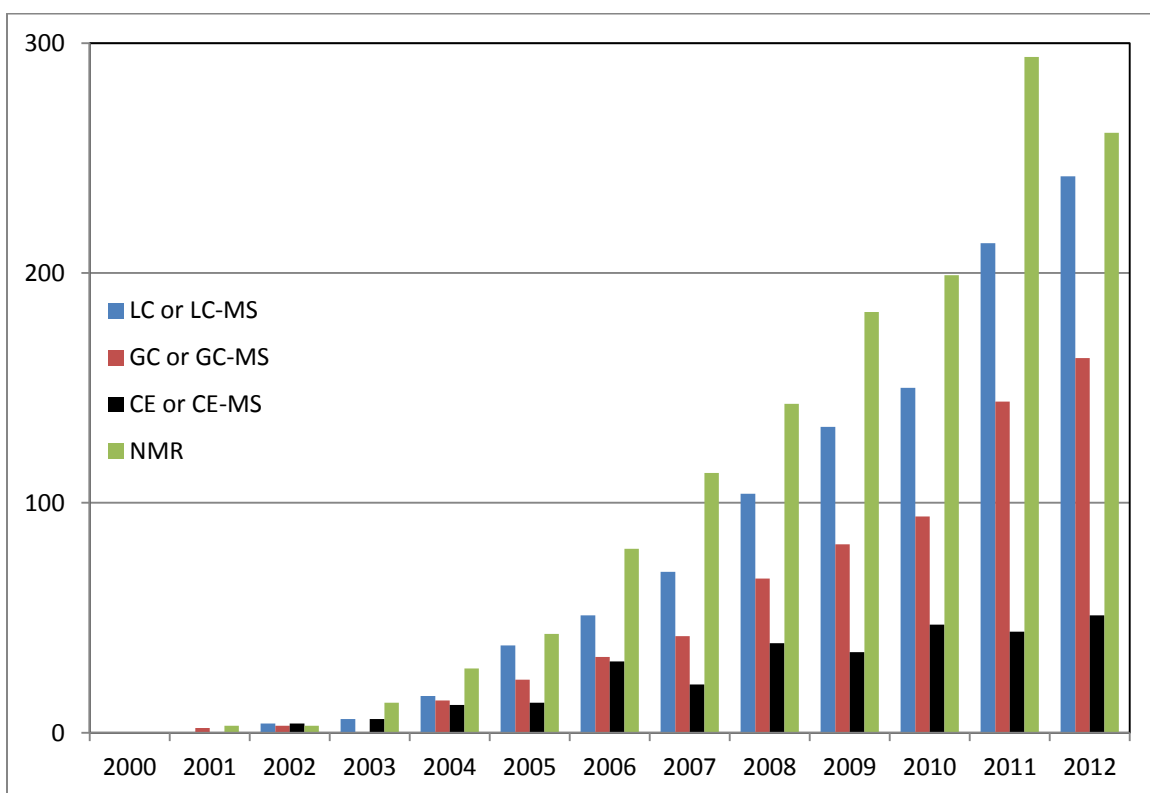


Figure 1.2 Number of publications containing “metabolomics” as a key word as of December 31st, 2012 as per Web of Science. The types of publications are classified according to the analytical platform used. The total number of publications in 2011 was 695 and the total number as of Dec. 31st 2012 was 717.

Although metabolomics is still a new field of research, recent technological developments have emerged which have allowed researchers to make great strides in the identifications of metabolites as biomarkers in health areas such as cardiovascular disease^{7,8}, liver injury⁹, various cancers^{10,11}, and exposure to environmental influences such as ionizing radiation^{9,12,13}. The research company Metabolon® alone has identified biomarkers which are currently used as clinical diagnostic tests for 4 types of cancer in addition to insulin resistance and amyotrophic lateral sclerosis. This is in stark contrast proteomics which, despite the huge resources expended and thousands of proposed biomarkers, has produced very little in terms of successful clinical applications or clinical methods¹⁴.

1.2 Challenges in comprehensive metabolomics

The “low molecular weight species” in a biological system encompass a staggering array of biochemicals ranging from small hydrophilic ions to reasonably large, neutral hydrophobic molecules. Unlike the similar types of chemical species encountered in gene analysis or protein analysis, the enormous chemical diversity within the metabolites presents significant challenges to the analytical chemist often leading to difficult analytical choices when attempting to perform comprehensive metabolomic analyses. For genomic or proteomic analyses, a small number of methods is suitable to measure all relevant genes or peptides; On the other hand no single analytical method can be optimized for the analysis of all biomolecules¹⁵. Another

challenge for comprehensive metabolomic analysis is that the current knowledge of metabolism and metabolic pathways in cells is surprisingly incomplete and this leads to a large number of metabolites being listed as “unknown”¹⁶. Identifying unknown metabolites can be an arduous and time-consuming process which is further complicated when the metabolite is found in small abundance. The current consensus on what is required for definitive metabolite identification is that at least two orthogonal or independent measurements must be available¹⁷. This criteria puts a premium on methodologies capable of providing orthogonal data in a single run.

The principal analytical challenge for comprehensive metabolomics is simply the sheer numbers of metabolites which are detected using modern, sensitive, instruments. In addition, the large range of metabolite concentrations (up to 14 orders of magnitude)¹⁸ poses a serious challenge. Thus, it is not possible to obtain quantitative measurements of all metabolites in a sample. Typically, for comprehensive metabolomic studies use a semi-quantitative approach where differences between “normal” or “control” samples are measured relative to “treated” or “affected” samples and reported as a fold change. While the “treated versus control” approach introduces some subjectivity into the data analysis, an international group in 2007 proposed experimental standards such as the minimal number of replicates which have helped offset some of this subjectivity^{17,19}.

1.3. Comprehensive Metabolomics as a Tool for Discovery of Biomarkers and Novel Pathways

A major application of comprehensive metabolomics has been in the discovery of biomarkers which will provide new, clinically relevant diagnostic targets or to discover novel metabolite pathways to provide clues pertaining to the general homeostasis of a living being. While there is no universal consensus on the definition of a biomarker, one of the most common definitions was provided by the United States Food and Drug Administration where a biomarker is “a characteristic that is objectively measured and evaluated as an indicator of normal biological processes, pathogenic processes, or biological response to a therapeutic intervention.”²⁰ Regardless of the definition, any metabolite which is considered to be a biomarker should be qualified by a rigorous, multiphase process which has unambiguously demonstrated its diagnostic and prognostic value.

The first phase of biomarker qualification, the discovery stage, is primarily concerned with identifying compounds which are either up or down-regulated or simply absent between a normal/control sample group and a treated/distressed sample group. It is this stage where comprehensive metabolomics has its greatest utility as a discovery tool. Compounds which appear to be significantly different between these groups are commonly referred to as differentiating markers. At this stage the full chemical identity of the marker may or may not be known but it needs to be accompanied by a unique set

of measurement features (e.g. retention time, accurate mass value, tandem MS spectra, etc.).

The next phase of discovery involves the full elucidation of the chemical identity of the differentiating marker followed by the analytical validation of the marker by an acceptable analytical method (targeted metabolomics). At this stage a differentiating marker becomes a candidate biomarker²⁰. The last phase of biomarker qualification involves the study of how the biomarker relates to biological mechanisms impacted by the event in question and the study of how clearly the candidate biomarker is indicative of a specific pathophysiology. In this last phase it is necessary to assess the potential for false positive and false negative results;²¹ this stage also encompasses pathway discovery²². Again, despite being in its infancy, comprehensive metabolomic approaches have been successfully used to discover novel biomarkers and pathways including but not limited to liver disease^{9,23}, chronic pain²⁴, and various cancer types^{10,11,25,26}. A number of these biomarkers are validated and are available for use in the clinic.

1.4. Sampling Considerations and Workflow in Comprehensive Metabolomics

To obtain a “real-time” assessment of homeostasis, all chemical reactions must be stopped as quickly as possible after collection of the sample to prevent unwanted degradation or alteration of metabolite levels. The most common means of achieving metabolic arrest is to immediately flash freeze samples in liquid nitrogen or a Dry-Ice

bath or to immediately extract/process samples so as to remove enzymes and other proteins from catalyzing any further metabolic reactions²⁷. Depending on which analytical method will be used, extraction can be performed in a variety of ways; however, a key requirement is that whichever extraction method is used, it should be capable of solubilizing all metabolites while excluding as much of the proteins and other higher molecular mass components as possible. Recovery standards are commonly added before any extraction process begins. Once extracted, internal standards may also be added and any chemical derivatization protocols may be carried out to prepare the sample for analysis. Once the sample has been prepared, the general consensus for workflow is diagrammed in Figure 1.3

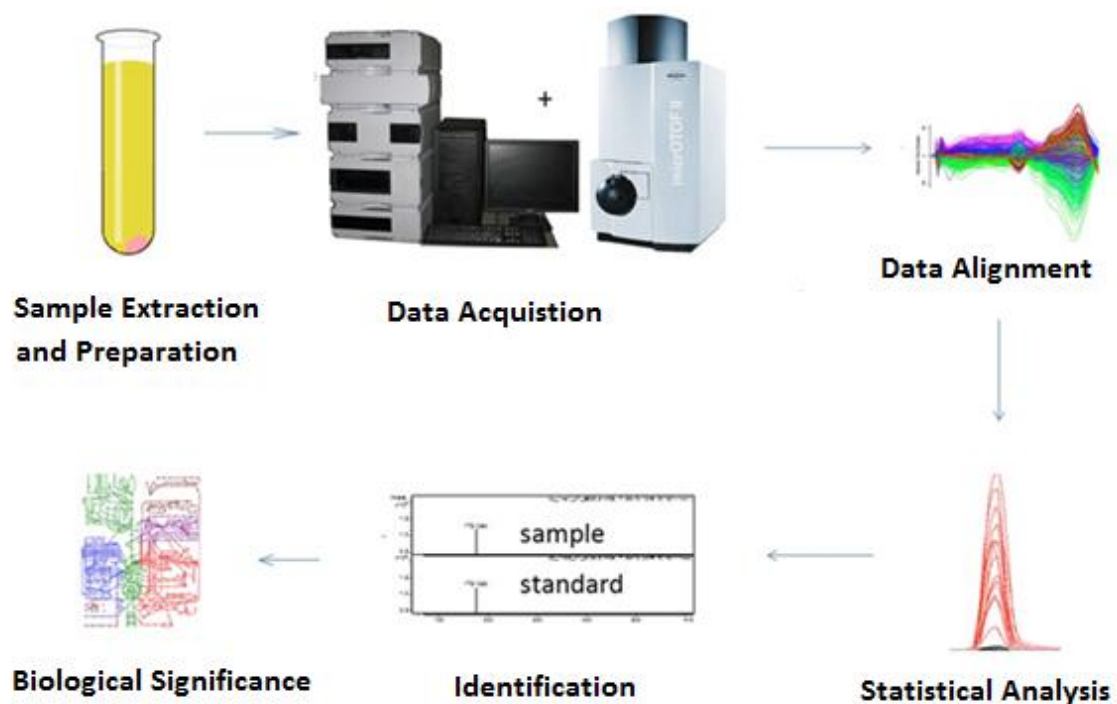


Figure 1.3. Typical Workflow for Comprehensive Metabolomics Analysis

1.5. Analytical Methods for Comprehensive Metabolomic Analysis

No single method or analytical platform exists which can simultaneously measure all low molecular mass compounds (<1500 Da) in a single analytical run.¹⁵ Analytical methods range from very highly specific for certain analytes such as immunochemical “kits” to low selectivity analyses such as optical methods. The latter are generally used only for targeted analysis of a small number of metabolites. By far the most commonly used methods used for comprehensive metabolomics are either

mass spectrometry-based or nuclear magnetic resonance-based due to the high selectivity of these methods.

NMR-based methods (including hyphenated techniques such as LC-NMR) are widely used for metabolomics due to the high quality of structural information which can be deduced from acquired spectra and the wide chemical range which can be detected with NMR²⁸. The primary drawback to NMR as a comprehensive tool is that NMR is relatively insensitive. NMR methods therefore only yield information about the most abundant 30-50 metabolites in the sample. This lack of sensitivity is a significant limitation to NMR techniques since many biomarkers and other relevant molecules are found in much lower concentrations than NMR can detect. Other drawbacks to NMR methods are that interpretation of NMR spectra can be complicated while the financial cost to purchase, operate and maintain these instruments is quite high. Nonetheless, NMR-based methods account for ~40% of all metabolomics papers published.

Mass spectrometry (MS)-based techniques are most common for comprehensive analyses due to the very high sensitivity, selectivity, and dynamic range of MS systems²⁹. MS systems also have the advantage of being easily coupled with separation platforms such as gas chromatography, liquid chromatography, capillary electrophoresis and super critical fluid chromatography. Despite the longer analysis times of these so called hyphenated techniques (e.g.,LC-MS), compared to direct infusion or flow injection sample introduction, these separation platforms can provide a degree of on-line sample

clean-up prior to MS analysis. These separations also provide chemical information arising from the observed retention/migration of the analytes that will aid in the characterization of the sample. The relative strengths and weaknesses of these techniques are compared in Figure 1.4.

	Infusion	Flow Injection	LC-MS	CE-MS	GC-MS	NMR
Throughput	Fast	Fast	Variable	Moderate	Slow	Moderate
Ease of Sample Preparation	Difficult	Difficult	Easy	Easy to Moderate	Difficult	Difficult
Quality of Structural Information	Moderate (MS ⁿ)	Low	Moderate	Moderate	Good	Excellent
Volume of Sample Required	μL-mL	μL	μL	nL- μL	μL	mL
Robustness	Moderate	Moderate	High	Moderate	High	High
Cost	Low	Low	Moderate	Moderate	Moderate	High

Figure 1.4. Summary of strengths and weaknesses of common analytical methods used for comprehensive metabolomics

Some MS instruments are capable of performing tandem (MS/MS) and multi-stage MS (MSⁿ) experiments which can provide a highly desired orthogonal measurement. Accurate mass measurements and isotopic abundance measurements are also useful for the determination of elemental composition.¹⁷

1.6. Fundamentals of Mass Spectrometry

All MS systems share 3 separate components; an ionization source, a mass analyzer, and an ion detector (most commonly an electron multiplier). MS detectors are

true quantity detectors rather than a concentration dependent detector³⁰. At least 70 unique types of ionization sources have been reported in literature although for comprehensive metabolomics analysis only three types have been used extensively: electron impact (EI), electrospray (ESI) and atmospheric pressure chemical ionization (APCI)³¹. Figure 1.5 illustrates the typical coverage that each ionization type provides based on analyte polarity and molecular mass.

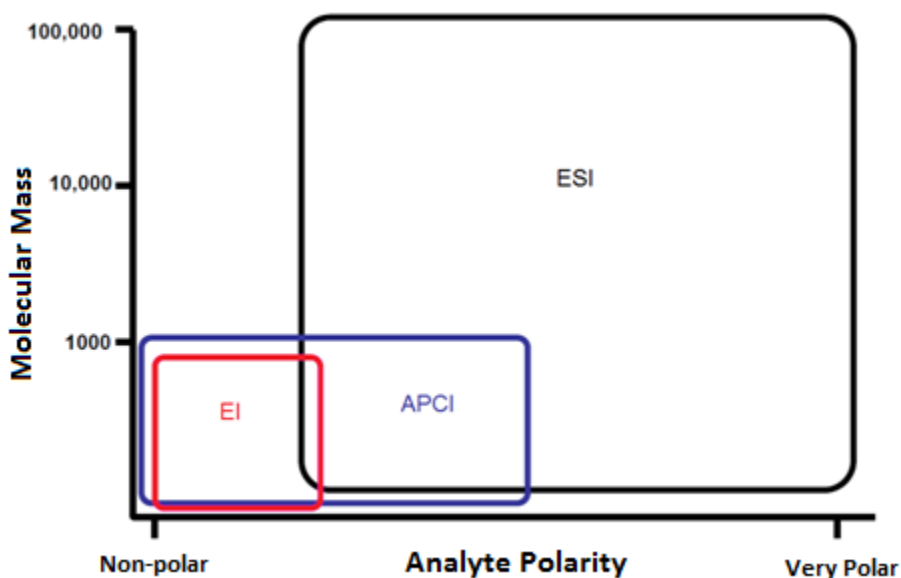


Figure 1.5. Comparison of commonly used ionization methods for comprehensive metabolomics analysis

EI is one of the oldest and most well understood methods of ionization; it is especially adept at providing structural information for molecules due to the high energy ions it produces and the resulting fragmentation induced in almost all molecules. The physical requirements of EI sources are most compatible with GC analysis, primarily

since the analytes must be in the gas phase in order to be ionized. Therefore molecules which are reasonably volatile are amenable to EI. Although EI-MS has many desirable analytical properties the requirement for analyte volatility renders it impractical for most metabolite classes which are polar and non-volatile unless chemically derivatized.

APCI is another well known and well understood ionization technique where a gas, typically nitrogen in the presence of water is ionized by a coronal discharge. This charged gas then proceeds to undergo a series of primary and secondary gas-phase reactions most commonly producing a solvated proton, a $H^+(H_2O)_n$ ion, which can transfer a proton to an analyte molecule in the gas phase. APCI offers significant advantages including the ability to produce ions from relatively non-polar molecules and its ability to maintain a high rate of ionization efficiency under high flow rate conditions; however, this technique requires some degree of volatility of the analyte and that the analyte be thermally stable due to the high temperatures required (~350-500°C).

1.7. Electrospray Ionization for MS Analysis

The most widely used ionization technique for comprehensive metabolomics is electrospray ionization (ESI).³² This type of ionization was first reported in 1937 by Chapman when he reported detecting “gas phase ions as a result of spraying an electrified salt solution from a metal tube”³³. Over the next 75 years, various models and hypotheses have been proposed to explain how gaseous phase ions are produced during the ESI process. The “ion evaporation” model proposed by Iribarne and

Thompson³⁴ and the “free-jet” dispersion model, more commonly known as Coulombic fission, originally proposed by Dole³⁵ are the most popular models. Both models stipulate that molecules are first chemically ionized by the adsorption or loss of an ion in solution to produce a chemical adduct. These charged droplets are sprayed from a capillary tube under an applied voltage to create the electrospray. The ion evaporation model, graphically presented in Fig. 1.6a predicts that excess ions in the droplet will coat the outer surface of the droplet sphere and as the droplet evaporates, the Rayleigh limit will be reached whereupon the force from the droplet surface tension is equal to the Coulomb repulsion of the ions. At this point the ions will become desolvated and “evaporate” into the gas phase.

Alternatively, the free-jet/Coulombic fission model represented in Fig. 1.6b predicts that solvent molecules will evaporate from the charged droplet compressing the ions left behind until the Rayleigh limit is reached. When the Rayleigh limit is exceeded, ion-ion repulsive forces cause the droplet to “explode” releasing some ions into the gas phase and producing smaller droplets which can repeat this ionization process.

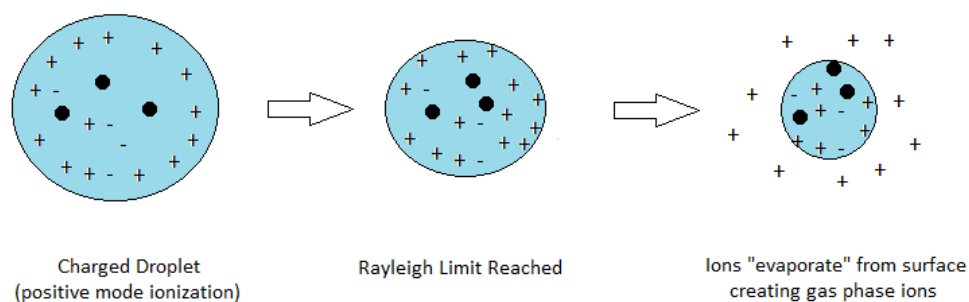


Figure 1.6a. Ion desorption model for production of gas phase ions from an electrically charged droplet.

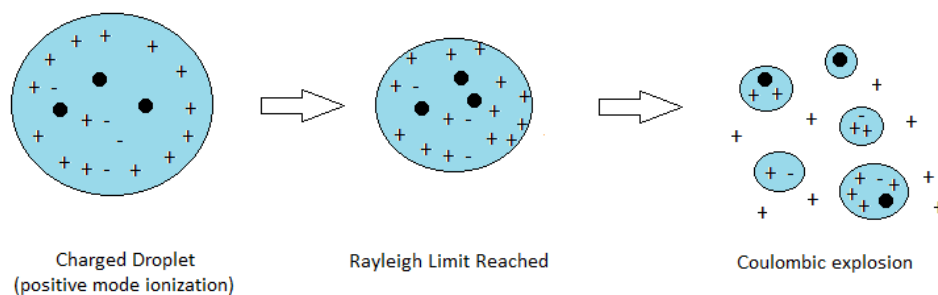


Figure 1.6b. "Free-jet" dispersion model for the production of gas phase ions from an electrically charged droplet.

There are three primary aspects of ESI which make it so attractive for metabolomics analysis. The first stems from the low energy of the ions which tend to produce intact, molecular ion species, with little or no fragmentation leading to relatively simple spectra which are easy to analyze and interpret. These low energy ions are also well suited for collision induced dissociation (CID) experiments which can provide an additional layer of structural information if desired³⁶. The second aspect of ESI that makes it attractive for metabolomics is that it is particularly adept at ionizing

polar and charged molecules that have low volatility. These compounds encompass the majority of metabolites found in living systems³⁷. Even metabolites which do not contain ionizable functional groups can be detected by ESI-MS by the formation of adduct ions with salts such as lithium, sodium, ammonium, and chloride. Finally, ESI is very easy to couple to liquid flow streams such as those found eluting from liquid chromatography columns without requiring specialized interfaces making it an ideal complement to LC²⁶.

Despite these considerable advantages, ESI does have weaknesses which must be contended with in order to ensure high quality data. One weakness to ESI is that the ionization efficiency of a given compound is very dependent on the chemical and physical properties of the analyte and solvent used including analyte hydrophobicity, molecular volume and solvent volatility³⁸. With so many factors impacting the ionization efficiency, the relative responses of molecules vary significantly. Indeed, it has been noted that observed response factors may vary by almost 4 orders of magnitude for a given set of experimental conditions³⁹. Instrumental performance is greatly influenced by experimental conditions such as the total flow volume or flow rate into the ESI capillary, the applied potential to the capillary and the temperature of the ESI source. In this respect ESI requires that the researcher places large importance on experimental “optimization” to determine the best set of operating conditions to perform measurements⁴⁰.

Finally the last weakness of electrospray is a phenomenon commonly known as ion suppression. For both the ion desorption model and the free-jet dispersion model of ESI, it is predicted that ions which occupy the surface regions of the charged droplet will be the ions which are most likely to be released as gas-phase ions. If the total ionic strength of the droplet is large (i.e., a high quantity of ions in the droplet) the surface quickly becomes saturated with ions. This saturation prevents all ions within the droplet to reach the surface which in turn causes a lower rate of desolvation and a falsely low MS signal. To overcome ion suppression, experimental parameters must be optimized to enhance ionization efficiency (e.g. low flow rates, highly volatile solvents etc.) or the total ionic strength must be reduced by dilution.

1.8. Mass Analyzers for Mass Spectrometry

The heart of any MS system is the mass analyzer which physically separates gas phase ions based on their mass-to-charge ratio (m/z). Modern mass analyzers in routine use for metabolomics are generally divided by their mass accuracy and resolution capabilities although other characteristics such as data acquisition rate, linear response range and ease of use are also important characteristics. Figure 1.7 gives a general capability overview of the six most commonly used mass analyzer types. Of the six types, time-of-flight mass analyzers are among the more popular for comprehensive metabolomics³⁷ especially when coupled to LC due to their good mass accuracy and sensitivity, very fast acquisition rate, and relative ease of use.

	Type of Mass Analyzer						
Characteristic	Magnetic Sector	Triple Quadrupole	Ion Trap	Orbitrap	TOF	QTOF	FT-ICR
Mass Range	~15000	~4000	~10 ⁵	~10 ⁵	Unlimited	unlimited	>10 ⁶
Mass Resolution	200k	unit	~100-1000	50k-100k	10k-70k	10k-70k	>10 ⁶
Dynamic Range	10 ⁵	10 ⁶ -10 ⁷	10 ⁵ -10 ⁶	10 ⁴	10 ⁴	10 ⁴	10 ⁴
MS/MS	Good	Good	Excellent	Excellent	N/A	Good	Poor
Separation Platform Compatibility	Low	High	High	Low	High	High	Low
Robustness	Poor	Excellent	Excellent	Poor	Excellent	Good	Poor
Throughput	Slow	Fast	Fast	Slow	Fast	Fast	Very Slow
Ease of Use	Difficult	Easy	Easy	Difficult	Moderate	Moderate	Very Difficult
Relative Cost	High	Low	Low	High	Moderate	Moderate	Very High

Figure 1.7. Common mass analyzer types and characteristics (adapted from Dass; "Principles and Practice of Biological Mass Spectrometry" Wiley Interscience New York 2001). (TOF=time-of-flight; QTOF=quadrupole-time-of-flight; FT-ICR=Fourier Transform-Ion Cyclotron Resonance).

1.9. Chemical Separations Prior to ESI-MS

The consensus of most researchers is that accurate mass measurement is insufficient for metabolite identification¹⁷. One acceptable form of orthogonal measurement in addition to accurate mass is the chromatographic or migration time through a separation platform. The use of a separation platform prior to MS detection, especially with ESI also provides an effective means to reduce the impact of matrix

interferences such as salts which impact the quality of the MS signal. This characteristic will be explored further in Chapter 3. Separation utilizing a chemical property other than m/z also allows for the measurement of isobaric species which otherwise could not be differentiated by MS alone. The two most common separation platforms used with ESI-MS are liquid chromatography (LC) and capillary electrophoresis (CE)⁴¹.

CE-based separations are primarily driven by differences in the charge-to-size ratio of ionized species in an electrically conductive buffer. This technique has been proven to be effective targeted metabolomic applications primarily. While CE has been used for comprehensive metabolomic applications, CE suffers from a number of technical challenges. One such challenge is that since electrophoretic mobility is strongly correlated with the effective charge of the ion or molecule, CE typically is only effective for molecules with reasonably good acidic or alkaline properties; molecules which have a net charge close to zero under a given set of buffer conditions can only be moved by electroosmotic forces which can be very weak depending on the separation conditions⁴². This challenge also leads to difficulty in the development of a single method which can be used for both anionic and cationic metabolites simultaneously with reasonable run times. Another difficulty with CE especially when coupled to MS is that the total sample loading capacity is very low due to the narrow capillary diameter. Since MS is a quantity-based detection system rather than concentration based, on-line preconcentration techniques such as electrophoretic stacking often need to be used to

achieve acceptable detection limits for low abundance metabolites. These pre-concentration techniques are not always applicable to all metabolite classes.

Liquid chromatography continues to be the most common chemical separation technique in metabolomics due to its ease of use and the diversity of applications to which it can be applied³². LC has also enjoyed recent advancements in column technology, specifically in packing materials including very small particle (<2 μ m) and fabricated superficially porous/core-shell particles which have given rise to so called “ultra-performance” liquid chromatography (UPLC). Due to these advancements, the total through-put of LC separations have improved enormously since the increased separation power allows the use of shorter columns with higher flow rates.

Historically, LC techniques have been divided into “modes” of operation which describe the general operating setup including the column type and the mobile phase characteristics. While many modes are available, comprehensive metabolomics analysis is typically done with either reversed phase (RP) elution, hydrophilic interaction (HILIC) or with a newly emerging mode, aqueous normal phase (AqNP) all of which are fully compatible with ESI-MS detection.

RP chromatography is performed with a stationary phase packed with a hydrophobic material, most commonly derivatized silica where hydrophobic ligands have been chemically bonded to the silica surface and a mobile phase which is a polar solvent. The primary retention mechanism for RP chromatography is well understood

and most often dominated by the partitioning of hydrophobic compounds into the non-polar region of the column packing although other interactions such as dipole interactions, hydrogen bonding and π -system interaction are also possible depending on the column type.

A number of well accepted tests for RP columns exist to characterize structure-selectivity relationships which add to the utility of RP chromatography since these tests can also be used for retention prediction. Retention prediction is a useful tool for metabolite identification where authentic standards are not readily available^{43,44}. While RP chromatography has wide-spread applications in the separation of many classes of metabolites and offers many other advantages such as de-salting capability, the non-polar nature of the column does not effectively retain a significant portion of the metabolome, i.e., polar hydrophilic molecules.

As an alternative to RP, hydrophilic interaction (HILIC) chromatography has received considerable attention for metabolomics applications recently due to its ability to effectively retain polar molecules. The first credited use of the term hydrophilic interaction chromatography was by Alpert in 1990 when he described a chromatographic system using a highly polar hydrophilic stationary phase with a polar mobile phase consisting of acetonitrile and water⁴⁵. In this work, Alpert proposed a mechanism, graphically represented in Figure 1.8 where a water-enriched pseudo stationary phase formed around the polar particles in the column.

The hypothesis of this mechanism is based on hydrophilic molecules partitioning into this enriched area leading to the prediction that retention should be inversely correlated with hydrophobicity. While there is evidence that such partitioning does take place, numerous other factors such as hydrogen bonding and other electrostatic interactions can have a profound impact on the retention and selectivity in HILIC chromatography. Recently, Kawachi performed a comprehensive study whereupon they developed a testing procedure to measure the relative contributions of 9 possible interactions relevant to HILIC which can be used as a basis for column selection similar to tools in routine use for RP column selection⁴⁶.

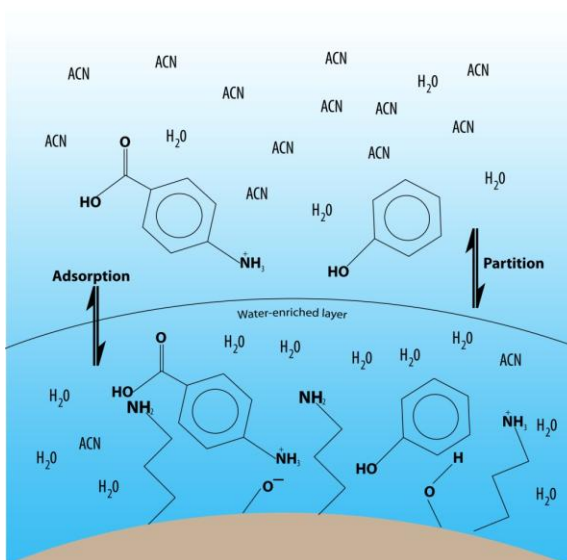


Figure 1.8. Formation and partition of water enriched pseudo stationary phase in HILIC chromatography with a polar Aminopropyl stationary phase

Beyond the ability of HILIC to retain polar molecules in a much more effective manner than RP, HILIC offers an unintentional but very welcome benefit when used with ESI-MS; the high concentrations of volatile solvents with low surface tension such as acetonitrile which must be used in HILIC offer enhanced conditions for both ion evaporation and Columbic fission leading to much higher ionization efficiencies compared to conditions with high water contents. The high organic content of the mobile phase is also very compatible with sample preparation methods which require extraction and protein precipitation with organic solvents.

A third LC mode which has recently attracted interest in metabolomics is based on modified high purity silica and has been labeled aqueous normal phase (AqNP) chromatography. In this chromatography mode, the silica used for the column packing has been derivatized to convert the surface silanol groups to silica hydride groups; this modified silica has been classified as type “C” silica (Figure 1.9).

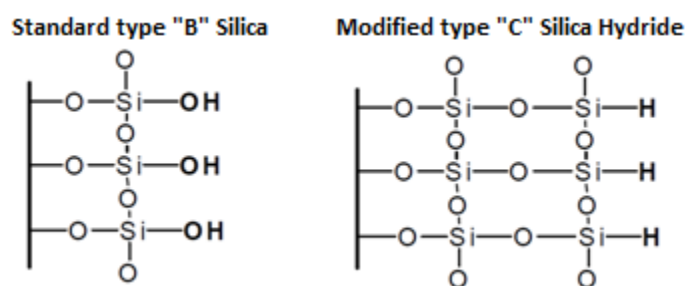


Figure 1.9. Standard “type B” silica and modified “type C” silica used in aqueous normal phase chromatography

Without silanol groups, the hydroscopic properties of the packing are greatly reduced, preventing the accumulation of a water layer surrounding the packing typical of HILIC⁴⁷. While the retention mechanism in AqNP is still to be fully elucidated, most experimental observations strongly suggest that analytes are retained by adsorption similar to what is found in standard normal phase chromatography when operated under high organic solvent conditions⁴⁸. Interestingly, these columns have been observed to have RP like retention characteristics when operated under high aqueous conditions making these columns useful in multiple chromatographic modes⁴⁹.

1.10. Allergy Mechanisms

Immunology is a branch of biological science which studies the function and mechanisms of the immune system of living systems encompassing the physiological state of an organism in both health and disease. In general, immune system disorders can be characterized into three categories; immunodeficiency where the immune system fails to respond, autoimmunity where the immune system attacks the host's own body, and hypersensitivity where the immune system inappropriately responds to harmless compounds or stresses. The third type of immune disorder, hypersensitivity, is more commonly known as allergy where various immune system cells such as mast cells, eosinophils and basophils, become sensitized or programmed to identify benign substances as antigens. While all allergies are not equal, certain primary or "classical" mechanisms are common to all types of hypersensitivity⁵⁰.

Any foreign molecule or protein may stimulate the production of antibodies of various classes (IgG, IgM, etc.); however, the primary antibody which is produced during hypersensitivity is the IgE type which exists as a monomer and binds very tightly to receptors found on mast cells and other immune-active cells. In normal, non-atopic individuals, benign proteins and molecules may initially illicit the production of IgM antibodies which are pentamers and generally cause agglutinating or clumping of antigens which aids in their elimination from the body. Under certain conditions however lymphocytes may initiate “class switching” which is primarily regulated by T-cells as a result of the production or presence of small molecules known as cytokines. These cytokines direct naïve T cells to become either the Th2 phenotype or the Th1 phenotype. This is an important event in sensitization since only Th2 cells produce Interleukins IL- 4 and IL-5 which are the primary signaling mechanism which simulates the production of IgE. Th1 cell on the other hand produce IL-10 and interferon- γ which inhibits IgE production. The propensity of an individual to produce a balance of Th2 greater than Th1 is of great importance in producing an atopic (favorable) profile for the development of allergies and it is suspected that a wide variety of chemical and biological factors may influence this balance⁵¹.

Once an allergen has bound to two or more surface IgE molecules on a mast cell, degranulation is immediately triggered, releasing chemical mediators and other bio-active molecules with histamine, platelet-activating factor (PAF) and lower potency cysteinyl-leukotrienes (cys-LT) such as LTC₄ being the most well known⁵². Histamine and

LTC₄ are vasodilators and also cause bronchial constriction along with increased mucus production where as PAF triggers the activation of blood platelets and attracts other lymphocytes.

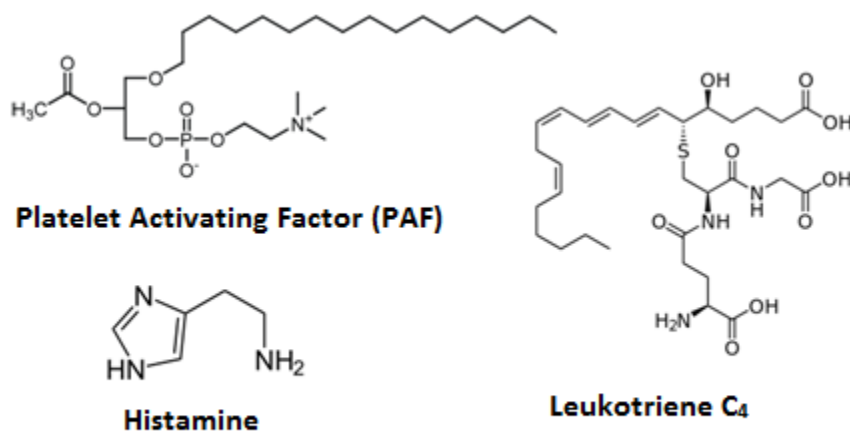


Figure 1.10. Chemical structures of select anaphylaxis mediators and biomarkers

In addition to this classical, IgE-mast cell driven event, alternative pathways and mechanisms which involve other lymphocytes and immunoglobulins may also contribute to the immune response^{52,53}. Figure 1.11 shows an overview of the three most commonly encountered lymphocyte-Ig mechanisms which arise during anaphylaxis. These events mark the early stages of anaphylaxis which is a term originally coined by Richet and Portier in 1902⁵⁴.

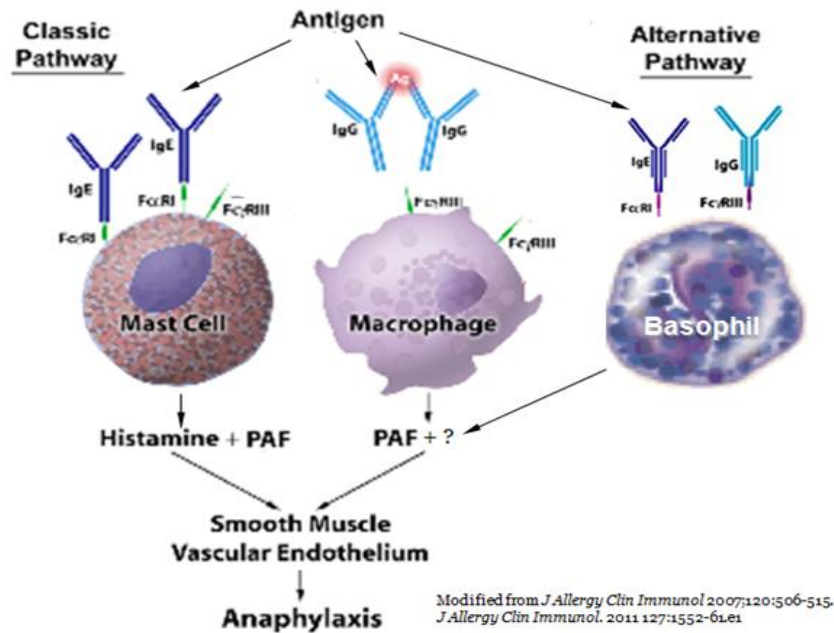


Figure 1.11. Common lymphocyte-Ig mechanisms which trigger anaphylaxis

There is no consensus on a definition of anaphylaxis. However, most proposed definitions involve the acute onset of one or more of the following symptoms:

1. Reaction of the skin or mucosal tissue
2. Respiratory compromise
3. Reduced blood pressure
4. Persistent gastrointestinal symptoms

Once other lymphocytes such as eosinophils arrive, the scavenging of the remains of mast cells begins; arachidonic acid and other phospholipids are released from the mast cell membrane. Scavenged arachidonic acid and LTC₄ are metabolized by the lipoxygenase and cyclooxygenase pathways, producing mediators such as LTD₄, LTE₄ and LTF₄ which are cysLT known to be up to 100x more potent vasodilators than histamine. This phase is referred to as late phase response. Since anaphylaxis is an

acute event, it is likely that small molecules which are quickly released or synthesized hold the most potential for indicators of anaphylaxis since larger molecules such as proteins and other polymer-based molecules will likely require too much time to be produced.

1.11. Anaphylaxis Mediators

Although researchers have been able to identify a number of biologically active metabolites which are released or produced during anaphylaxis which also fit the criteria as biomarkers, another level of bio-activity is possible namely anaphylaxis mediators. These are molecules which are directly responsible for inciting anaphylaxis⁵⁵. While histamine and the cysLT series of arachidonic acid metabolites have been demonstrated to have vaso-active properties, blocking their effects has a negligible effect on stopping the onset of anaphylaxis and their observed levels during anaphylaxis do not correlate to the severity of the attack. While these biomarkers have a limited capacity for diagnostic purposes they are not useful therapeutic targets. Anaphylactic mediators on the other hand, such as PAF directly cause anaphylaxis and blocking the receptors for PAF has shown to be effective in reducing the severity of an allergic attack⁵⁶.

For the study of anaphylaxis and allergy research, comprehensive metabolomics offers a number of specific advantages compared to other techniques. Metabolomics methods offer the ability to study not only metabolites which are endogenous but also

exogenous metabolites. Exogenous metabolites are especially important for allergy research since it is widely believed that hypersensitivity is not a natural response but is caused instead by external factors which cause the immune system to mount an inappropriate response. Metabolomics also has an advantage for allergy research due to its ability to describe the real-time chemical state of the system. In the case of allergic response and anaphylaxis changes occur rapidly and observing the changing chemical profiles during these events is likely to be important.

1.12 Thesis Objectives

The overall goal of this thesis at the outset was to develop practical liquid chromatography protocols which when coupled to electrospray mass spectrometry would afford improved metabolite coverage for comprehensive metabolomics applications. The second overall goal was to apply this approach to problems in allergy research. A summary of the specific objectives outlined in this thesis are:

1. To investigate of a variety of liquid chromatography columns and column combinations for use in metabolomics analysis,
2. To develop and validate liquid chromatography-mass spectrometry methods which would be appropriate for the simultaneous retention of a wide range of polar and non-polar metabolites with minimal ion suppression,
3. To develop robust experimental protocols for metabolomic studies of blood serum samples,

4. To utilize the developed LC-MS comprehensive metabolomics methods as a discovery tool for the identification of metabolites which may have adjuvant properties causing hypersensitivity to peanuts,
5. To utilize the developed LC-MS protocol to discover peanut-induced anaphylaxis biomarker and mediator candidates
6. To assess the suitability of comprehensive metabolomics as a diagnostic tool to determine whether peanut hypersensitivity exists in a mouse subject by the analysis of the subjects blood serum metabolome.
7. To assess metabolomic changes occurring in the blood serum of peanut allergic children after an oral peanut challenge

Chapter 2. Methods and Materials

2.1 Equipment and Chemicals

2.1.1 LC-ESI-TOF-MS instrumentation

Throughout this thesis the primary LC-MS system which was used was an Agilent 1200 “RR” series LC coupled to a Bruker micrOTOF II time-of-flight mass spectrometer (~10k FWHM resolution) equipped with an Agilent electrospray ionization source setup in an orthogonal configuration. Mass calibration was performed by internal calibration with sodium formate clusters using the enhanced quadratic calibration algorithm (Bruker DataAnalysis®) to obtain mass accuracies of approximately 1-3 ppm. In addition to the primary system, a Dionex 3000 RS series LC coupled to a Bruker Maxis 4D ultra-high resolution QTOF (~60k FWHM resolution) was used for high resolution and MS/MS measurements (refer to section 2.10).

The seven 2.1x50mm LC columns utilized in this thesis were: LUNA Aminopropyl (Phenomenex, Torrance CA, USA); Kinetix HILIC (unmodified silica) (Phenomenex); ZIC HILIC Sulfonylebetaine (SeQuant, Umeå, Sweden); Diamond hydride type “C” silica (Cogent, Eatontown NJ, USA); Kinetix PFP (Pentafluorophenyl) (Phenomenex); RP-Amide (Halo, Wilmington DE, USA); Kinetix XB-C18 ((Phenomenex). Column details are listed in Table 2.1. A pre-column filter (0.2µm) was also used with each column or column set.

Table 2.1. LC Columns Investigated and Column Details

Column type	Primary Separation Mechanism	Dimensions	Particle size/type
Aminopropyl	HILIC	2.1 x 50 mm	3µm / fully porous
Silica	HILIC	2.1 x 50 mm	2.7µm / core shell
Sulfonylbetaine	HILIC	2.1 x 50 mm	3µm / fully porous
Silica hydride	Aqueous Normal Phase	2.1 x 50 mm	4µm / fully porous
Perfluorophenyl	Reversed Phase	2.1 x 50 mm	2.7µm / core shell
RP-amide	Reversed Phase	2.1 x 50 mm	2.7µm / core shell
XB-C18	Reversed Phase	2.1 x 50 mm	2.7µm / core shell

2.1.2. Other Instrumentation

For all methods, chemical standards were weighed on a Mettler AC 100 series analytical balance and pH of the aqueous LC mobile phases was measured with a pH209 series benchtop pH meter. For methods requiring the pelleting of precipitated materials an Eppendorf 5414R chilled centrifuge was used.

2.2. Liquid Chromatography Mobile Phases and Extraction Solvents

For all LC-MS methods, mobile phase solvents were HPLC grade or higher including acetonitrile, water and methanol. The aqueous mobile phase used for all experiments was prepared using ammonium acetate (Caledon; Georgetown ON.) and concentrated formic acid (Fisher Scientific; Ottawa ON.). Extraction solvents used for blood plasma and serum analysis were HPLC grade methanol and ethanol (Caledon).

2.3. Chemical Standards

Isotopically labeled amino acids, L-phenylalanine-d₈, L-methionine-d₃ and L-tryptophan-d₅, were obtained from Cambridge Isotope Laboratories (Andover MA, USA) and the cystenyl-leukotrienes C₄,D₄,E₄,F₄ and N-acetyl-E₄ were obtained as a mixed solution in ethanol from Cayman Chemical (Ann Arbor MI, USA). All other chemical standards used in this work were obtained from Sigma-Aldrich (St. Louis, MO, USA). A full listing of all chemical standards used may be found in Appendix 1.

2.4. LC Gradients and MS Parameters

For determination of orthogonality between columns, two LC gradients were used at a flow rate of 200µL/minute with a column temperature of 50°C. Mobile phase A was acetonitrile and mobile phase B was 5mM ammonium acetate with formic acid added until pH 3 was reached. A “HILIC style” gradient began at 95%A with a linear gradient to 35%A over 10 minutes, a hold at 35%A for 3 minutes followed by a linear increase to 95%A over one minute. Equilibration was done for a period equaling 15 column volumes of solvent. A “RP style” gradient was used beginning at 15%A with a linear gradient to 85%A over 10 minutes, a hold at 85%A for 3 minutes followed by a linear decrease to 15%A over one minute and hold at 15%A for a re-equilibration period equaling 15 column volumes of solvent.

All injections were 2µL in volume and two separate chromatograms were obtained under positive and negative ionization modes. Relevant MS conditions for the

column orthogonality experiment used a mass range of 50-1000 m/z with a scan rate of 2 Hz, a nebulizing gas pressure (N₂) of 3 bar, a dry gas (N₂) flow rate of 6 L/minute and a chamber temperature of 250°C. The capillary potential for positive mode ionization was set at 4.5 kV and for negative mode at -3.8 kV.

For the analysis of blood serum extracts, the LC column set used were a SeQuant ZIC HILIC column (2.1x50mm) followed by a Halo RP-Amide column (2.1x50mm) coupled in series. Elution was carried out at 200µL/min at a column temperature of 50°C. The gradient used was “HILIC style” where solvent “A” was acetonitrile and solvent “B” was 10mM ammonium acetate brought to a pH of 3 by the addition of formic acid. Initial gradient conditions began at 95%A and holding at 95%A for 0.5 minutes followed by a linear decrease over 9.5 minutes to 30%A, a hold at 30%A for 5 minutes, then a linear increase to 95%A over 2 minutes. Between runs the columns were reequilibrated at 95%A for 13 minutes. MS detection was carried out over a mass range of 75-1000 m/z at an acquisition rate of 2 Hz, a drying gas (N₂) flow rate at 6 L/min, nebulizing gas pressure at 3.0 bar and a capillary potential of 4.5kV in positive mode and -3.8 kV in negative mode. All injections were 2µL (0.4µL serum equivalent injected on column). Injections of a pooled sample were carried out in pentuplicate prior to injections of individual samples, and after every 10th sample throughout the sample set then again in pentuplicate after the last sample to track instrumental performance throughout the analysis of a given sample set.

2.5. MS/MS Spectra Acquisition

The acquisition of MS/MS spectra was performed on a Bruker Maxis 4D ultra-high resolution QTOF (~60k FWHM) coupled to a Dionex 3000 RS UPLC. Mass calibration was performed by internal calibration with sodium formate ion clusters using the enhanced quadratic calibration algorithm to obtain mass accuracy of approximately 1-2 ppm. LC gradient conditions and columns were identical to those used for serum analysis. ESI settings for MS/MS were set at 3.5 kV for positive ion mode and -3.0 kV for negative ion mode with nebulizing gas and dry gas settings identical to those used in section 2.6. Collision energy for collisionally induced dissociation (CID) was set at 30 eV as default. In cases where a lower CID energy was more appropriate a collision energy of 10 eV was used.

2.6. Tandem Column Configuration

The instrumental configuration for tandem column analysis involved the serial connection of columns via a short length (~3cm) of PEEK tubing (0.005" i.d.). A diagram of the column configuration may be found in Figure 2.1.

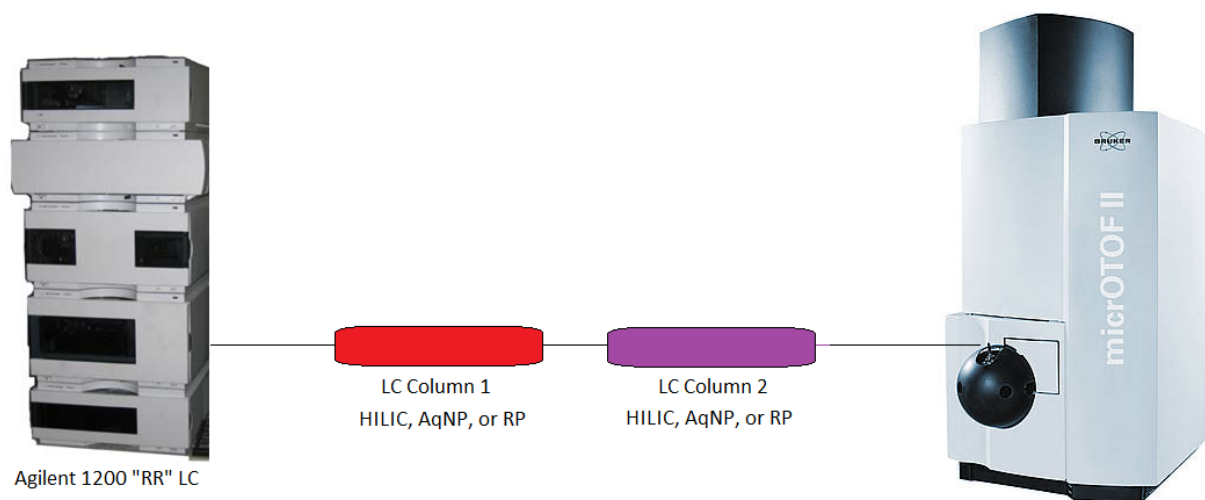


Figure 2.1. Instrumental setup for the tandem column configuration used in liquid chromatography-mass spectrometry experiments

2.7. Post Column Addition Experiments – Ion Suppression Determination

Post column addition was performed by continuous infusion of a 15 μ M solution of L-phenylalanine- d_8 in methanol at 5 μ L/min using a Hamilton syringe pump via a T-joint inserted after the columns and prior to the ESI source. All other LC-MS conditions were identical to those used for the determination of column orthogonality experiments.

2.8. Data Alignment, Preprocessing, and Extraction

Prior to analysis, raw data collected from LC-ESI-TOF-MS experiments was processed using the open source program XCMS (Scripps Institute for Metabolomics).

This software aligned peaks in a set of chromatograms, extracted and integrated chromatographic features. After data alignment, extraction and integration, the XCMS companion software package called CAMERA (Scripps Institute for Metabolomics) was used to identify isotope signals and to identify ion adduct peaks and in-source fragmentation peaks. The areas of integrated peaks were then compared to peak areas of an internal standard (glycyl-phenylalanine) to obtain relative peak areas for both the positive ion and negative ion modes. Full XCMS parameters used for data extraction and peak alignment may be found in Appendix 2.

2.9. Criteria for Metabolite Identification

Criteria outlined in Sumner et al. was used as the basis for identification of metabolites¹⁷. In cases where authentic chemical standards were available, metabolite identification was confirmed by comparing the accurate mass values, chromatographic retention times, and MS/MS spectra between the peak found in the sample with the corresponding features of the authentic standard. Where authentic chemical standards were not available, metabolite identification was based on accurate mass measurements, observed isotopic ratios, and reported MS/MS spectra found in publically available databases such as METLIN (Scripps Institute) and the Human Metabolomic Database (Genome Canada/University of Alberta).

2.10. Statistical Analysis

Principal component analysis (PCA) and orthogonal partial least squares-discriminate analysis (OPLS-DA) were performed using the data analysis software package SIMCA P+ (version 12.0.1.0). For all analyses unit variance scaling with a 1/square root block weight was applied. Student's t-test and analysis of variance (ANOVA) statistical analyses were performed using Microsoft Excel. Student's t-test calculations assumed a 2-tail distribution with heteroscedastic scattering. ANOVA was done with 2-factor (2-way) with replication.

2.11. Peanut Sensitization Protocol and Intraperitoneal Challenge

Female C57BL/6 mice (6-8 weeks old) were sensitized to peanuts by oral gavage treatment weekly with 1 mg peanut protein from Kraft peanut butter⁵⁷ and 10 μ g cholera toxin (List Biological Laboratories) in 100 μ L of sterile water. The complete treatment schedule required four weeks and is summarized graphically in Figure 2.2. Oral gavages were done using intragastric feeding needles (#01-290-2B; Fisher Scientific). Intraperitoneal challenge was performed by injecting 5 mg of crude peanut extract (Greer Laboratories) in 500 μ L of PBS into the peritoneal cavity. After challenge, the core body temperature of the mice was monitored using a rectal probe.

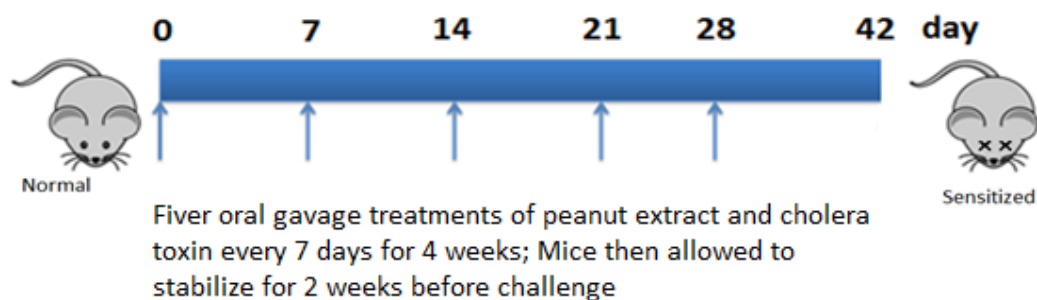


Figure 2.2 Treatment schedule for the sensitization of mice to peanut protein

2.12. Blood Sample Collection, Preparation, and Extraction

For experiments involving mice, whole blood was obtained by retro-orbital bleeding of anesthetized mice by puncture of the ocular vein with a glass capillary tube. For human subjects, blood was collected by venipuncture. For the preparation of blood serum, whole blood was allowed to clot at room temperature for ~15 minutes whereupon the clear fluid was separated from the solid clot and other blood cells by centrifugation at 5000 x g at a temperature of 4°C. For the preparation of blood plasma, whole blood was either collected in EDTA-treated collection tubes in the case of human blood or whole blood was centrifuged immediately at 5000 x g, 4°C in the case of mouse samples before clotting.

Precipitation of blood plasma/serum proteins and extraction of metabolites was performed by the addition of a 50:50 v/v solution of methanol:ethanol with a solvent to plasma/serum ratio of 4:1 as per Bruce et al.⁵⁸ and vortexed for 2 minutes. Typically 120µL of MeOH:EtOH was added to 30µL of serum/plasma. This alcohol/serum mixture

was then immediately centrifuged at 5000 x g at 4°C for 10 minutes resulting in a clear supernant with a well packed protein pellet. Typically, ~140µL of supernate was removed and flash frozen in liquid nitrogen. Samples were stored at -80°C until LC-MS analyses were performed.

Chapter 3. LC-MS Method Development

3.1. Method Development Considerations and Challenges

Comprehensive metabolomic studies present the analyst with a variety of analytical challenges.^{59,60} The wide range of chemical and physical properties of chemical species in biological matrices present significant challenges for any chromatographic system. Second, the enormous range of metabolite concentrations, typically over 12-14 orders of magnitude far exceeds the linear dynamic range of any modern detection system. While ESI-MS continues to be the most popular platform for the comprehensive analysis of biomolecules, this ionization method has some limitations which restrict its ability and capability for quantitative or semi-quantitative analyses.

ESI exhibits a very wide range of relative response factors (RRF) for analytes; for example, the RRF for alanine is approximately 100-fold less than for phenylalanine due to chemical properties such as hydrophobicity and molecular volume.³⁸ ESI also struggles to ionize inherently neutral molecules efficiently such as sugars compared to compounds with functional groups which are easily ionized.

Finally, ion suppression which is often discussed but rarely addressed with direct experimentation represents the “Achilles heel” of ESI. Indeed ion suppression may have a serious impact on the observed signal intensity and because of this, the total ionic strength of the solution must be kept as low as possible to prevent falsely low signals.

This suppression effect is especially common in methods using direct infusion or flow injection analysis. Ion suppression results in a loss in mass accuracy and response linearity^{40,61}. A widely accepted approach to limiting the impact of matrix interferences is the use of a front end separation platform prior to ESI-MS detection.

Currently, LC-based separations are the most widely used platforms prior to ESI-MS analysis^{26,32,41,62,63}; unfortunately, no single LC column is capable of retaining and separating all metabolite classes which range from highly polar and charged water-soluble compounds to extremely non-polar compounds such as some lipids. The selection of an appropriate LC column from the wide array of available column types and selectivities is daunting since in non-targeted analysis it is not known which compound types will emerge as the most important species in a given system or study.

A common approach to the problem of dealing with a wide range of analyte polarities has been to use two (or more) modes of chromatography (e.g., reversed phase, hydrophilic interaction, ion exchange, etc.) or to use columns with different selectivities and then analyze samples or sample fractions on each column individually. Performing multiple analyses can be an effective strategy; however it is impractical when analyzing large numbers of samples or samples of wide range of analyte types.

An approach used in both small molecule analysis and proteomics is the use of comprehensive two-dimensional LC analysis where the eluent from one column is collected in a sample loop and then injected onto a second column exhibiting different

separation properties⁶⁴⁻⁷². While some of these reports are alternatively named “coupled column chromatography”, they all require specialized, complex equipment such as dual pumping systems and complicated valve setups which are either not commonly found in most laboratories or are beyond the capabilities of less experienced users. Another disadvantage common in many of these approaches is that considerable sample dilution can occur depending on the differences in flow rates between the two pumping systems⁷². Finally, software to effectively deal with the visualization of these data sets has only become available recently.

A less studied but possibly effective alternative to 2D-LC is the use mixed-bed columns containing two or more types of chromatographic packings in a single column yielding different selectivities^{73,74}; while mixed bed columns hold promise regarding their ability to separate a much wider range of compound classes, a major obstacle to adopting mixed bed columns is the lack of equipment and expertise to pack such columns reproducibly at the standard research lab level.

The successes of some mixed bed LC column approaches inspired us to explore the potential of linking two LC columns in series such that the paired columns would have different selectivities and could be used with a single LC gradient system using a conventional LC-MS system. An obvious LC column combination would be a reversed phase column coupled with a normal phase column. Normal phase chromatography

typically uses solvents such as hexanes and dichloromethane which, in addition to being immiscible with aqueous mobile phases are not suitable for ESI-MS.

We were attracted to the potential of pairing hydrophilic interaction (HILIC) columns with reversed phase columns owing to the effectiveness of HILIC phases in the separation of polar components and the effectiveness of partition chromatography in the separation of non-polar compounds. We also sought to explore the use of aqueous normal phase (AqNP) chromatography which has enjoyed recent successes in metabolomics applications^{47,75}. Solvent compatibility would not be an issue since these column types can be operated with solvents such as methanol or acetonitrile and water.

Multiples of the same column or very similar columns have been linked together to create a much longer LC column^{65,76–78}; however, this work is the first report of directly linking two orthogonal columns without employing a second pumping system to change the solvent composition prior to separation on the second phase. It should be noted that this approach is not intended to provide “optimal” LC peak capacities; rather, it is intended to provide optimal ESI-MS conditions by reducing the total numbers of metabolites entering the ESI source at any one time. The reduction of the total numbers of metabolites entering the ESI source should also reduce the degree of ion suppression observed, especially in the region near the void volume.

To demonstrate the potential of this proposed methodology for the untargeted analysis of blood plasma/serum samples, we first examined both mixtures of metabolite

standards encompassing a wide range of chemical properties and then examined a pooled blood serum sample taken from over 100 wild type mice. The separations afforded by seven columns encompassing the three most widely used separation modes in untargeted metabolomic analysis were RP, HILIC, and AqNP columns were determined and suitable tandem column combinations were proposed. Next, the analytical advantages of using columns in tandem were assessed based on the total degree of retention observed for components in the pooled mouse serum extract and on the relative amount of ion suppression across the chromatogram based on post-column addition experiments.

Beyond the analytical challenges of comprehensive metabolomics, another factor which was addressed in this work was to evaluate which type of blood fluid preparation, namely serum or plasma would be the most appropriate for the study of peanut allergies. To determine this, a previously reported extraction procedure for plasma which has been proven to remove at least 99% of all protein while still offering good metabolite recovery for both polar and non-polar metabolites⁵⁸ was used on both plasma and serum samples originating from the same whole blood sample.

3.2. Results

3.2.1. Initial Screening of LC Columns and Determination of Column Orthogonality

To begin the initial screening of which LC columns would hold the most promise for comprehensive metabolomic analysis and for use in tandem column configurations a

set of 100 metabolite standards in an ethanol:methanol:water solution (2:2:1), similar to the composition of the blood plasma/serum extraction solution, was injected in triplicate on each column using both HILIC and RP type gradients (Section 2.4). These standards are listed in Appendix 1 and were chosen to encompass 12 metabolite classes representing both polar and non-polar compounds. Based on the measured retention times of all standards, the orthogonality between a pair of columns was assessed by calculation of Pearson product-moment correlation coefficients (r). The r value is a form of regression analysis measuring the linear dependence between two data sets (retention data) as given by the formula given in equation 3.1.

$$r = \frac{n \sum xy - (\sum x)(\sum y)}{\sqrt{n \sum x^2 - (\sum x)^2} \sqrt{n \sum y^2 - (\sum y)^2}}$$

Equation 3.1 Pearson product-moment correlation coefficient

Pairings showing an r value of ± 1 are considered a perfect correlation where all data points in a scatter plot lie exactly on a linear line with either positive or negative slope as indicated by the positive or negative value. Values between 1.0 to 0.8 (and -1.0 to -0.8) are considered to be strongly correlated, values between ± 0.8 and ± 0.5 are described as weakly correlated and values less than ± 0.3 are described as non-correlated (good orthogonality). Table 3.1 outlines the calculated orthogonality as per their Pearson number for the studied columns and Figure 3.1 shows selected scatter plots of the observed k' between the columns.

Table 3.1. Pearson Correlation Coefficients Between HILIC, AqNP and RP Columns

Column Type	Silica	Aminopropyl	Sulfonyl-Betaine (ZIC)	Silica Hydride	PFP	C18
Aminopropyl	0.422	-	-	-	-	-
Sulfonylbetaine (ZIC)	0.803	0.610				
Silica Hydride	0.851	0.509	0.807	-0.416	0.716	-
PFP	0.168	0.490	0.173			
C18	-0.089	-0.565	-0.234	-0.280		
RP-Amide	-0.248	-0.485	-0.244	-0.408	0.735	0.504

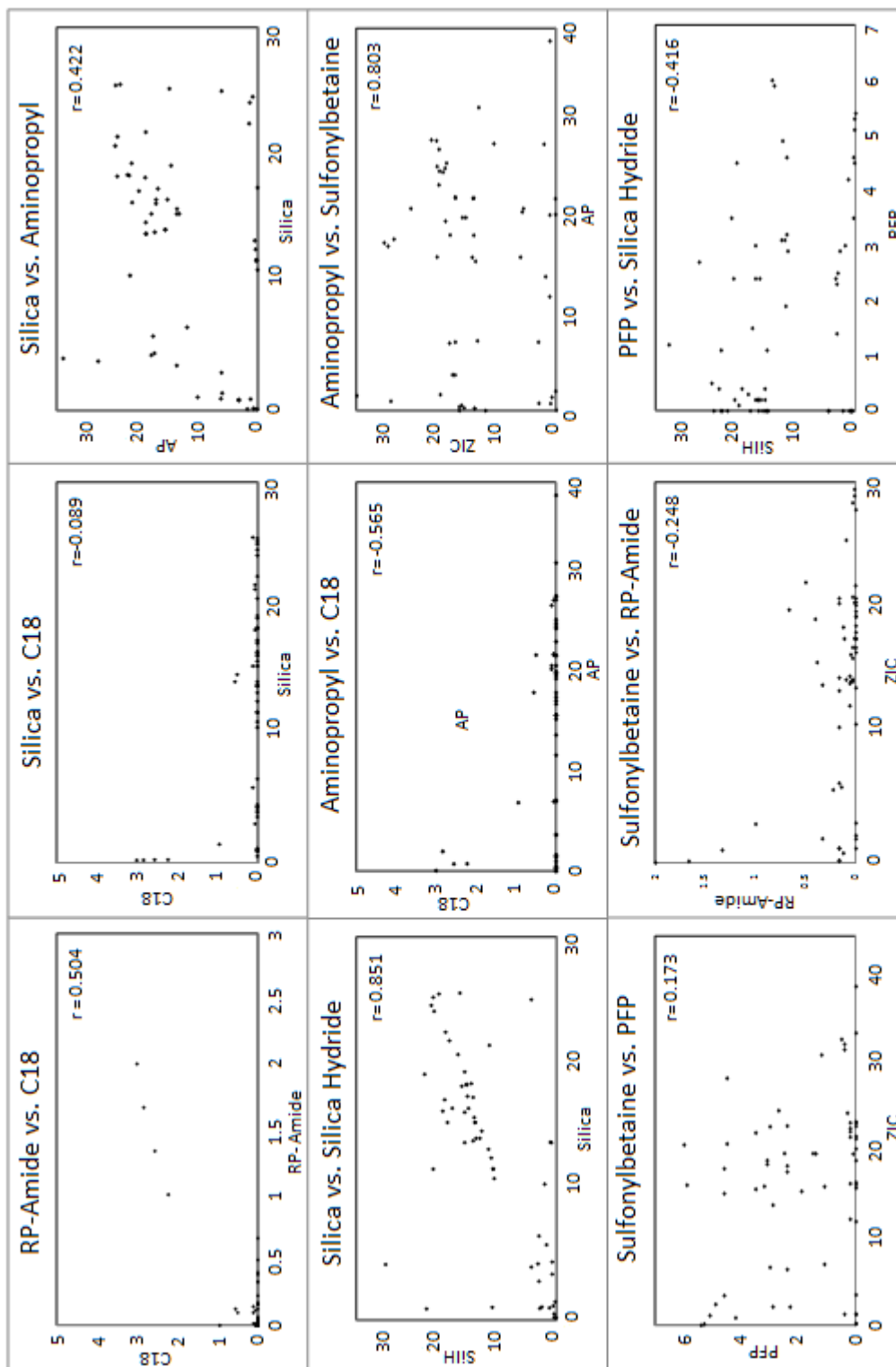


Figure 3.1. Pair-wise comparison of relative retention (k') of 100 metabolite standards on seven LC stationary phases under HILIC gradient conditions (Note different k' and r values represented on each panel).

3.2.2. Determination of Ion Suppression Observed with Blood Serum Extract

Ion suppression/enhancement can be a serious issue in the LC-MS analysis of complex biological samples due to loss of linearity in response for affected analytes⁷⁹. To determine the chromatographic regions where ion suppression was a factor in the analysis of blood serum extract, post-column addition experiments were performed for analyses on each column and with a selection of column combinations exhibiting at least some degree of orthogonality under both HILIC and reversed phase gradient elution conditions. Figures 3.2 and 3.3 shows the intensity of the $[M+H]^+$ ion of phenylalanine- d_8 that had been infused post column during analyses on the silica column alone, the PFP column alone and the silica-PFP combination in positive ion mode scaled by retention factor and retention time respectively. Decreases in signal intensity of the $[M+H]^+$ ion are an indication of ion suppression.

Ion suppression was observed early in the chromatograms of all columns and column combinations between apparent k' values of 0 and up to 4, depending on the column and the column combination. Ion suppression was also observed later in the chromatograms of some individual columns (e.g., silica only and PFP only chromatograms in Figures 3.2 and 3.3). However, when two columns were coupled in series (e.g., silica followed by PFP), the degree of ion

suppression was significantly reduced and was only observed early in the chromatograms. The regions of ion suppression for each column and column combination under both HILIC and reversed phase gradient elution conditions are summarized in Table 3.2 and illustrated in Figure 3.4.

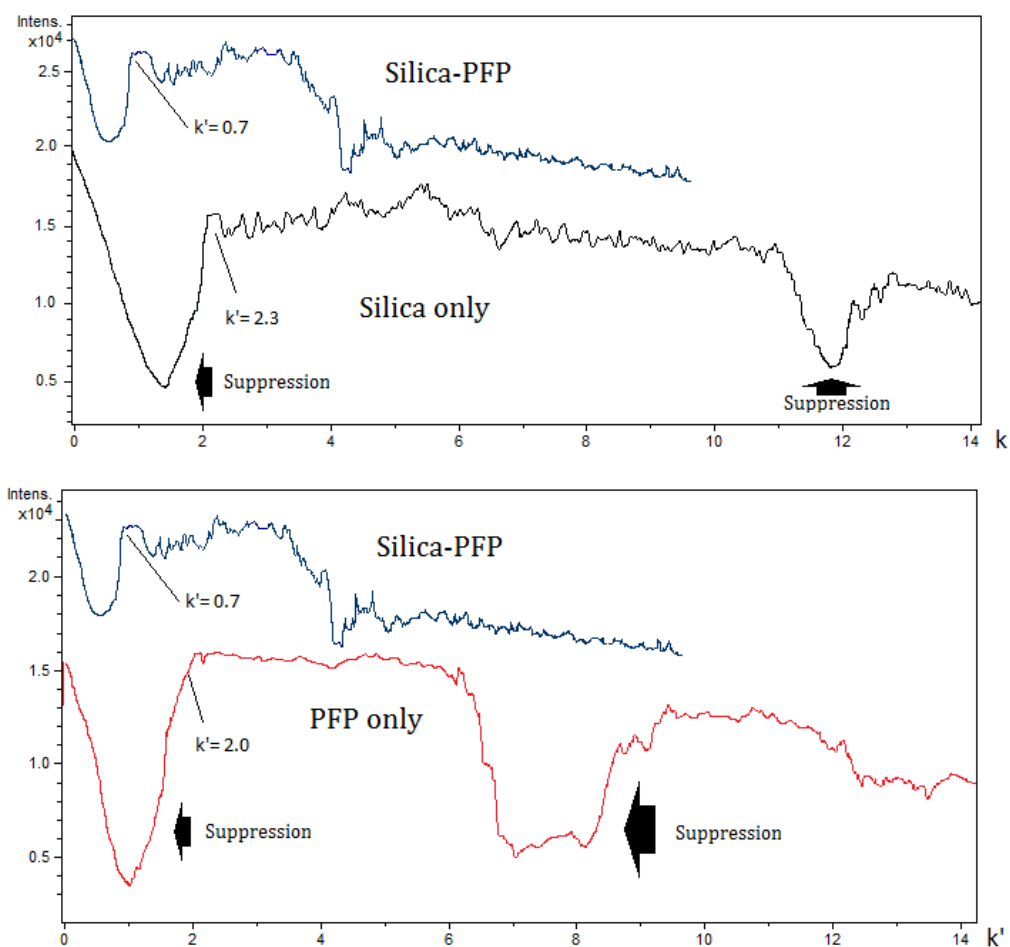


Figure 3.2. Mass chromatogram scaled by retention factor (k') of the $[M+H]^+$ ion of L-Phenylalanine- d_8 added post column following the separation of mouse serum on silica and PFP columns alone and a silica-PFP column combination in positive ion mode using "HILIC style" gradient.

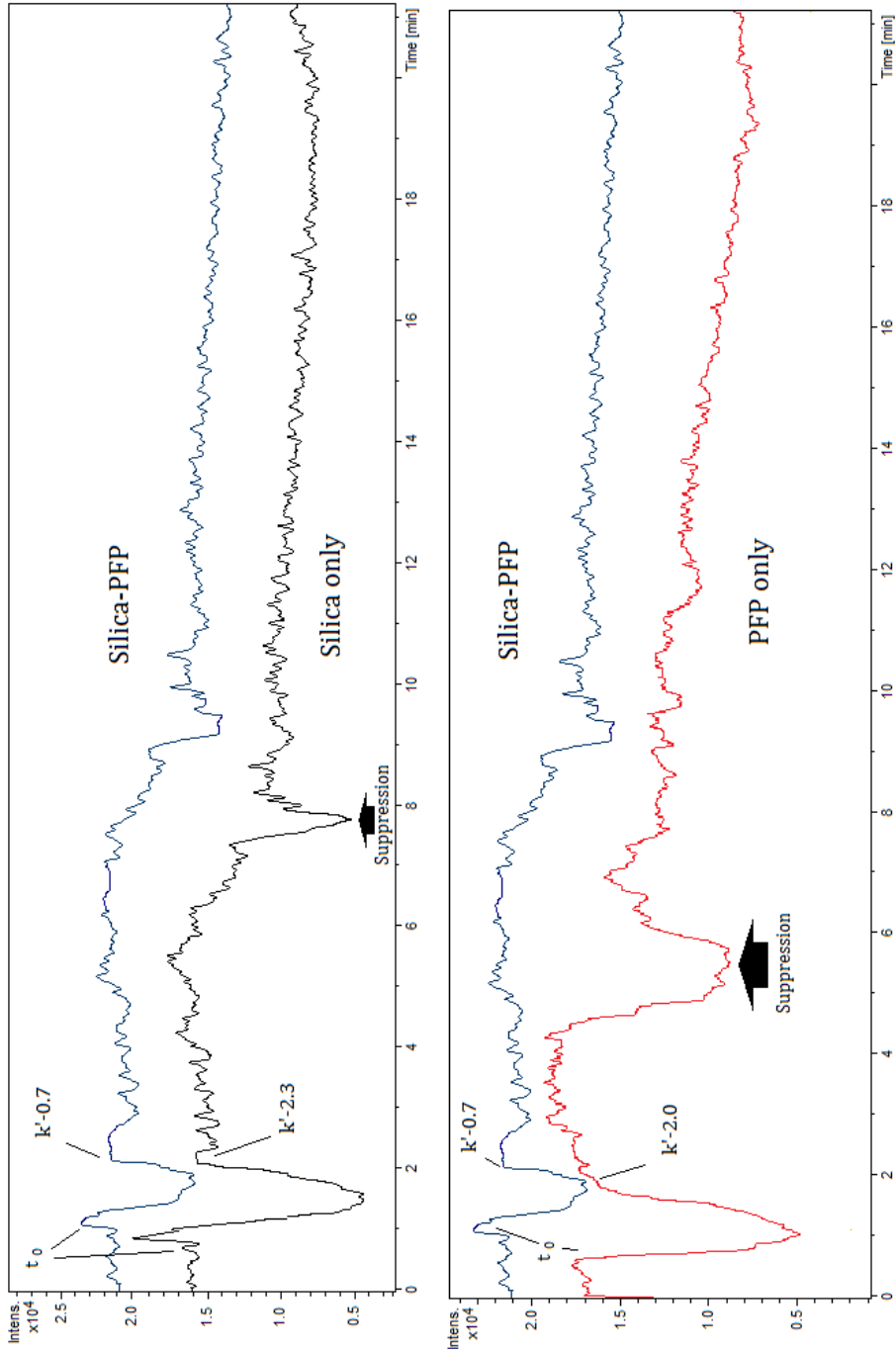


Figure 3.3. Mass chromatogram scaled by retention time of the $[M+H]^+$ ion of L-Phenylalanine- d_8 added post-column following the separation of mouse serum on silica and PFP columns alone and a silica-PFP column combination in positive ion mode using "HILIC" style gradient

Table 3.2. Summary of regions where ion suppression was observed for various columns and column combinations under HILIC and reversed phase gradient elution conditions.

Column or Column Combination	t_0 (min)	Early Ion Suppression Region (min)	Early Ion Suppression Region (k')	Other Region of Ion Suppression (min)
Sulfonylbetaine (ZIC)	0.7	Both modes, 0.7-2.0	Both modes $k'=0-1.8$	7.5-7.8 min (HILIC mode)
Amide	0.6	Both modes, 0.6-2.3	Both modes, $k'=0-2.8$	None
Silica	0.6	HILIC, 0.6-2.0 RP, 0.6-2.3	HILIC, $k'=0-2.3$ RP, $k'=0-2.8$	7.4-8.0 min (HILIC mode)
PFP	0.6	HILIC, 0.6-1.8 RP, 0.6-1.6	HILIC, $k'=0-2.0$ RP, $k'=0-1.7$	4.4-6.0 min (HILIC mode)
Silica Hydride	0.8	Both modes, 0.8-1.7	Both modes, $k'=0-1.1$	none
C18	0.6	Both modes, 0.6-2.2	Both modes, $k'=0-2.7$	none
Aminopropyl	0.7	HILIC, 0.7-4.0 RP, 0.7-3.6	HILIC, $k'=0-4.7$ RP, $k'=0-4.1$	none
ZIC-Amide	1.3	Both modes, 1.3-2.2	Both modes, $k'=0-0.7$	none
Amide-ZIC	1.3	Both modes, 1.3-2.2	Both modes, $k'=0-0.7$	none
Silica-PFP	1.3	Both modes, 1.3-2.1	Both modes, $k'=0-0.7$	none
Silica Hydride-C18	1.4	Both modes, 1.4-2.7	Both modes, $k'=0-0.9$	none
Aminopropyl-C18	1.3	Both modes, 1.3-3.4	Both modes, $k'=0-1.6$	none

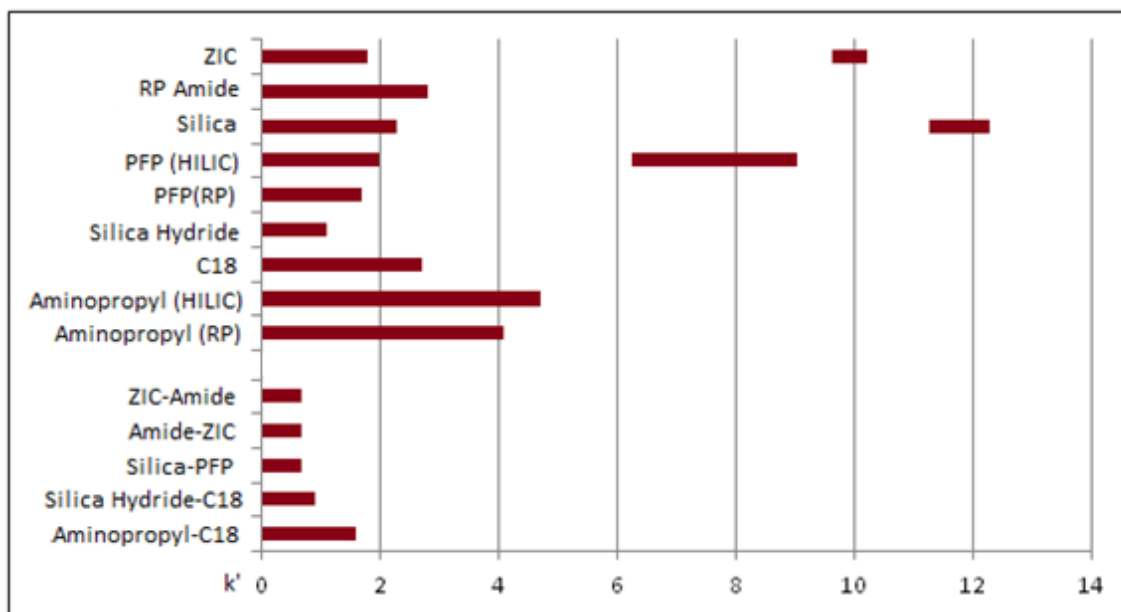


Figure 3.4. Regions of ion suppression observed in chromatograms by post column addition. All individual columns and select select column combinations are shown.

3.2.3. Evaluation of Retention Properties of Single Columns Compared to Columns Operated in Tandem

To evaluate whether the tandem column approach would increase the retention of both polar and non-polar substances, the 100 metabolite standards used in the orthogonality determination experiments were spiked into a pooled mouse serum extract. The chromatographic performance of these metabolites along with a large number of other serum metabolites were evaluated using three orthogonal column combinations. Figure 3.5 shows superimposed extracted ion chromatograms (EIC) for a number of metabolite standards on the ZIC HILIC column, the RP amide column and the ZIC-RP amide tandem combination. The ZIC HILIC column was observed to retain and

separate polar, hydrophilic metabolites quite well. Lipid soluble fatty acids, leukotrienes and lyso-phosphatylethanolamines, on the other hand, were observed to elute near the dead volume (t_0) where significant ion suppression was known to occur (Table 3.2).

Conversely, the reversed phase column retained the lipids well, even when using a HILIC style gradient but did not retain the polar compounds to a significant degree, regardless of the gradient type. Many polar compounds eluted near the dead volume on each RP column and were not detected in the serum extract due to severe suppression in that region. When the two columns were coupled in series and run under HILIC gradient conditions, both classes of substances were retained and eluted in regions of the chromatogram ($k' > 1$) where there was negligible ion suppression. The peak widths using the coupled columns were similar to the peak widths observed on either of the individual columns. In simple terms, chromatographic retention was good for all classes of compounds with little or no loss of chromatographic performance.

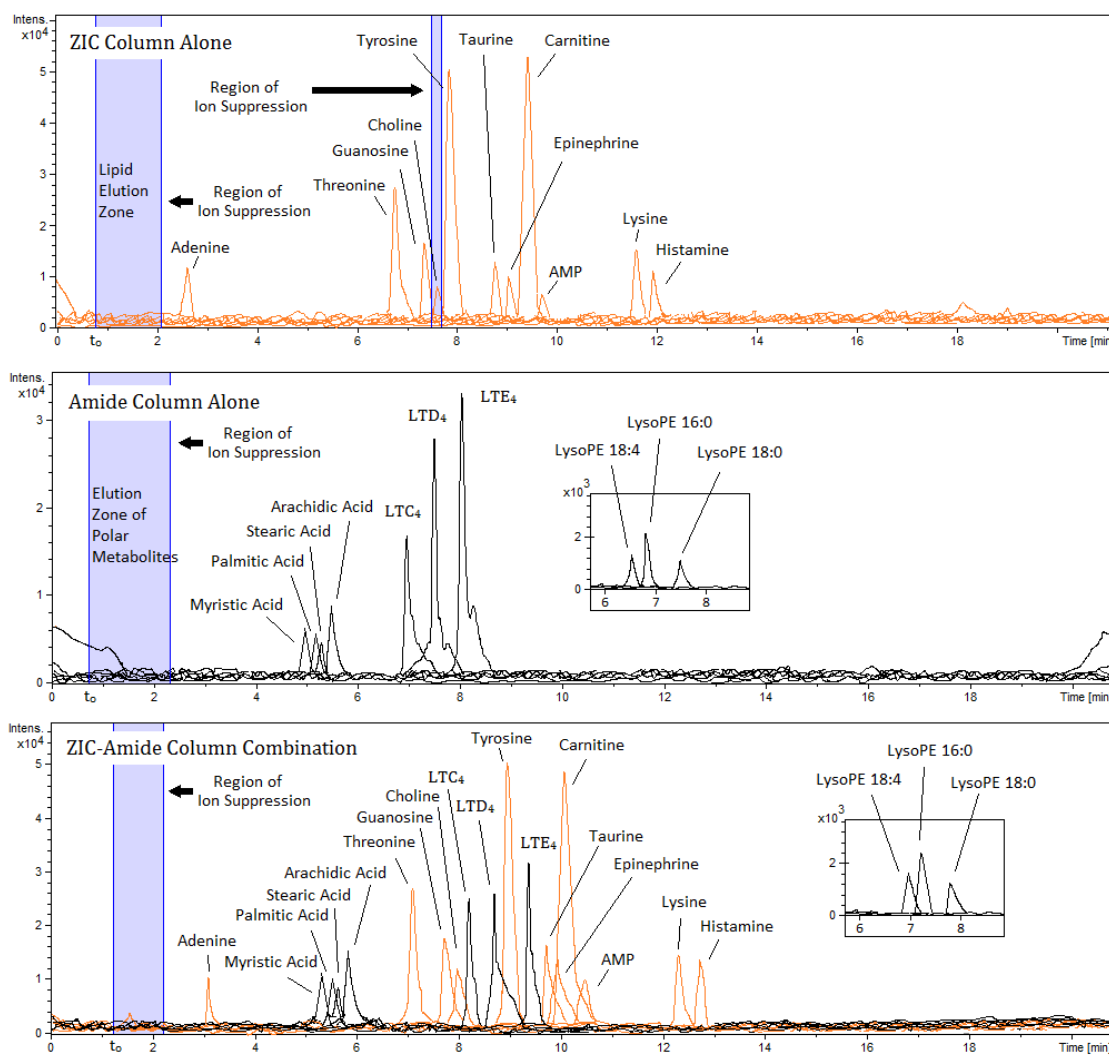


Figure 3.5. Retention of a variety of polar metabolites on the ZIC column alone (top panel), the retention of non-polar metabolites on RP-amide column alone (middle panel) and on the ZIC-amide combination under HILIC gradient conditions (bottom panel). Measurements of authentic chemical standards confirmed that polars eluted in dead volume of RP column and non-polars eluted in dead volume of HILIC column. Regions of ion suppression have been shaded.

3.2.4. Total Feature Retention

Due to the wide array of possible column-solute interactions available with two different column types, more substances in a complex mixture should be retained using the tandem column approach compared to using a single column alone. To evaluate this hypothesis quantitatively, the total number of unique mass spectral features that could be identified in a pooled mouse serum sample was determined using XCMS and CAMERA. It was decided to use a minimum signal-to-noise ratio greater than 10. These data are summarized in Table 3.3.

Table 3.3. Numbers of mass spectral features detected in a pooled mouse serum sample following analysis on various LC columns and column pairings. Columns were run using either a “HILIC gradient” or a “reversed phase gradient” (see materials and methods).

Individual Column	Number of features (HILIC gradient)	Number of features (RP Gradient)	Column Pairing	Number of features (HILIC gradient)	Number of features (RP Gradient)
ZIC	1932	659	Amide-ZIC	2770	2692
Amide	993	2195	ZIC-Amide	2661	2782
PFP	1925	2451	Silica-PFP	3073	2609
Silica	2373	932			
SilH	2376	1954	SilH-C18	2893	2471
C18	1177	2369			
AP	1394	456	AP-C18	1227	2397

ZIC= Sulfonylbetaine; PFP= perfluorophenyl; SilH= Silica Hydride; AP= Aminopropyl

Each chromatographic data set was evaluated in an identical fashion using XCMS to align peaks; redundant peaks (isotope peaks, adduct ions, in-source fragments, etc.) were eliminated from each data set using the annotation package CAMERA. The total number of unique mass spectral features detected ranged from 456 (aminopropyl column alone in reversed phase mode) to 3073 (silica-PFP combination under HILIC gradient conditions). In all cases the number of mass spectral features reported were those features that were not in regions of the chromatogram which were affected by ion suppression (see Table 3.2). Overall, the tandem columns resulted in the detection of more mass spectral features than any single column under either the HILIC or reversed phase gradient elution conditions. There are two key factors responsible for this increase in the number of quantifiable features: first, the ion suppression zone in tandem column combinations is significantly narrower than for each column on its own; second, the tandem columns afford increased retention of analytes into regions with no ion suppression.

3.2.5. Retention Time Reproducibility

In order to assess the retention time reproducibility, all 100 serum samples which were used to make up a single pooled sample were injected onto the ZIC HILIC-RP Amide column combination over a period of 3 days; a typical time-frame for an assessment of retention reproducibility. Of the metabolite features which were detected in at least 80 samples (1695 total) a retention variation was found to be

between $\pm 2-5$ seconds over a 20 minute chromatographic run. These data are comparable to the inter-day and intra-day reproducibility normally observed with either single column. Moreover, this narrow range is well within the alignment capability of most software packages such as XCMS.

3.2.6. Comparison of Blood Serum vs. Blood Plasma

Comparison of samples prepared from blood plasma and blood serum is important because in many cases only one type of blood preparation is available. Experiments were conducted where whole blood samples from 10 mice were prepared as both plasma and as serum. Our concern was that some metabolite levels may change during the time required for clotting in the preparation of serum; Since plasma can be processed immediately, we were concerned that there may be slight differences between the two sample types. These plasma/serum samples were extracted and run in triplicate on the ZIC-RP amide column combination using the HILIC gradient. After peak alignment by XCMS, it was determined that greater than 99% of all features observed in plasma (~4000 between both ionization modes) were also observed in the serum equivalent. Student's t-test was performed on all peak areas of metabolite features extracted by XCMS. Over 95% of the normalized peak areas were found to be identical with a confidence level greater than 95% ($p > 0.05$) between the two sample sets.

Previous studies comparing plasma and serum demonstrated that while levels of some metabolites, especially lipids may be slightly higher or lower between the sample types, the overall reproducibility and reliability are equivalent^{28,80–82}.

3.3. Discussion

3.3.1. Ion Suppression Reduction

Ion suppression, a surprisingly common phenomenon in electrospray ionization mass spectrometric analyses, is due primarily to an overload of ions competing for limited space on the surface of sprayed droplets⁸³. The most effective strategy to eliminate ion suppression is to limit the total concentration of ions in the eluent going into ESI source by dilution or by separation⁸⁴. When ion suppression occurs, the resulting data is considered qualitative rather than quantitative since suppression results in a loss of linearity and/or accuracy⁸⁵. An unexpected yet welcome benefit of coupling HILIC and reversed phase columns in series was the significant reduction in ion suppression during chromatography, save for those components which elute with apparent k' values less than 1 and in some cases less than 0.7 (Figure 3.2). The hypothesis put forth in this work is that the complementary nature of paired columns results in the separation of the ion suppression-causing components retained on one column by the second column, such that the ionic strength of the eluent from the second column has been decreased sufficiently such that ion suppression is no longer observed. Between $k'=0$ and 1 many poorly retained components elute such that there

is significant ion suppression, likely due to the sheer number of components eluting simultaneously.

3.3.2. Tandem Column Retention Characteristics and Total Feature Detection in Blood Serum Extracts

The general retention characteristics of each column types can be described by their retention mode; HILIC phases retain polars and RP phases retain non-polars albeit each with different specific selectivities. Figure 3.5 demonstrates that operating two columns in tandem imparts the retention characteristics of both columns simultaneously resulting in retention of both compound types. It should be noted that the observed retention times of compounds shift by a time roughly equal to the volume required to carry it through the ineffective column. This observation precludes the possibility that the increase in retention is caused by the doubling in column length since the retention factor (k') effectively decreased.

The total number of mass spectral features observed in non-ion suppressed regions of the chromatograms with a S/N ratio above 10 increased about 20-30% when a HILIC column was coupled to a reversed phase column and eluted with a HILIC gradient (Table 3.3), compared to running either column alone. One notable exception to this trend was the coupling of an aminopropyl column to a reversed phase column. Aminopropyl columns are known to retain anionic compounds strongly, resulting in poor chromatographic performance⁸⁶. Similarly, when using the silica hydride column with

the C18 column a very modest increase of only 102 extra signals were observed with a RP gradient compared to the C18 alone. A possible explanation for this would be that since silica hydride has been shown to be quite effective in RP mode^{47,75} a number of compounds were retained to such a large degree that they did not elute during the programmed gradient and by the time they did elute the degree of broadening was so large that they could not be reliably detected with the minimum S/N ratio. Overall a 20-30% increase in the number of mass spectral features detected in any sample is significant, and is particularly useful in untargeted metabolomic investigations.

3.3.3. Column Order, Gradient Type, and Other Considerations

In theory the order in which two complementary columns are connected should not have a significant impact on the total number of features observed or on the degree of ion suppression since unretained material on the first column will pass quickly to the second. To confirm this, the ZIC and Amide column combination was tested with each in front of the other and the total number of features tallied. For elution with both types of gradient used, the number of features for both configurations were similar varying by less than 3% and the retention times of the common features varied between the two configurations by less than 2% indicating that the column order indeed has little impact on the retention characteristics.

While the order that the columns are connected may be arbitrary, the gradient profile may have a significant effect on the total number of features detected depending

on the columns used, especially when using the silica HILIC phase where the primary retention mechanism is based on partitioning into a fluid pseudo-stationary water layer as described by Alpert⁴⁵ where secondary interactions are minimal. In this case, using a HILIC-like gradient beginning at high organic composition has positive impacts since eluting with a high water composition minimizes the effectiveness of this column.

For functionalized HILIC columns such as the zwitterionic-sulfonylbetaine column (ZIC) which can retain based on secondary mechanisms such as ion exchange the effect seems to be minimal. Another well known advantage of using a HILIC-like gradient is that the high organic composition often leads to higher ionization efficiency due to the higher volatility of solvents such as acetonitrile and methanol compared to aqueous buffers. Overall, the conclusion that a HILIC-like gradient should be desirable compared to a typical RP like gradient when in use with ESI-MS.

Another consideration which must be made prior to column selection arises due to the tendency of certain columns to strongly or even irreversibly retain certain types of molecules or to have very poor performance characteristics. In lipid analysis, it is well known that many lipid classes such as triglycerides and cholesteryl esters are very strongly retained by C18 bonded phases rendering the required time for elution to be impractical. In these cases using a less hydrophobic column would be ideal. Similarly many amine-containing molecules are known to elute with poor peak shapes when using non-encapped silica-based columns rendering these types of column unsuitable

regardless of which orthogonal column is used in tandem. Due to these issues which are specific to each column type, care must be exercised in selecting columns to use in tandem since other factors beyond the orthogonality need to be considered.

3.4. Conclusions

When performing comprehensive metabolomic analyses of complex biological samples it is not possible to develop a truly “optimized” LC method due to the sheer number of substances and the diversity of their chemical properties. On the other hand, it is possible to utilize LC to ensure that the total ionic strength of the solution reaching the ESI-MS source at any one time is within a range where no ion suppression occurs. By using orthogonal columns in tandem, not only can the separation be increased relative to the capability of a single column but that ion suppression can be decreased and confined to a region where apparent capacity factors are less than 1. The result is that a greater number of mass spectral features can be quantified in a single analytical injection using simple setup with conventional LC equipment. In principle any HILIC column could be coupled with any reversed phase column to afford a combination that should have increased separation capabilities for complex biological samples compared to either the HILIC or the reversed phase column alone. For the work presented in the remainder of this thesis, the ZIC-RP Amide column combination using a HILIC gradient was used due to the high orthogonality between these columns, the low degree of ion

suppression observed with these columns operated in tandem, and the total numbers of unique features observed in the pooled blood serum sample.

Chapter 4. Metabolomic Analysis of Mice Undergoing Sensitization to Peanuts

4.1 Introduction

The preceding chapter outlined a novel LC-MS approach for the simultaneous screening of polar and non-polar metabolites in blood serum. As an application of this methodology, we chose to study the metabolomic effects on mice which have undergone a procedure to induce hypersensitivity to peanuts.

The vital questions to be addressed in this chapter are what metabolomic changes are occurring in the mice as sensitization process progresses and are these changes causing hypersensitivity. Another vital question to be addressed is whether changes at the metabolomic level are capable of diagnosing peanut allergies. To answer these questions, a series of mice were treated with peanuts and a known adjuvant, cholera toxin, and their metabolic profiles were compared to mice which were not hypersensitive to peanuts.

**Disclaimer: All work described in this chapter was approved by the Research Ethics Board of McMaster University. All animal handling/treatment procedures, clinical measurements of anaphylaxis and immunology experiments were performed by Joshua Kong; Dept. of Pathology and Molecular Medicine, McMaster University. Animal blood samples were processed by both the author and by Joshua Kong. All other work described in this chapter was performed by the author.*

4.1.1. Development of Peanut Hypersensitivity and the Role of Animal Models for Allergy Research

The maintenance of homeostasis (tolerance) to peanuts is dependent on complex interactions between foods and the immune system components which reside in the digestive tract⁸⁷. Under normal conditions, the interaction of peanut protein with the intestinal epithelium is harmless resulting in immune responses which promote tolerance. Alternatively, under certain special conditions immune system cells found in the gut such as dendritic cells may be stimulated and T regulatory cells may polarize, resulting in the production of immune-regulatory cytokines which, in turn, causes the production of antibodies that are specific to peanut protein; at this point the individual becomes hypersensitive to peanuts⁸⁸. Subsequent exposure to peanuts causes an inappropriate immune response which may lead to anaphylaxis. While a number of key cytokines such as interleukin-4 and interleukin-10 have been identified⁵¹, knowledge of what initially causes the immune cells to polarize and produce these cytokines is severely lacking.

Due to this knowledge gap, we sought to apply comprehensive metabolomics using LC-ESI-TOF-MS to study changes in the blood serum metabolome during development of hypersensitivity to peanuts. Since a study of human subjects that are in the process of becoming hypersensitive to peanuts would be nearly impossible to conduct, a well-characterized mouse model was used to simulate immune system activation.

Although animal models often have limitations, their use has led to major contributions to the general understanding of the tolerance versus sensitization paradigm, including the elucidation of mechanisms involved with intestinal anaphylaxis^{89,90} and pharmacological modulators of anaphylaxis⁵⁰. One obstacle to using an animal model is that most animals do not naturally develop hypersensitivity to peanuts⁹¹. In these cases an adjuvant must be administered along with the antigen (peanut) to illicit hypersensitivity. The most commonly used adjuvant in experimental immunology is cholera toxin (CT) due to its high capacity to activate the immune system⁹². While CT is not involved with sensitization in humans, it is a useful tool that has been shown to be a reliable and applicable surrogate in mice for inducing hypersensitivity to a wide array of antigens including peanuts⁵². Despite its wide-spread use, the mechanism of how CT invokes an inappropriate allergic response is still poorly understood⁹³.

4.1.2. Research Objectives

The overall plan for the work presented in this chapter is the determination of the comprehensive metabolomic profiles of mice undergoing artificially induced hypersensitivity to peanuts. Concurrent administration of peanut protein and cholera toxin to mice would induce this hypersensitivity. While considerable effort has been spent studying the proteomic and genomic aspects of the development of hypersensitivity, very little is known about hypersensitivity at the metabolite level. The

basic hypothesis of this work is that the metabolomic profiles of allergic subjects become altered during the sensitization process and that these altered metabolite levels are indicative of or result in biological outcomes that are markers of the immune system responses to peanut sensitization.

The discovery of the bio-active compounds which cause adjuvant effects or the metabolic pathways which are disturbed during sensitization would be a key step in improving our understanding of the mechanisms which are responsible for hypersensitization to allergens. An in-depth understanding of these mechanisms may also lead to clues pertaining to the question of why peanut allergy is so prevalent in some regions of the world but not in others and why peanut hypersensitivity is so persistent compared to other food allergies⁸⁷. Additionally, metabolomics may lead to a greater understanding of the mechanism of CT in its role as an immune system activator.

The two overall goals of the work in this chapter are as follows:

1. To assess the capability and utility of comprehensive metabolomics as a discovery tool for identification of key molecules and/or metabolic pathways involved in sensitization and,
2. To determine the diagnostic ability of comprehensive metabolomics in differentiating sensitized versus non-sensitized subjects based on their blood serum metabolite profiles.

4.2 Experimental Design

For the assessment of the metabolomic profiles found in sensitized mice, three separate experiments were carried out. A summary of each experiment may be found in Figure 4.1.

	Control Mice	# of Mice	Treated Mice	# of Mice
Experiment #1	No Pre-treatment	5	Pre-treatment for 6 weeks with PN + CT	5
Experiment #2	Pre-treatment with PN for 6 weeks	7	Pre-treatment for 6 weeks with PN + CT	7
Experiment # 3	Pre-treatment with phosphate buffer for 6 weeks (sampled every 2 weeks)	7	Pre-treatment for 6 weeks with PN + CT (sampled every 2 weeks)	7
	Pre-treatment with PN for 6 weeks (sampled every 2 weeks)	7	Pre-treatment for 6 weeks with CT (sampled every 2 weeks)	7

Figure 4.1. Summary of three experiments performed for the metabolomic analysis of mice undergoing sensitization to peanuts. PN= Peanut, CT= Cholera Toxin.

Each experiment included the analysis of pooled samples (i.e., an integrated sample composed of small aliquots of all individual samples) for the assessment of analytical reproducibility throughout the LC-MS analyses. Pooled samples were analyzed throughout the sample set in addition to blanks (see Section 2.4).

Experiment one involved the comparison of the blood serum metabolomes of five mice which were not treated (naïve mice) and of five mice treated with peanut extract and cholera toxin (sensitized) using the protocol outlined in Section 2.11. Serum samples were taken at the end of the six-week sensitization protocol.

Based on the results of this pilot experiment, a second experiment was carried out with a slightly larger number of mice per group (7 mice vs. 5 mice) to improve the statistical robustness. This experiment also compared the serum metabolomes of mice which had been treated with peanut extract by oral gavage with mice that received peanut and cholera toxin. The peanut only treatment was done to account for metabolomic changes that may occur due to the administration of peanuts. These serum samples were collected after the full six-week protocol had ended.

Finally, a third experiment was performed where the blood serum metabolomes were monitored in a comprehensive fashion, bi-weekly, throughout the sensitization protocol outlined in Section 2.11. In this third experiment, 28 mice were divided into four groups of seven mice each. Each group of seven were treated with one of the following: (1) an isotonic phosphate buffer at normal physiological pH (naïve), (2) a peanut extract solution only, (3) cholera toxin only, and finally (4) peanut extract with cholera toxin. The goals of this experiment were three-fold; first, to determine if the results of the previous experiments were reproducible and consistent; second, to determine whether changes due to the administration of cholera toxin along with both positive and negative controls (peanut and naïve mice); third, to monitor the metabolomic changes occurring in the mice during the sensitization period. These mice were bled every two weeks as summarized in Figure 4.2.

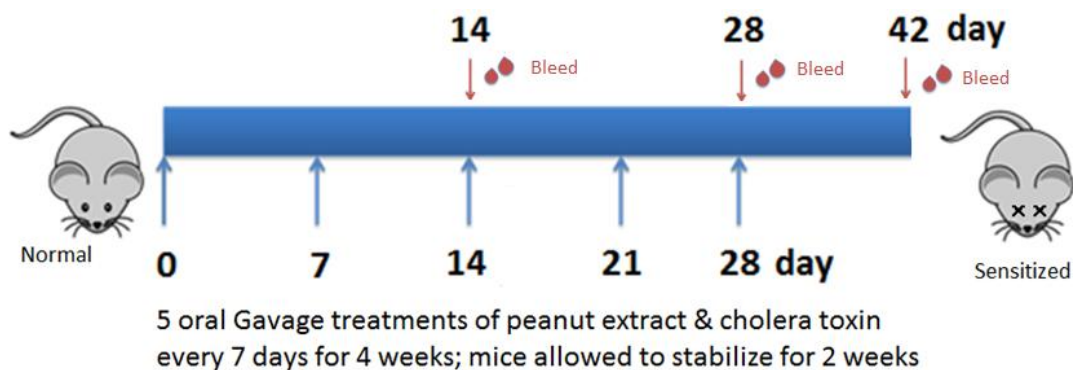


Figure 4.2. Gavage treatment schedule and bleeding schedule for metabolomic study of mice undergoing sensitization with peanut and cholera toxin.

4.3 Results

4.3.1. Experiment One: Metabolomic Profiles of Naïve Mice Compared to Sensitized Mice

To assess metabolomic differences between “healthy” (naïve) and “allergic” (sensitized) mice, the metabolite levels in the blood serum of 5 mice which had undergone peanut/cholera toxin sensitization were compared to 5 “naïve” mice which had not been treated. After blood sample collection, the ten mice were then challenged with an intraperitoneal injection of peanut extract. The sensitized mice were observed to undergo moderate to severe peanut-induced anaphylaxis based on clinical observations such as a decrease in core body temperature, an increase in hematocrit (percent volume of blood cells per total blood volume) and other behavioral hallmarks such as scratching. These observations were in contrast to the naïve mice which showed no clinical symptoms whatsoever. These results matched previous observations made

by the Jordana group in sensitized mice and provided a clear indication that mice that had been treated with peanut and cholera toxin were indeed sensitive to peanuts.

The blood samples of all ten mice were then extracted; aliquots of each sample were pooled and HILIC-RP LC-ESI-MS analyses were carried out as described in Section 2.4. The metabolite data obtained from these analyses were aligned, extracted and normalized using XCMS/CAMERA. The data were analyzed using OPLS-DA which allowed the comparison of the two treatments. The OPLS-DA analysis showed that pooled samples clustered tightly, indicating good instrumental reproducibility throughout the period of the analysis. Next, metabolite features which showed poor analytical reproducibility (RSD >20%) within the pooled sample replicates were removed. This was done due to the recommendations of Dunn et. al.⁹⁴ who determined that features with poor analytical reproducibility (>20%) coupled with their normal biological variability would be too unreliable for analysis. In this analysis approximately 100 features identified using XCMS fit the criteria for removal. After removal of these metabolite features with high analytical variability, the pooled sample data were removed from the data set. OPLS-DA analysis was then performed on the data from the ten samples (Figure 4.3).

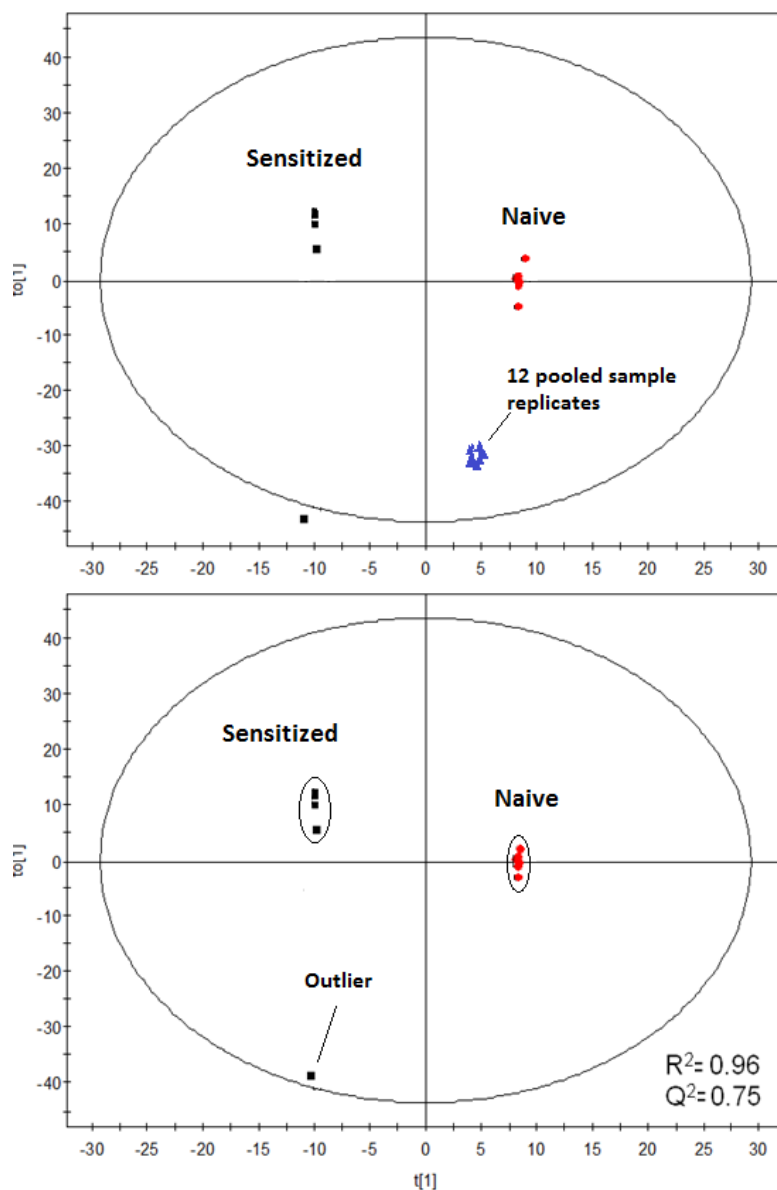


Figure 4.3. OPLS-DA analysis of the blood serum metabolome encompassing ~2100 metabolomic features comparing naive mice to sensitized mice. Top panel includes pooled sample replicates; bottom panel excludes pooled sample replicates. High R^2 and Q^2 scores indicate that the experimental data is consistent with a robust predictive model.

Preliminary OPLS-DA analysis revealed a clear separation between the two groups of mice with high “regression” and “goodness of fit” scores ($R^2=0.96$, $Q^2=0.75$ respectively) despite the appearance of one sensitized mouse sample outlier which cannot be rationalized by clinical outcome. While the analysis of these scores is somewhat subjective, it is generally accepted that regression and fit scores above 0.6 are indicative of a highly robust model⁹⁵. Interestingly, Student’s t-test comparison between the two groups revealed that, of the 2100 unique metabolite features found by XCMS and CAMERA, only 15 metabolites (Table 4.1) were statistically different between the two sample types (p values less than 0.05).

Table 4.1. Fifteen Metabolites exhibiting statistically significant fold changes ($p < 0.05$) out of 2100 total features comparing naïve (not treated) and sensitized mice (treated with peanut and cholera toxin) in the first pilot experiment. Metabolites appearing in green were identified unambiguously by comparison to authentic chemical standards; metabolites in yellow were identified based on matches between their mass spectra and mass spectra found in databases; chemical formulae of metabolites in light red were assigned based on accurate mass and isotope ratio measurements.

m/z	RT (min)	ID/Formulae	p-value (t-test)	Fold Change	Identification Confidence
(+)136.064	3.5	Adenine	0.036	2.7	ID with standards
(-)151.025	4.0	Xanthine	0.0001	4.1	
(-)167.021	8.2	Uric Acid	0.0005	1.5	
(-)178.050	2.7	Hippuric acid	0.009	1.8	
(-)267.075	6.8	Inosine	0.0005	4.6	
(+)268.108	3.5	Adenosine	0.040	2.8	
(+)626.393	8.0	Leukotriene C4	0.025	1.4	
(-)161.044	2.7	Hydroxymethylglutaric acid	0.014	2.3	ID by Database/ MS ²
(-)253.216	2.2	Palmitoleic acid (16:1)	0.023	0.6	
(-)281.247	2.8	Oleic acid (18:1)	0.022	0.7	
(+)476.278	7.3	lysoPE(18:3)	0.044	1.3	
(+)502.295	7.2	lysoPE(20:4)	0.004	1.7	
(+)526.296	7.1	lysoPE(22:6)	0.002	1.8	
(+)160.134	10.0	C ₈ H ₁₈ NO ₂	0.006	1.2	Formula only
(+)700.578	4.8	C ₄₀ H ₇₈ NO ₈	0.027	1.3	

4.3.2. Experiment Two: Sensitized Mice Compared to Mice Treated with Peanut Only

In light of these encouraging results a second experiment involving 7 mice per group (increased from 5 mice in experiment one) was performed. In addition to the increase in sample size, this second experiment differed from the first in that untreated, naïve mice were replaced with mice treated with peanut extract only (no adjuvant). The serum metabolomes of these peanut-treated mice were then compared to 7 mice treated with peanut and cholera toxin (sensitized mice). This experiment has the potential to differentiate between effects resulting from the administration of peanuts.

Similar to the previous experiment, mice that had been treated with peanut and adjuvant showed a strong anaphylactic response after challenge whereas mice treated only with peanut did not show any clinical symptoms. These observations were consistent with observations previously made by members of the Jordana group.

After sample collection and processing, LC-MS analyses were performed. Data processing on all samples including pooled samples was performed identically on all samples using the protocol developed in experiment one (Section 4.3.1.). Approximately 2200 unique metabolomic features were detected in the two groups, a number similar to that observed in experiment one. These data were analyzed by OPLS-DA. Pooled samples clustered tightly indicating good instrumental reproducibility throughout the sample set analysis. As in experiment one, approximately 100 features with poor analytical reproducibility (>20% RSD) in the pooled sample replicates were removed

from the data set. OPLS-DA analysis was then applied to the two sample groups in the absence of the pooled samples. Clear separation between sensitized and non-sensitized mice was evident and the R^2 and Q^2 scores of 0.61 and 0.57, respectively, indicate good model robustness (Figure 4.4).

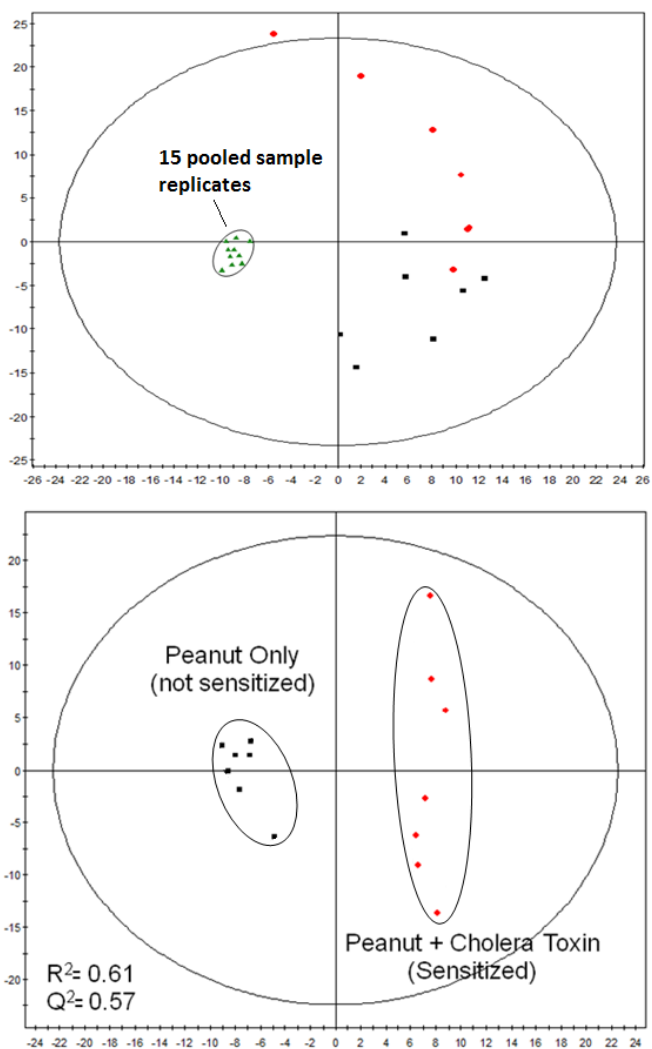


Figure 4.4. OPLS-DA analysis of the mouse blood serum metabolome with pooled samples (top) and without pooled samples (bottom) comparing mice treated with peanut extract only to fully sensitized mice.

Student's t-test comparison of sensitized mice versus peanut only treated mice detected 6 features with a p value of less than 0.01 and an additional 20 less than 0.05 as given in Table 4.2.

Table 4.2. List of twenty-five metabolites (out of approximately 2200) exhibiting statistically significant fold changes between mice treated with peanut extract and cholera toxin versus mice treated only with peanut extract in the second sensitization experiment. Metabolites appearing in green were identified unambiguously by comparison to authentic chemical standards; metabolites in yellow were identified based on matches between their mass spectra and mass spectra found in databases; metabolites in light red represent unknown compounds.

m/z	rt (min)	ID	p-value (t-test)	Fold Change	Identification Confidence	
(-)102.054	3.1	γ -aminobutyric acid	0.025	0.8	ID with Standards	
(-)115.040	3.5	Levulinic acid	0.012	1.3		
(-)108.011	3.9	Hypotaurine	0.006	0.4		
(+)136.064	3.3	Adenine	0.028	2.7		
(+)137.052	3.9	Hypoxanthine	0.008	0.2		
(+)139.053	3.3	4-Hydroxybenzoic acid	0.049	0.6		
(-)151.028	3.9	Xanthine	0.017	0.4		
(-)267.074	6.6	Inosine	0.026	0.3		
(+)268.107	3.4	Adenosine	0.021	2.8		
(-)283.072	7.1	Xanthosine	0.012	0.6		
(+)624.328	7.9	Leukotriene C4	0.017	1.2		
(-)128.036	8.0	Pyroglutamic acid	0.022	0.7		ID by Database
(+)188.173	13.3	N-acetylspermidine	0.008	0.7		
(-)506.329	2.4	LysoPE(20:1)	0.003	1.5		
(-)736.517	6.3	PE(36:5)	0.041	1.8		
(+)744.551	28.6	PC(33:2)	0.045	1.4		
(+)755.566	6.3	PA(40:3)	0.032	1.5		
(+)762.510	22.9	PC(36:4)	0.035	1.3		
(+)766.541	29.0	PC(35:4)	0.019	1.5		
(+)778.532	23.4	PC(36:6)	0.045	1.3		
(+)804.547	23.7	PC(38:7)	0.018	1.2		
(+)848.558	7.5	PE(44:6)	0.005	1.6		
(-)450.116	8.7	Unknown	0.049	0.6	True Unknown	
(+)485.243	9.0	Unknown	0.006	0.5		
(+)634.538	25.2	Unknown	0.013	1.8		

4.3.3. Experiment Three: Time-Course Analysis of Mice Undergoing Sensitization

The third and final experiment involved monitoring of the metabolomes of mice as they were sensitized with peanut and cholera toxin, along with a negative control group (naïve mice) and positive control groups (mice treated with peanut only and cholera toxin only) as outlined in Figure 4.1. This experiment was conducted over a 6-week period with blood samples taken every 2 weeks. All serum samples from this experiment were stored at -80°C and were analyzed as one large analytical sample set. Samples were processed in the same fashion as the previous two experiments (as described in Sections 4.3.1 and 4.3.2). A pooled sample was created from the individual samples and was analyzed many times throughout the analytical schedule. A tight clustering of the pooled sample replicates (Figure 4.5) indicated good instrumental reproducibility throughout the analysis. XCMS and CAMERA were used to process these data and approximately 2500 unique metabolomic features were identified in positive and negative ESI ionization modes. Out of these 2500 metabolomic features approximately 150 were removed due to their high analytical variabilities (>20%) in the pooled sample.⁹⁴

The global metabolite analysis of mouse serum after two weeks of treatment is shown in Figure 4.5. The top plot of this figure shows very tight clustering of the 20 pooled samples while the bottom plot shows a small degree of separation of between the treatment groups with low regression and goodness of fit scores (0.47 and 0.27

respectively) indicating poor reliability in the model's predictive capability⁹⁵. No metabolite feature in this data set yielded a t-test or an analysis-of-variance (ANOVA) p value below 0.05. In other words, there were no statistically significant metabolites after two weeks of treatment.

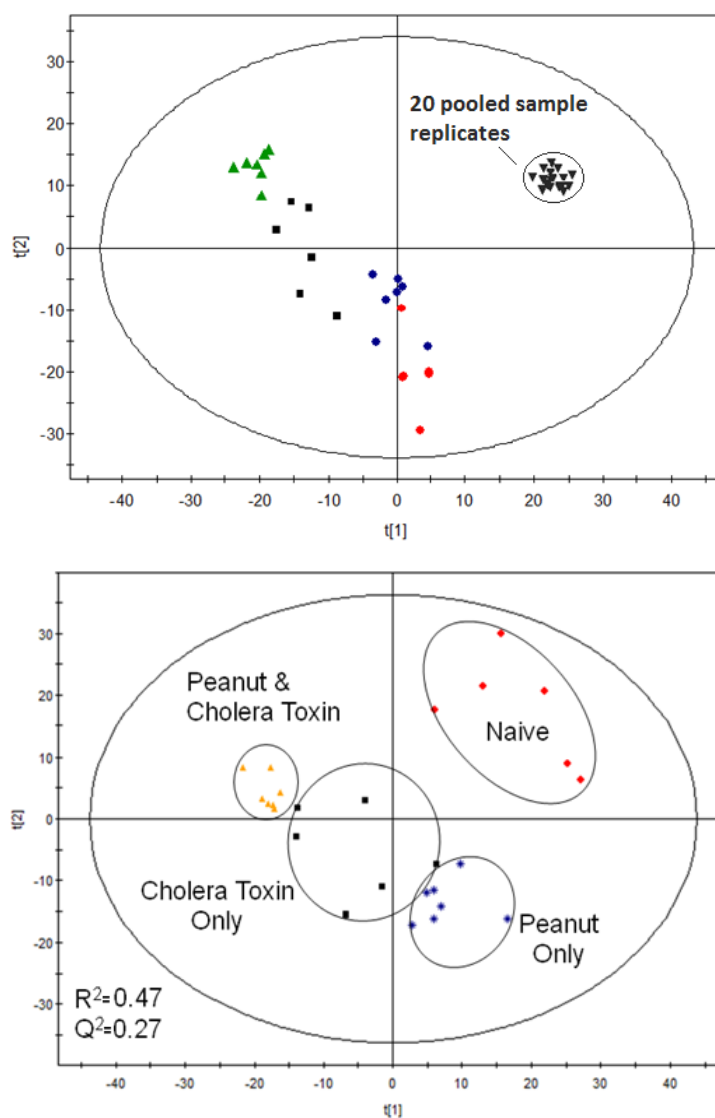


Figure 4.5. OPLS-DA analysis of blood serum metabolome after 2 weeks of treatment encompassing ~2500 metabolite features comparing mice treated with peanut extract only, CT only, naïve mice, and fully sensitized mice. Top panel shows the full data set including pooled sample replicates; bottom panel excludes pooled sample data.

After four weeks of treatment, global metabolomic analysis by OPLS-DA (Figure 4.6) showed increased separation between the treatment groups. The regression and fit scores (0.59 and 0.36 respectively) have improved slightly over the two-week data set but still do not suggest a very robust predictive model. It is clear that some changes at the metabolomic level have begun to occur. Despite the tight clustering of the pooled samples and the tightness of the treatment groups (similar to Figure 4.5) the total biological variability was quite high in these samples, often exceeding 90% relative to the mean. ANOVA analysis revealed only 8 features which had p values less than 0.01.

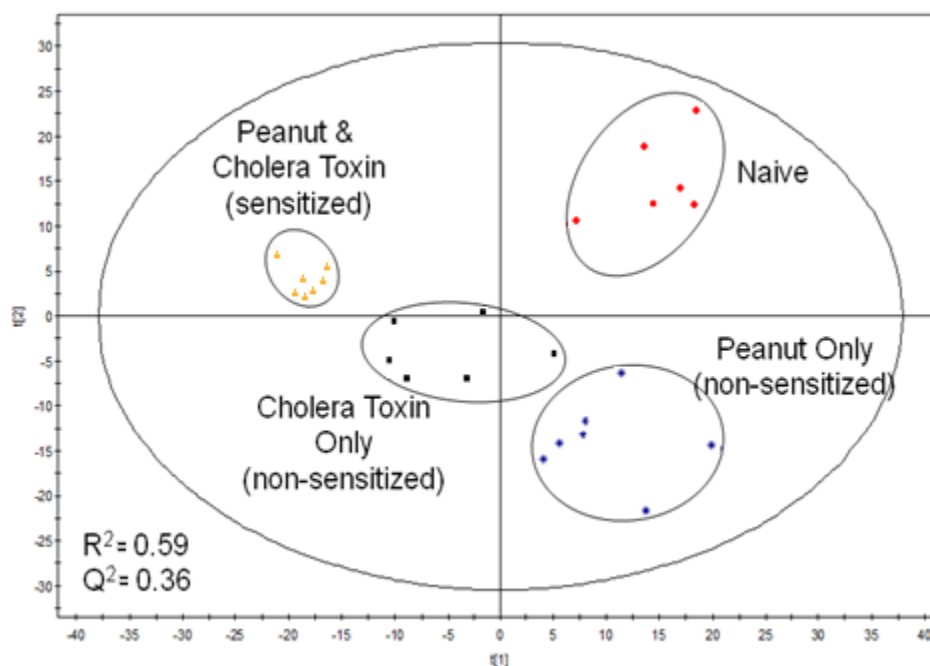


Figure 4.6. OPLS-DA analysis of blood serum metabolome after four weeks of treatment. These data encompass ~2500 metabolite features and show four treatment groups: mice treated with peanut extract only, CT only, naïve mice, and fully sensitized mice.

The last set of sensitization samples were collected six weeks following the initial treatment. The OPLS-DA analysis of these samples revealed that two groups, the peanut-only and the CT-only mice, were virtually overlapped; the sensitized and naïve mice are very well separated (Figure 4.7). Due to the strong overlap of the two former groups, the R^2 and Q^2 scores were modest (0.55 and 0.27). A second OPLS-DA analysis was performed in which the data from the two non-sensitive groups were combined (Figure 4.8). The predictive scores improved dramatically, reaching R^2 of 0.60 and Q^2 of 0.59 indicative of a strong, robust predictive model⁹⁵. ANOVA analysis of the metabolomic features revealed 18 features had p values less than 0.01 with 7 of these less than 0.001. These data are summarized in Table. 4.3.

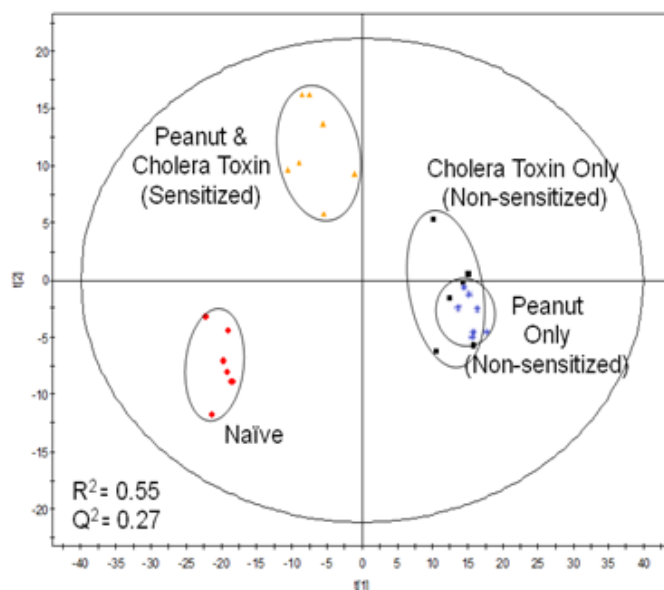


Figure 4.7. OPLS-DA analysis of blood serum metabolome after six weeks of treatment. These data encompass ~2500 metabolite features and show four treatment groups: mice treated with peanut extract only, CT only, naïve mice, and fully sensitized mice.

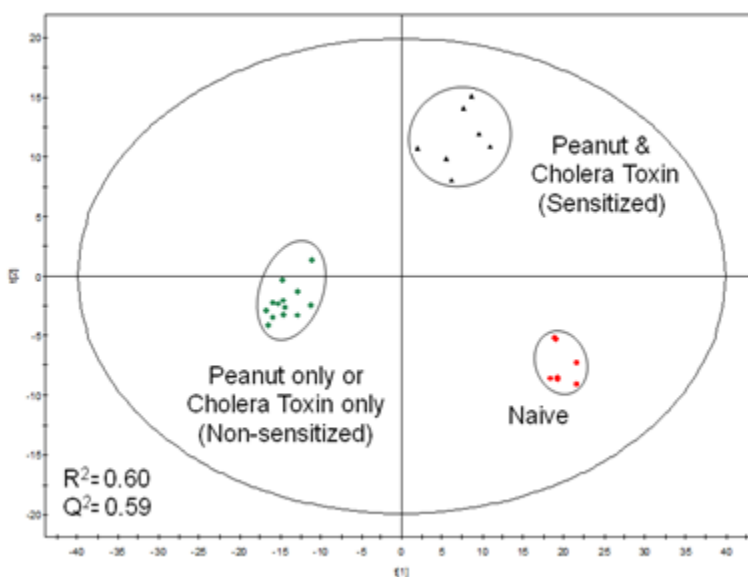


Figure 4.8. OPLS-DA analysis of blood serum metabolome comparing mice treated with peanut extract only, CT only, naïve mice, and fully sensitized mice after six weeks of treatment. In this analysis peanut extract only mice and cholera toxin only mice were combined into a single group.

Table 4.3. Nineteen metabolites (out of ~2500) exhibited statistically significant differences ($p < 0.01$) between naïve mice, mice treated with peanut extract only, mice treated with CT and fully sensitized mice from the third sensitization experiment. Metabolites appearing in green were identified by comparison to authentic chemical standards; metabolites in yellow were identified compared to database spectra or MS^2 analysis; metabolites in light red are unknown

m/z	rt (min)	ID	p-value (ANOVA)	Fold Change	Identification Confidence
(+)136.073	3.4	Adenine	<0.001	3.0	ID with Standards
(+)137.056	4.0	Hypoxanthine	<0.001	0.5	
(-)151.026	4.0	Xanthine	<0.001	0.6	
(-)167.021	8.0	Uric acid	0.003	1.7	
(+)244.099	7.6	Cytidine	<0.001	0.7	
(-)267.074	6.6	Inosine	0.01	0.7	
(+)268.115	3.5	Adenosine	<0.001	3.5	
(+)269.117	3.5	Arabinosylhypoxanthine	<0.001	2.7	ID by Database
(+)540.430	21.8	Hexacosanoylcarnitine	<0.001	2.0	
(+)584.454	21.7	lysoPC(18:0)	<0.001	2.4	
(+)762.568	20.9	PC(34:0)	<0.001	1.5	
(+)764.536	23.0	PS(34:0)	0.002	1.6	
(+)275.264	21.7	Unknown	<0.001	1.9	True Unknown
(-)309.002	6.7	Unknown	<0.001	0.6	
(+)319.289	21.6	Unknown	<0.001	1.7	
(+)380.342	21.5	Unknown	<0.001	1.6	
(+)512.422	21.3	Unknown	0.002	1.7	
(+)614.478	21.5	Unknown	0.001	1.8	
(+)628.482	21.6	Unknown	<0.001	2.4	

4.4 Discussion

4.4.1. Metabolite Profiles Reveal Significant Differences in Serum Metabolome

OPLS-DA analysis of sensitized mice compared to naïve mice and sensitized mice compared to peanut-fed mice (first and second sensitization experiments respectively), revealed that these groups can be differentiated quite easily based on “regression” and “goodness of fit” scores. Similarly, the third sensitization experiment also showed a high degree of separation between fully sensitized mice compared to negative control (naïve mice) and positive control (peanut-only treated and cholera toxin-only treated) groups. Interestingly, out of the ~2500 mass spectral features which were used in the global OPLS-DA analysis, only 25 features were found to be statistically different in these experiments.

A number of the significant metabolites were common to all experiments. Six of the common metabolites were associated with purine metabolism pathway which ends at uric acid in humans. Adenine, adenosine, inosine, hypoxanthine, xanthine and uric acid were all found to have statistically significant p values (Table 4.3). These metabolites played a significant part in differentiating hypersensitive mice from mice which were tolerant to peanuts.

4.4.2. Alteration of Purine Levels in Fully Sensitized Mice

The levels of some metabolites involved in purine metabolism were found to be significantly altered in each of the three experiments performed. Of interest, the levels of guanosine and guanine which are associated with a different branch of this pathway do not change significantly. Thus, guanosine and guanine are potential benchmarks for normalization of other purines; use of a purine ratio (i.e., [purine]/[guanine]) would compensate for analytical errors such as dilution. Similarly, other purine ratios such as the ratio of uric acid to xanthine may provide a diagnostic test for peanut hypersensitivity.

Figure 4.9 displays the purine degradation pathway along with the observed changes in each metabolite at six weeks in the experiment which tracked changes during the sensitization process (third experiment).

Examination of the relative levels of each purine in the uric acid pathway after six weeks of treatment shows that while uric acid is significantly increased relative to both peanut-only and naïve mice, the increased level is not significant compared to mice treated with cholera toxin (Figure 4.10). Also of note, the levels of the direct precursors to uric acid along one branch of the pathway, namely xanthine, hypoxanthine and inosine are noticeably decreased in sensitized mice compared to mice treated only with peanut, suggesting an activation of this portion of the purine metabolomic pathway (Figure 4.10).

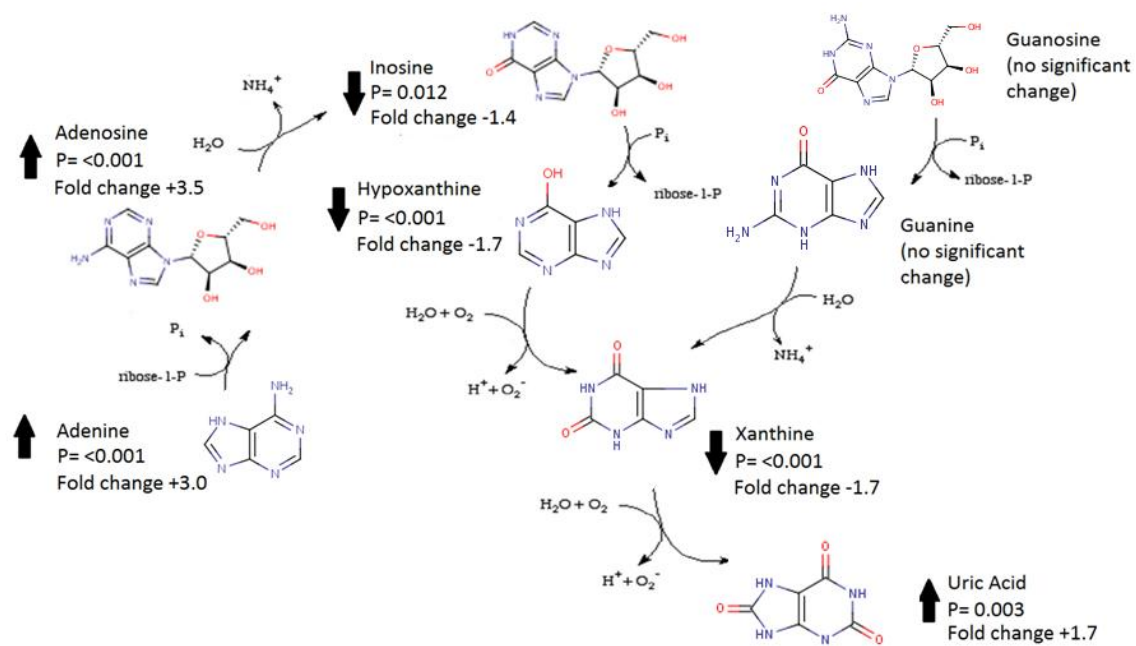


Figure 4.9. Observed fold changes in metabolite levels in the purine metabolism pathway due to treatment with peanut and cholera toxin compared to peanut-treated mice six weeks after initial treatment.

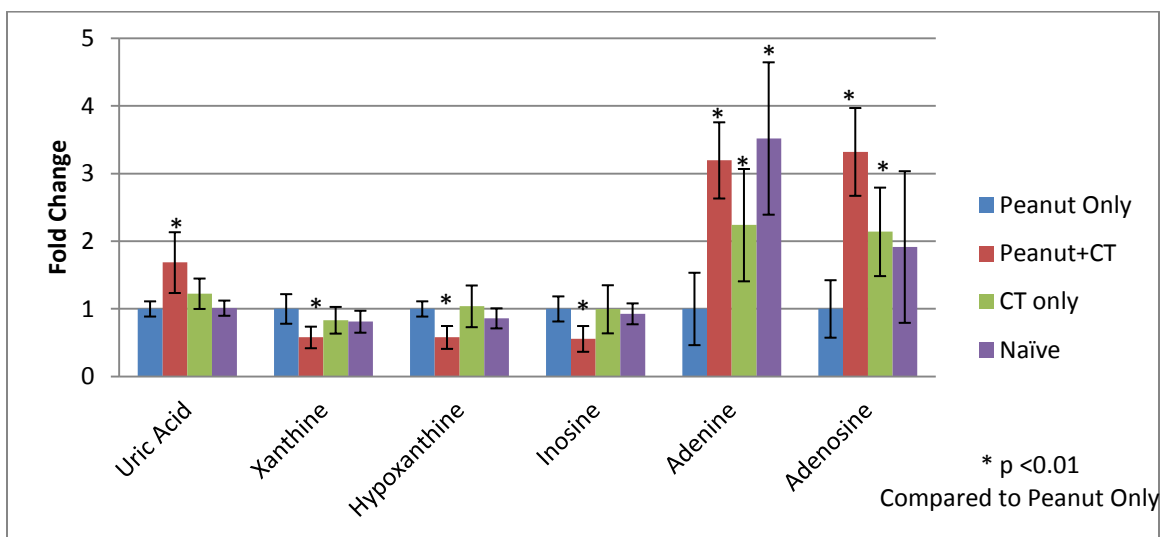


Figure 4.10. Relative levels of purines involved in uric acid pathway after six weeks of treatment from the third sensitization experiment. All levels were normalized to mice treated with peanut only to compensate for changes due to the digestion of peanuts.

As the sensitization period progressed, the purine which marks the end of the purine degradation pathway in humans (i.e., uric acid), begins to show marked elevation after four weeks (Figure 4.11). These data correlate with observations made by the Jordana group where they noted that the four-week mark is the minimum required time for sensitization⁵⁷. However, the relatively large variation seen in the peanut-fed mice at four weeks precludes a conclusive indication of elevation. A large degree of variability was also observed in the levels of other purines.

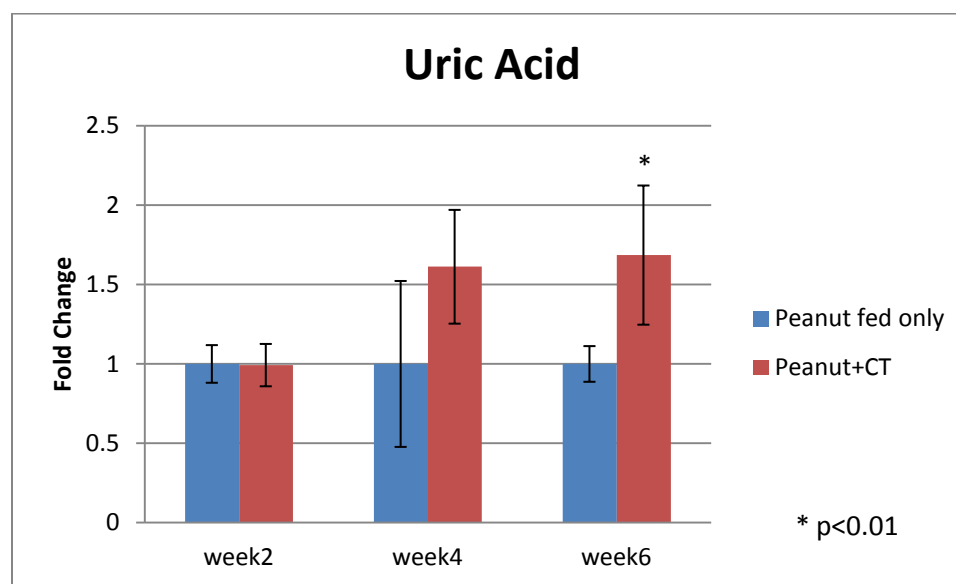


Figure 4.11. Relative levels of uric acid in sensitized mice treated with peanut and cholera toxin compared to mice treated only with peanut extract.

The purine metabolic pathway has not been identified previously as having a role in the development of peanut allergy. However, uric acid is known to be a danger-associated molecular pattern (DAMP) or alarmin, which is a compound released during

severe physical or metabolic stress conditions. This DAMP is indicative of a high rate of cell death or cell damage⁹⁶. High levels of uric acid have also been correlated to diets high in meat protein,⁹⁷ typical of developed regions. Previous reports have also noted that uric acid has a role in inducing T helper 2 (Th2) cell immunity involved with inhaled allergens such as dust mites and is an inflammatory mediator of allergic asthma⁹⁸. A correlation between the high prevalence of peanut allergy in developed regions and uric acid could be due to high protein diets which in turn, lead to high uric acid levels or the increased rate of gut flora death caused by the overuse of antibiotics and general aseptic conditions encouraged in modern developed nations.

4.4.3. Uric Acid as an Adjuvant and Critical Signaling Molecule for the Induction of Peanut Hypersensitivity

The application of comprehensive metabolomic screening in the development of sensitivity to peanuts has led to the discovery of an impact on purine metabolism, specifically on uric acid. Previous reports identified uric acid as having a negative impact on immune function.⁹⁸ This discovery prompted members of the Jordana group to investigate the role of uric acid as both an adjuvant and as a critical molecule required for sensitization. To test whether uric acid can act as an adjuvant, a series of mice were treated with the sensitization protocol used previously in this work. Briefly, mice were divided into groups of three; peanut and CT treated (known sensitivity), peanut only (known tolerant), and mice treated with peanut and uric acid. After six weeks of treatment, these mice were challenged with an intraperitoneal injection of peanut

extract. Clinical observations of these mice show that uric acid-treated mice clearly became anaphylactic as measured by the drop in core body temperature and their increase in hematocrit, although not to the same extent and severity as the CT treated mice (Figure 4.12). This result strongly suggests that uric acid is indeed an inducer of immune system cells triggering hypersensitivity. This result provides additional evidence for uric acid as a DAMP. It should be noted that this experiment alone does not provide evidence that this pathway is essential for sensitization.

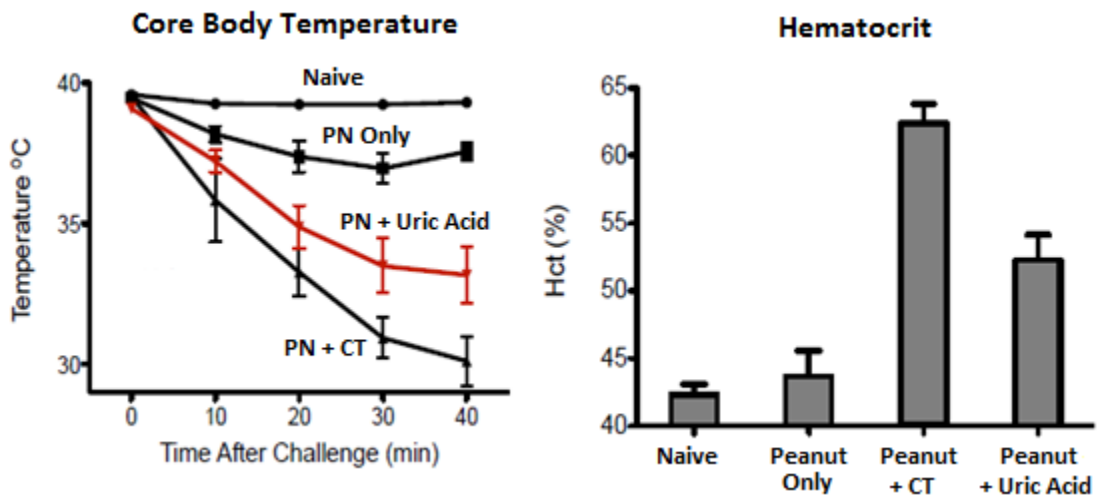


Figure 4.12. Observed clinical responses in mice treated with peanut extract and uric acid compared to non-sensitive mice and mice treated with peanut and cholera toxin after intraperitoneal peanut challenge. Decreases in core body temperature (right) and increase in hematocrit indicate levels measured at 20 minutes post challenge show clear signs of anaphylaxis. (PN +CT= mice treated with peanut and cholera toxin; PN= mice treated with peanut only; PN + Uric acid= mice treated with peanut and uric acid). Data provided by J. Kong and M. Jordana.

To investigate whether uric acid is an essential compound for immune system activation, a follow up experiment was performed recently by the Jordana group where

mice treated with peanut and CT were also given an intraperitoneal injection of uricase. Uricase is an enzyme that converts uric acid to allantoin. This treatment was carried out for a six-week period as in the previous studies, together with control mice treated with peanut and cholera toxin (no uricase) and naïve mice. The hypothesis behind this experiment was that uricase would prevent uric acid accumulation, thereby decreasing any effects of uric acid on the immune system. After intraperitoneal peanut challenge, mice treated with peanut and cholera toxin responded as expected with a sharp increase in hematocrit levels along with decreases in core temperature (Figure 4.13). Alternatively, mice which had been given uricase did not show any signs of anaphylaxis despite being treated with peanut and CT (Figure 4.13). This result is clear evidence of uric acid's function in the activation of the immune system during sensitization. These findings were only made as a result of the lead provided by the findings made using a comprehensive metabolomics approach. This use of comprehensive metabolomics as a discovery tool led to the confirmation of new metabolites which cause immune system dysfunction.

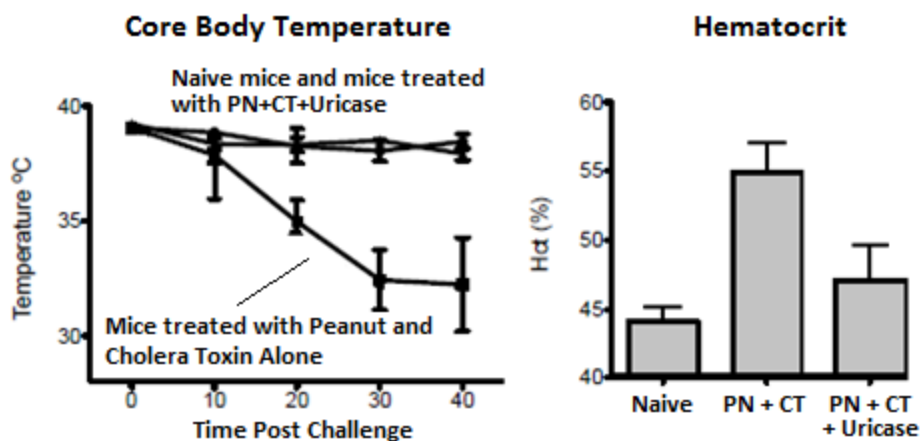


Figure 4.13. Clinical observations of mice treated with peanut, cholera toxin and uricase compared to naïve and sensitized mice after intraperitoneal peanut challenge. No changes in core body temperature (right) and only slight changes in hematocrit levels (left) indicate no anaphylaxis occurred in uricase treated mice (PN +CT= mice treated with peanut and cholera toxin; PN +CT+uricase= mice treated with peanut, cholera toxin and uricase). Data provided by J. Kong and M. Jordana.

4.4.4. Effect of Cholera Toxin on Levels of Uric Acid and Other Purines

Cholera toxin is a widely used and accepted adjuvant for the induction of hypersensitivity to a variety of antigens⁹². Cholera toxin's role as an activator of dendritic cells and as a promoter of interleukin production has also been well studied⁹³. However, cholera toxin's effects at the molecular level are for the most part unknown. Analysis of purine levels in mice treated only with CT (Figure 4.9) shows that with the exception of adenine and adenosine levels which are clearly elevated, the levels of the other purines are not significantly different from levels in peanut-treated mice or mice treated with both peanut and cholera toxin. Uric acid levels while slightly elevated in cholera toxin-treated mice are not statistically different from controls. These data suggest that metabolomic changes from administration of CT alone are not sufficient to

account for the effects arising from the purine pathway alteration. These findings are the first of their kind and show that, although cholera toxin does impact metabolite levels, its effects at the molecular level are clearly different compared to those observed when a potential antigen (peanut protein) is present.

These findings inspired the Jordana group to monitor uric acid levels in mice which are undergoing a sensitization method currently under development. This novel sensitization method which does not require an adjuvant is also marked by increases in uric acid. Work is still on-going to provide further evidence on the essential role of uric acid in the induction of hypersensitivity.

4.5. Conclusions

This study represents the first documented use of comprehensive metabolomics as a discovery tool for the study of food hypersensitivity development. The comprehensive metabolomic analysis of mice undergoing a sensitization procedure utilizing cholera toxin as an adjuvant was able to reliably differentiate between normal, non-sensitized mice (regardless of what agents were administered) and mice in which hypersensitivity had been induced. These findings address and fulfill the first goal of this thesis. Furthermore, metabolomic analysis was able to identify that the purine degradation pathway was altered in sensitized mice resulting in the perturbation of blood serum levels of purines such as uric acid as well as uric acid precursors along one branch of the purine pathway. Based on this work, the Jordana group has since

demonstrated that uric acid is not only capable of inducing sensitization to peanuts in mice but appears to be an essential compound to activate the immune system to develop hypersensitivity. Based on these metabolomic results, the Jordana group has recently monitored uric acid levels in mice undergoing a sensitization method that does not require an adjuvant and they also observed an increase in uric acid in these mice. Furthermore, this discovery may lead to the development of novel diagnostic ratios using uric acid metabolites such as xanthine. This analytical method may allow the diagnosis of peanut hypersensitivity without the need to perform potentially dangerous peanut challenge experiments on humans. These findings are a clear indication of the power of comprehensive metabolomics in the discovery of novel mechanisms in immunology.

Chapter 5. Metabolomic Screening of Peanut Induced Anaphylaxis in a Murine Model

5.1 Introduction

The preceding chapter showed that peanut-sensitized mice have different metabolomic profiles compared to naïve mice and that uric acid and its associated pathway plays a critical role in the activation of the immune system in the development of hypersensitivity to peanuts.

The next vital question to address is what metabolomic changes occur during anaphylaxis and what metabolic pathways are involved. To answer these questions, mice which have been sensitized to peanuts were challenged via an intraperitoneal injection of a peanut extract and the time course of their reaction tracked using a comprehensive metabolomic approach.

5.1.1. The Health Problem

Beyond the biological considerations which were discussed in Sections 1.10 and 4.1, food allergies are an increasingly problematic health concern which currently affects about 3.5% of the North American population⁹⁹.

**Disclaimer: All work described in this chapter was approved by the Research Ethics Board of McMaster University. All animal handling and hematocrit measurements were performed by Joshua Kong, Dept. of Pathology and Molecular Medicine McMaster University. Animal blood samples were processed by both the author and by Joshua Kong. All other work described in this chapter was performed by the author.*

Allergic reactions to ingested foods may cause physical symptoms ranging from hives and diarrhea to full blown, life-threatening anaphylaxis. Among all food allergy types, hypersensitivity to peanuts has been determined to be present in approximately 1-2% of children in North America¹⁰⁰. Accidental exposure to peanuts or products containing peanut protein for these individuals leads to peanut-induced anaphylaxis (PIA) which is accountable for almost 60% of fatal or near-fatal food-related allergic reactions¹⁰¹. Most worrisome, current evidence suggests that the prevalence of peanut allergies has doubled in the past 10 years and, unlike many other food allergies, peanut hypersensitivity is unusually persistent¹⁰². Indeed, the most current data estimates that only 20% of all peanut allergy sufferers will ever outgrow or overcome their hypersensitivity, meaning that for four out of five patients diagnosed with peanut allergy, it will be a life-long affliction⁸⁸.

Unlike many other food allergies there are no safe or reliable diagnostic tools currently approved which can accurately assess the presence or severity of the allergic hypersensitivity; clinicians must rely on visual and anecdotal evidence given from the patient upon oral challenge (with peanuts) which is both potentially dangerous and difficult to interpret⁵⁵. This difficulty in diagnosis often leads to clinicians being reluctant to make a definitive diagnosis since a false positive will lead to unnecessary burden on the patient and family. A false negative, on the other hand, may lead to a potentially life-threatening reaction.

There is also a severe lack of effective treatment options available for peanut allergy. Unlike many other food allergies, oral immunotherapy treatments have been shown to be ineffective and, as such, cannot be recommended as a viable treatment option for peanut-allergic individuals¹⁰³. At this time the only approved option for patients with peanut allergy is strict avoidance of peanuts and peanut products which leads to an undeniable societal impact, especially in schools where peanut-avoidance guidelines must be enforced to limit the exposure of anaphylactic children to foods and products containing peanuts.

Peanut allergy issues also have had a significant economic impact for the food and restaurant industries. Under new regulations food producers are required to provide warning labels to limit accidental ingestion of peanut products and are encouraged to produce foods in “peanut-free” facilities. Despite these efforts it has been reported that approximately 50% of allergic individuals will accidentally ingest a peanut-containing product every 3-4 years¹⁰⁴.

The current level of understanding regarding the immune response mounted by the body upon the onset of PIA is woefully incomplete. Recent studies have provided evidence in experimental models to suggest that IgG₁ and macrophages are also involved in PIA, in addition to the normal IgE-mast cell mechanism¹⁰⁵. This pathophysiological complexity suggests that many additional compounds which are yet

to be identified are likely involved in the anaphylactic process when triggered by peanut exposure.

Further evidence to support this hypothesis is that the blockade of platelet activating factor (PAF) which is one of the very few confirmed mediators of PIA will only limit the severity of attack rather than completely stopping the reaction⁵⁶. This means that other mediators, yet to be identified, must also be present. Also of concern, known markers of anaphylaxis such as histamine and the leukotrienes which have bio-active properties but are not mediators themselves are insufficient to provide an accurate and reliable diagnosis in human patients¹⁰⁶. This is due to ethical considerations which dictate that challenge experiments in humans must be stopped before PIA has an opportunity to occur, meaning that these compounds rarely emerge in sufficient quantities for detection.

A considerable knowledge gap exists regarding the molecular basis of anaphylaxis in humans, specifically identification of potential biomarkers which could aid in the diagnosis of peanut allergy and more importantly, the identification of key PIA mediators (i.e., molecules responsible for inducing anaphylaxis). These mediators represent potential therapeutic targets for amelioration of PIA.

5.1.2. Research Objectives

The objective of the work outlined in this thesis chapter was to apply a comprehensive metabolomic approach to identify novel anaphylactic biomarkers and

mediators utilizing a murine model developed by the Jordana research group (Department of Pathology and Molecular Medicine, McMaster University). Only one study utilizing a comprehensive metabolomics approach for the study of anaphylaxis appeared recently in the literature. This study used gas chromatography-mass spectrometry (GC-MS) to examine serum samples from guinea pigs sensitized to ovalbumin and/or cattle albumin¹⁰⁷. While this study reported some metabolomic differences between anaphylactic and non-anaphylactic subjects, samples were collected at only one time point which was well after challenge. The authors acknowledged that the only metabolites found to be altered were the result of downstream effects such as glucose depletion. Metabolites which may be mediators or biomarkers of anaphylaxis were not reported.

In this work we studied the blood serum metabolome of mice using LC-ESI-TOF-MS at various stages of PIA with the goal to identify early-stage and late-stage mediators and biomarker candidates as well as any other molecules that changed or were released during PIA. The overall objectives of this work can be summarized as:

1. To assess the capability of comprehensive metabolomics to differentiate anaphylactic subjects from non-anaphylactic subjects (i.e., as a diagnostic tool), and to assess the ability of comprehensive metabolomics to accurately reflect the severity of anaphylaxis being experienced (i.e., as a tool to diagnose exposure threshold levels).

2. To identify key metabolites and metabolic pathways which are involved during various stages of PIA and which may serve as candidate biomarkers and mediators of PIA.

5.2. Experimental Design

The design of experiments used in this investigation was crucial in order to allow us to differentiate between the key metabolite changes due to PIA from other unrelated metabolomic changes resulting from other factors including the handling of mice, the physical stress on the mice from intraperitoneal injection, sample collection (orbital bleeding), etc. The determination of time-dependent changes in the serum metabolome will be critical to assessing metabolite changes during anaphylaxis.

A key design feature unique to this series of experiments (compared to typical comprehensive metabolomics studies) is that a simple “treated” versus “control” comparison was not possible. First, the work in Chapter 4 showed that there were significant pre-existing metabolomic differences between sensitized and non-sensitive mice. In other words, the control sample mice (naïve or peanut-only treated) are already different from the sensitized mice. Second, there are two different comparisons which can be examined as outlined in Figure 5.1, (a) direct time-series comparisons of the sensitized mice versus the non-sensitive mice and (b) time-progression comparisons within groups of sensitized mice (or non-sensitive mice). The time-series comparisons give information regarding which metabolites are changing in sensitized mice compared to changes in naïve mice the administration of peanuts. Time-progression comparisons

on the other hand, give information pertaining to the total metabolomic changes happening over a period of time which describe the stage of PIA being experienced.

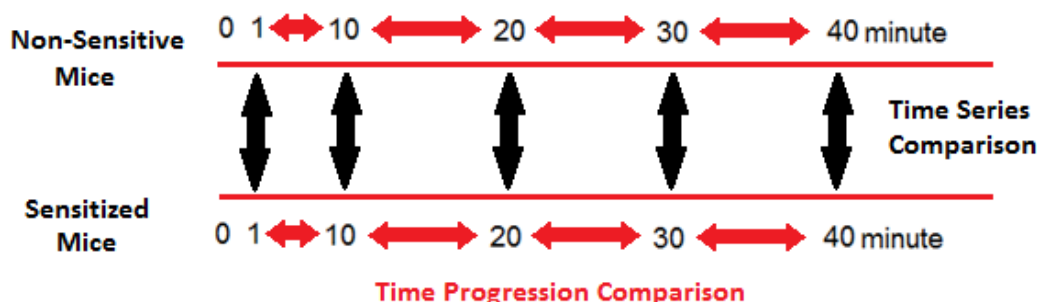


Figure 5.1. Types of time-based, metabolomic comparisons possible in peanut challenge experiments. Time series comparisons (black arrows) compare sensitive to non-sensitive mice at matching time points after challenge. Time progression comparisons (red arrows) compare metabolomic changes within a group type as time progresses.

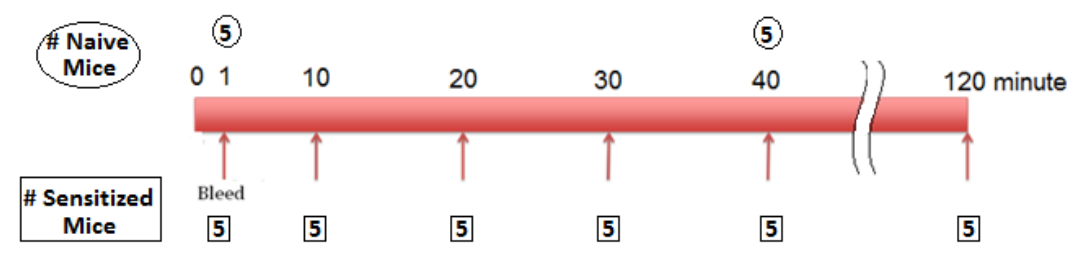
5.2.1. First Challenge Experiment

The first set of experiments performed with mice involved the sensitization of 35 mice with an additional 15 mice which were not pre-treated (naïve) which were used as the control group (Figure 5.2.A).

Prior to challenge, 5 sensitized mice and 5 naïve mice were bled to establish the starting, pre-challenge metabolite levels in each type of mouse as discussed in chapter 4. The remaining mice (both types) were then challenged with an intraperitoneal injection of peanut extract; after challenge, the mice were bled and sacrificed at the

time points described in Figure 5.2.A. The last time point (120 minutes) was used to encompass the anaphylactic period and most of the “recovery” period. All mice were sacrificed after blood sample collection because repeated sampling of the mice may result in metabolomic changes due to the additional stress of repeated bleeding. These changes would complicate interpretation of the changes due to peanut exposure. The objective of this first experiment was to assess whether significant metabolomic changes were occurring in the time-progression comparisons.

A. 1st challenge experiment sampling schedule



B. 2nd challenge experiment sampling schedule

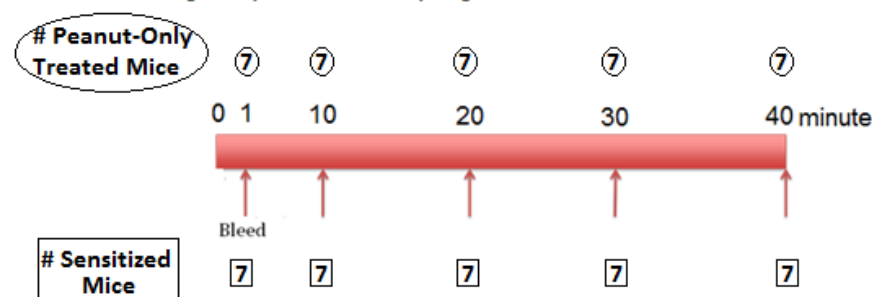


Figure 5.2. Sampling schedule for bleeding and sacrifice after intraperitoneal challenge (at time=0) of mice with peanut extract for the first and second peanut challenge experiments. The first challenge experiment required 35 mice including pre-challenge and control mice arranged in groups of 5. The second challenge experiment required a

total of 84 mice including pre-challenge and control mice arranged in groups of 7 mice each.

5.2.2. Second Challenge Experiment

The first challenge experiment was a pilot experiment that clearly demonstrated that large-scale metabolomic changes had occurred during PIA. In order to perform a time series comparison experiment, time-matched control mice were required that corresponded to the treated mice. In the first challenge experiment, un-treated mice were used as “control” mice. Thus, any metabolic changes in the mice that were due to administration of peanuts by oral gavage could not be accounted for.

To address these limitations, a second experiment was performed as outlined in Figure 5.2.B. Each sensitized challenge group was matched with a corresponding “control” group of mice that had been treated with peanut extract. The mice were challenged and bled at the same five time points as described in Figure 5.2.B.

The sample size of this second experiment increased from five mice to seven mice per group (for a total of 84 mice) to provide greater statistical power to address biological variations. By matching the sensitized groups with control groups (peanut-only treated) at each time point it was felt that it would be possible to determine which metabolites were changing due to PIA as opposed to other effects such as the metabolism of peanuts (time-series comparisons). This experiment also aimed to account for any metabolomic effects resulting from the oral gavage feeding over the six-week period. This experiment did not include time points within the recovery period

(i.e., times later than 40 minutes) where clinical symptoms were known to begin to return to normal. The exclusion of the recovery period was the recommendation of our collaborator, Dr. Jordana since the information gained during this period was deemed to be not worth the financial cost of 14 mice.

5.3 Results

5.3.1 Clinical Measurement of PIA Severity-First Challenge Experiment

The core body temperatures of all mice were measured rectally during the experiment to ensure that the mice (either sensitized or non-sensitized) were responding physiologically and to gauge the severity of PIA. Also, hematocrit levels were measured in all mice to determine the degree of anaphylaxis⁵⁷. In the first peanut challenge experiment, noticeable drops in the core body temperatures of sensitized mice were observed following i.p. injection (Figure 5.3). This temperature change was accompanied by elevated hematocrit levels, clearly showing that the sensitized mice had experienced PIA as a result of peanut challenge. The severity of the anaphylactic reaction increased and peaked at approximately 20-30 minutes as judged by the hematocrit levels although the lowest body temperatures occurred between 40 and 70 minutes before recovering. (Figure 5.3)

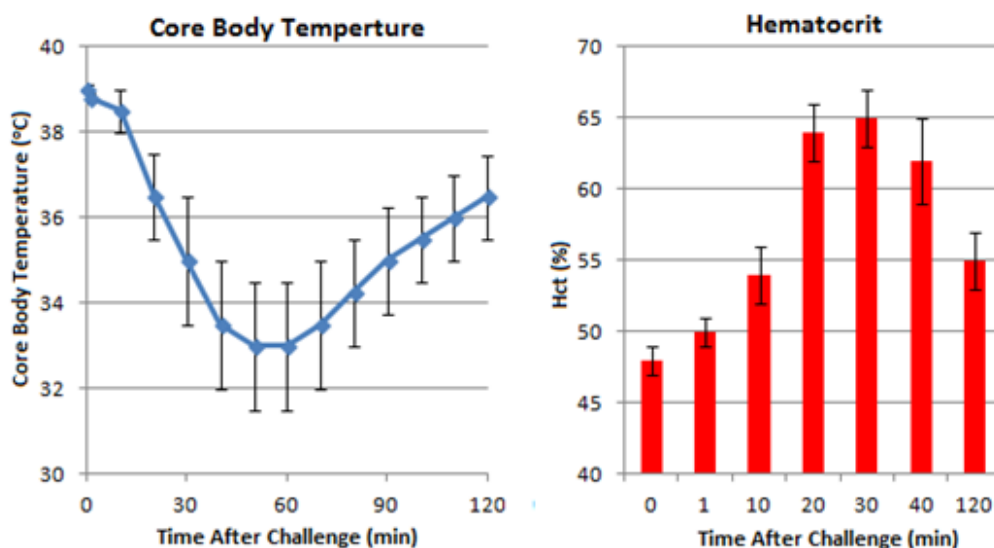


Figure 5.3. Core body temperature and hematocrit levels of mice undergoing peanut-induced anaphylaxis as a function of time post *i.p.* challenge with peanut extract in the first peanut challenge experiment.

5.3.2. Global Metabolite Profiling - First Experiment

The entire LC-MS data set from the first challenge experiment was aligned, extracted, integrated and normalized using XCMS and, after removal of isotopic peaks and adduct ions using CAMERA, approximately 2700 metabolomic features with unique mass values and retention times were identified. The metabolite levels in all samples, including the pooled sample replicates, were subjected to analysis using OPLS-DA. A tight clustering of the pooled sample replicates indicated good instrumental reproducibility throughout the sample set (Figure 5.4, upper panel).

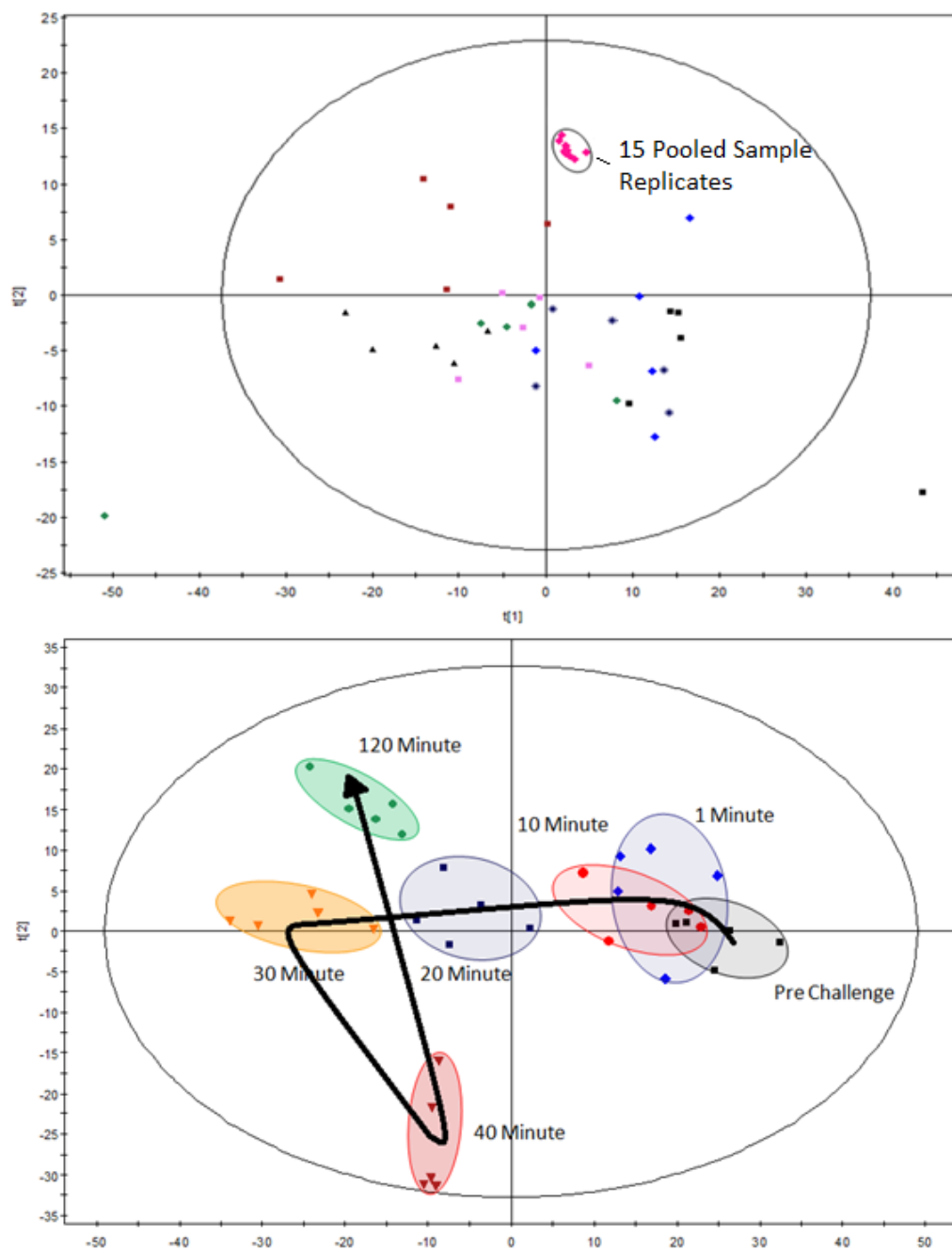


Figure 5.4. OPLS-DA score plot of metabolomic features found in the first peanut challenge experiment. Top panel includes pooled sample replicates; bottom panel excludes pooled sample data. Each time point includes 5 mice per group and each sample encompasses values for ~2700 metabolite features. Pre-challenge mice were also sensitized.

Next, metabolite features which showed poor analytical reproducibility (RSD >20%) within the pooled sample replicates were removed. This reduction in the data set was done based on the recommendations of Dunn et al. They determined that features with poor analytical reproducibility in the pooled sample (>20%) in addition to their normal biological variability would be too unreliable for analysis⁹⁴. Approximately 150 features fell beyond the 20% analytical variability threshold and these were removed from the data set.

The final, data set excluding data from the pooled sample replicates and those features with high analytical variability were then re-analyzed by OPLS-DA (Figure 5.4, bottom panel). The OPLS-DA scores plot displays a clear progression of sample classes from early to late anaphylaxis groups. The 20-minute mice are fully separated from the pre-challenge mice. At 40 minutes a sharp change is seen in the groupings corresponding to the leveling of hematocrit levels with another sharp change being observed in the 2-hour (120 minute) group. There is no overlap between the 10-minute, 20-minute, 30-minute, 40-minute and 120-minute groups.

5.3.3. Comparison of Metabolomic Profiles of Mice During PIA Found in the First Challenge Experiment

The OPLS-DA analysis of data from the first challenge experiment (Figure 5.4) demonstrated that significant changes occurred in mice as PIA progressed. The stage of anaphylaxis (early-late-recovery stage) was manifest as increasing

separation with time. In this respect the first challenge experiment was successful as a time-progression comparison.

In the first experiment, control mice were only available at 1 minute and at 40 minutes post-challenge. This was done to limit the financial cost of this pilot experiment. Time-series comparisons therefore could only be made at 1 minute and 40 minutes. At the 1 minute time point, the direct comparison of control and treated mice showed that 11 metabolites had changed significantly (Table 5.1); no fewer than 70 metabolites had undergone significant changes by the 40-minute time point (Table 5.2.). From this perspective this first trial experiment was a success because it clearly showed that there were significant changes to the mouse metabolome due to peanut challenge. This success gave the impetus to undertake a second, more expensive study with control mice at each time point.

5.3.4. Global Metabolite Profiling of Mice - Second Experiment

In the second challenge experiment more mice were used in each time group (seven mice compared to five) including matched time controls. To better account for metabolome changes occurring from the feeding of peanuts (by oral gavage) the control mice were treated with peanut extract (without adjuvant) on the same treatment schedule as the sensitized mice (treated with peanut and cholera toxin).

Table 5.1. Metabolites in sensitized mice that were found to be significantly different ($p < 0.05$) one minute post challenge compared to naïve mice in the first challenge experiment. Metabolites highlighted in green were identified by comparison to authentic chemical standards; metabolites in yellow were identified based on good matches between their mass spectra and mass spectra in databases; chemical formulae of metabolites in light red were assigned based on accurate mass and isotope ratio measurements.

Accurate Mass	RT (min)	ID	p-value (t-test)	Fold change	Identification Confidence
(+)112.0871	13.6	Histamine	<0.001	>100	ID with standards
(-)157.0362	7.8	Allantoin	0.005	0.78	
(+)198.0987	8.5	Metanephrine	<0.001	0.73	
(+)126.1025	13.2	Methylhistamine	0.036	1.3	ID by Database/MS ²
(+)832.5767	27.2	PC(40:7)	0.02	1.2	
(+)806.5629	27.3	PC(38:6)	0.039	1.2	
(-)163.0614	8.5	C ₁₀ H ₁₁ O ₂	0.002	0.65	Formula only
(-)243.0635	7.3	C ₉ H ₁₁ N ₂ O ₆	0.003	0.76	
(+)582.4254	8.7	Unknown	0.025	1.3	Unknown

Table 5.3. Twenty-eight metabolites exhibiting statistically significant fold changes out of 2100 total features comparing naïve (not treated) and sensitized mice (treated with peanut and cholera toxin) in the first, pilot experiment 40 minutes post-challenge. Metabolites appearing in green were identified unambiguously by comparison to authentic chemical standards; Metabolites in yellow were identified based on matches between their mass spectra and mass spectra found in databases; chemical formulae of metabolites in light red were assigned based on accurate mass and isotope ratio measurements. An additional forty-two unknown features were also found to be significant (not shown).

m/z	rt (min)	ID	p-value (t-test)	Fold Change	Identification Confidence
(+)104.039	2.2	2-hydroxybutyric acid	0.026	1.8	ID with Standards
(+)104.109	8.5	4-aminobutyric acid	0.008	0.6	
(+)114.068	6.5	Creatinine	0.005	0.6	
(-)124.005	9.4	Taurine	0.001	0.6	
(+)132.077	9.8	Creatine	0.007	0.8	
(+)156.077	12.2	Histidine	0.015	0.5	
(-)175.023	3.1	Ascorbic Acid	0.006	0.4	

(+)204.123	9.6	Acetylcarnitine	0.009	1.4	
(-)192.066	2.5	2-Methylhippuric acid	0.030	0.2	
(-)206.080	2.4	N-Acetyl-Phenylalanine	0.030	0.5	
(-)243.062	4.3	Uridine	0.002	1.7	
(+)253.130	5.3	Deoxyinosine	0.039	2.2	
(+)170.093	12.4	Methylhistidine	0.004	0.6	ID by Database
(+)189.159	13.0	N6,N6,N6-trimethyl-lysine	0.014	0.6	
(-)250.044	4.8	Norepinephrine Sulfate	0.001	0.3	
(-)429.371	25.6	Cholesteryl Acetate	0.020	1.9	
(+)480.308	8.0	lysoPE(18:0)	0.023	1.3	
(+)480.311	7.4	lysoPE(18:1)	0.047	0.7	
(-)599.380	7.7	Erythroanthin	0.010	0.5	
(+)672.427	7.4	PE(32:2)	0.014	0.4	
(+)782.561	29.6	PC(36:4)	0.014	0.6	
(+)826.565	28.9	PC(40:9)	0.030	0.6	
(-)134.062	2.6	C ₈ H ₈ NO	0.013	0.5	
(+)166.018	6.4	C ₄ H ₇ NO ₄ S	0.001	0.5	
(+)190.051	2.8	C ₁₀ H ₈ NO ₃	0.019	0.4	
(+)314.181	5.8	C ₂₀ H ₂₅ O ₃	0.024	2.5	
(+)341.183	6.4	C ₂₀ H ₂₄ N ₂ O ₃	0.025	2.4	
(+)399.271	2.2	C ₄₄ H ₇₉ O ₁₀ P (z=2)	0.001	0.2	

The mice were challenged with an i.p. injection of peanut extract and the core body temperatures and hematocrit levels were monitored. The severity of PIA in the sensitized mice was approximately equivalent to that observed in the first experiment. However, the onset of anaphylaxis peaked at approximately 10-20 minutes, judging by the hematocrit levels, as opposed to 20-30 minutes as in the first challenge experiment. The core body temperature and hematocrit data from the second challenge experiment are shown in Figure 5.5.

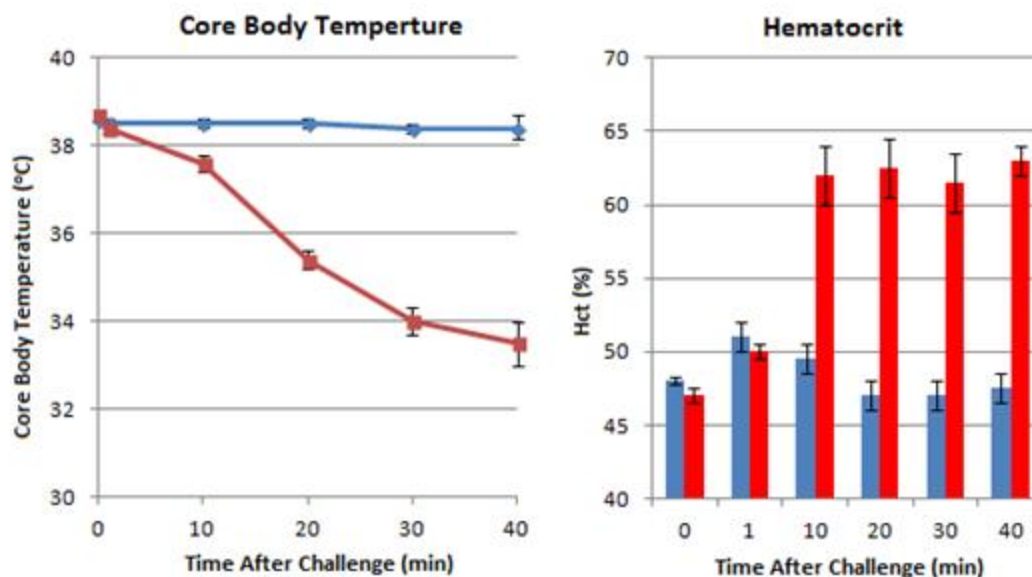


Figure 5.5. Core body temperature and hematocrit levels in mice undergoing peanut-induced anaphylaxis as a function of time post *i.p.* challenge with peanut extract in the second peanut challenge experiment. Data for sensitized mice is in red and for mice treated with peanut extract only are in blue. Data provided by J. Kong and M. Jordana.

Analysis of second challenge data set was performed in a manner identical to the first challenge experiment and yielded about 3500 unique metabolomic features. OPLS-DA was then performed on this total data set including the pooled sample replicates. Again, the pooled samples were found to cluster tightly indicating good instrumental performance (Figure 5.6, top panel).

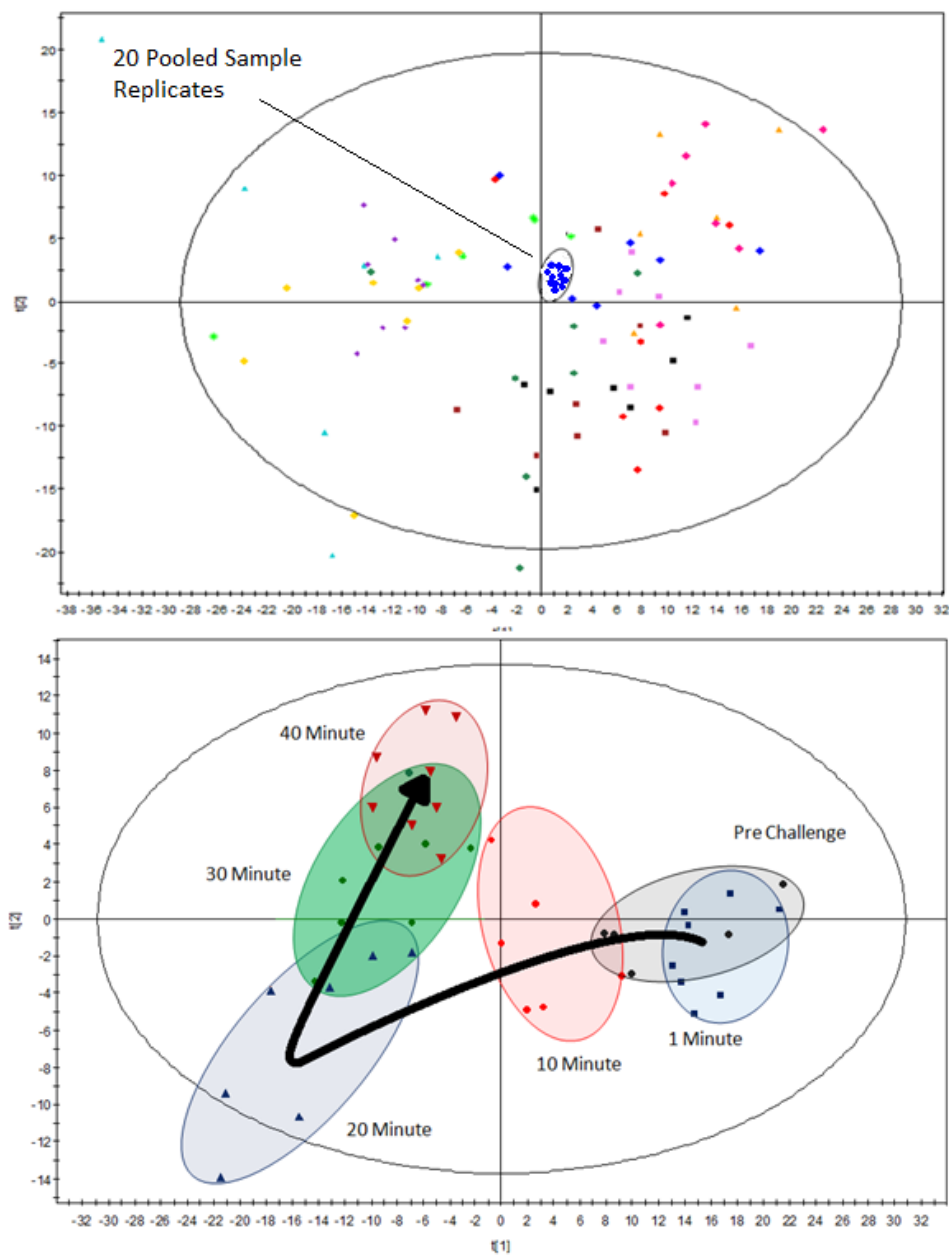


Figure 5.6. OPLS-DA score plot of metabolomic features for sensitized mice in second challenge experiment. Each time point includes 7 mice per group and each sample encompasses ~3500 metabolomic features. Pre-challenge mice were also sensitized.

After removing about 200 features with a high degree of variation within the pooled sample replicates (i.e., >20% analytical variation) and the pooled sample data, OPLS-DA was performed on the resulting data set. A similar but even more differentiated trend was observed in these data compared to the first challenge experiment. In the second experiment, a clear differentiation between groups can be seen as early as 10 minutes post-challenge. By 20 minutes post-challenge, groupings are fully separated (Figure 5.6, bottom panel).

The time-matched control mice allowed direct comparison of control (peanut-only treated mice) and fully sensitized mice (Figure 5.7). This analysis showed that while some separation does occur in these non-anaphylactic mice post-challenge, the total degree is rather low with no discernible pattern. This indicates that metabolomic changes in these control mice are not likely to be correlated with PIA.

The OPLS-DA analysis of metabolite profiles of sensitized mice (Figure 5.6 bottom) showed increasing time-progression separation. This analysis did not reveal which time point marks the first major separation of anaphylactic mice from control mice. By performing OPLS-DA on treated and control mice matched by time point (time-series comparison), serum metabolite profiles were observed to be differentiated to a quantitative degree of robustness^{95,108} ($R^2=0.63, Q^2=0.60$) by 20 minutes post-challenge (Figure 5.8).

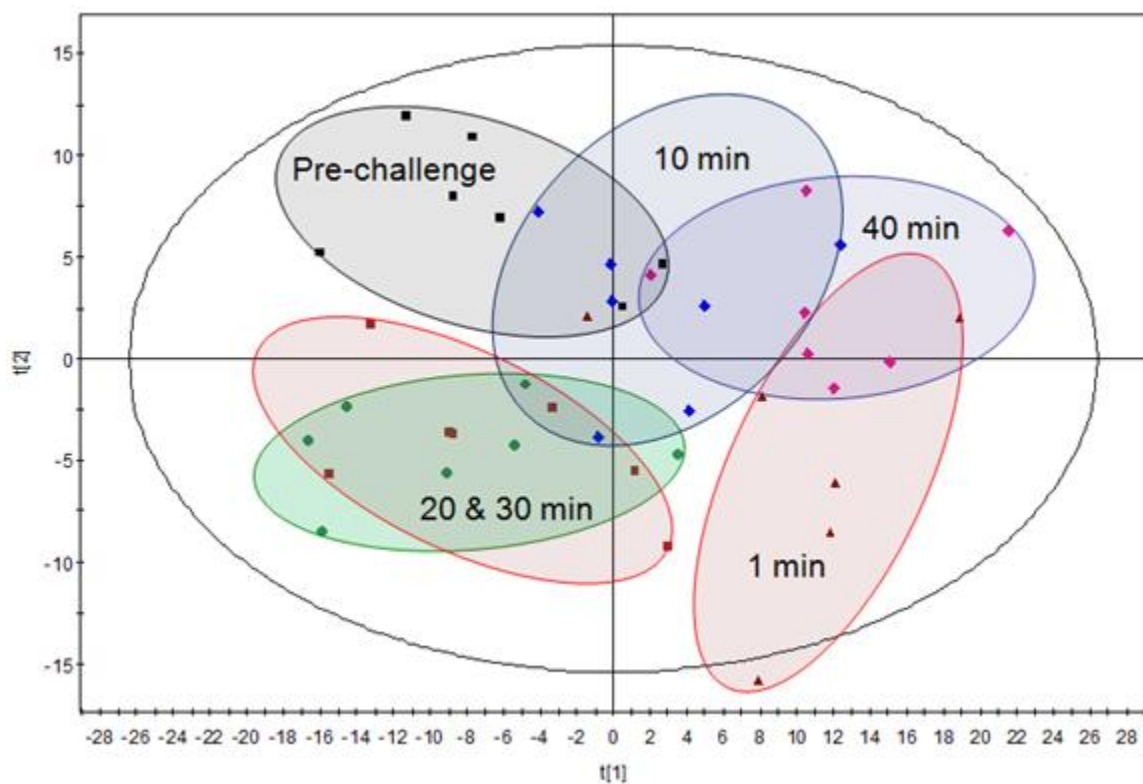


Figure 5.7. OPLS-DA score plot of metabolomic features in non-sensitized, peanut-only treated mice from second challenge experiment. Each group contains 7 mice encompassing ~3500 metabolomic features per sample. All mice in this data set did not show any anaphylactic symptoms post-challenge.

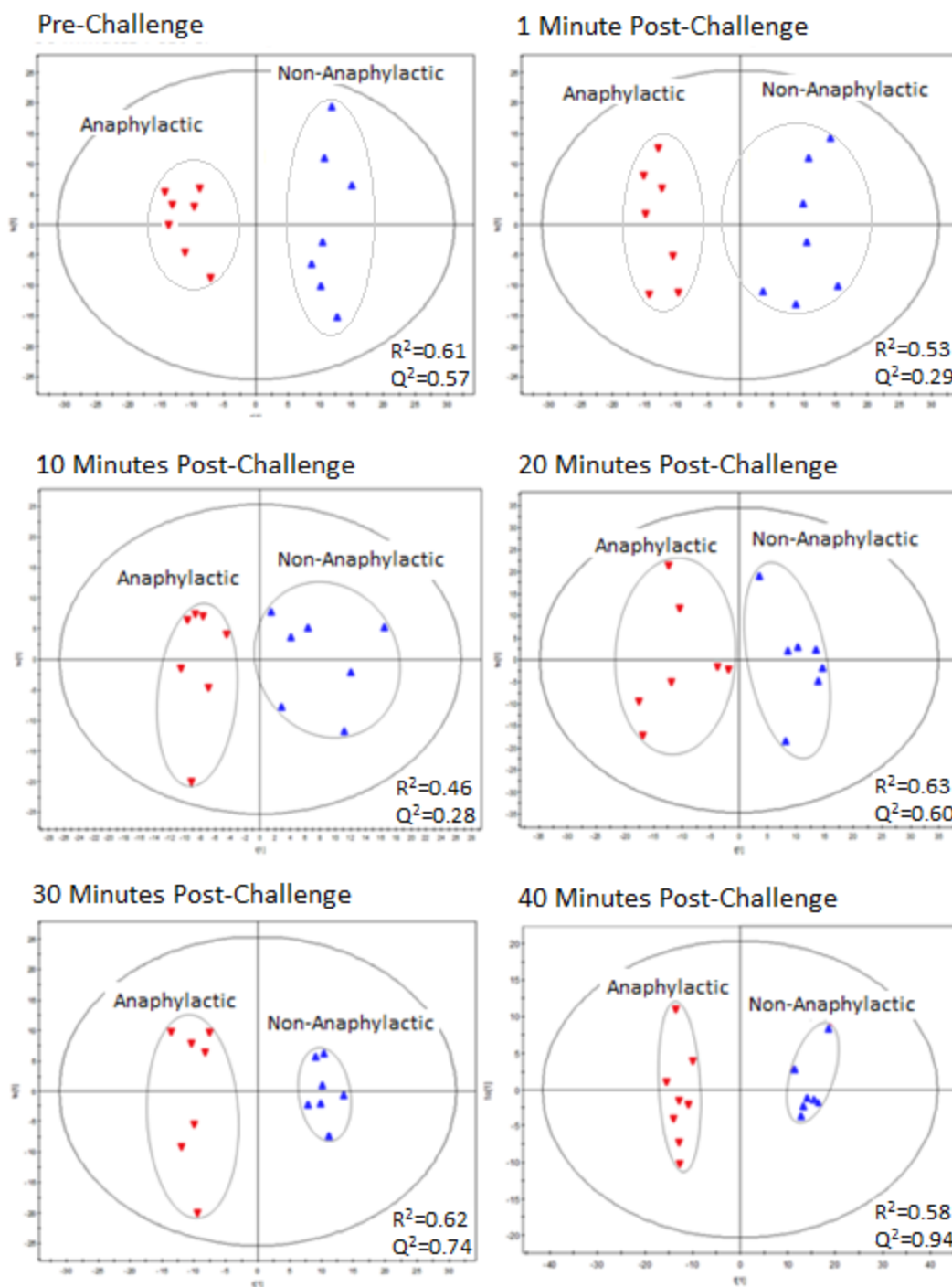


Figure 5.8. OPLS-DA plots of treated and control mice at various times post-challenge. The high “regression” and “goodness of fit” scores (R^2 and Q^2) are provided for each analysis.

5.3.5. Comparison of Metabolomic Profiles of Mice During PIA Found in the Second Challenge Experiment

With the inclusion of time-matched control groups in the second challenge experiment, direct statistical time-series comparisons could be made at each point to determine which metabolomic features had undergone significant change. This experiment involved the sacrifice and sampling of 14 mice at each time point (7 control mice and 7 sensitized mice) at 6 time points for a total of 84 mice.

Student's t-test p-values and fold changes were calculated for each of the approximately 3500 metabolite features. Table 5.2 lists the numbers of statistically significant features observed at each time point, together with the accumulated number of total features. To ensure statistical significance, analysis of variance (ANOVA) was also performed on features which had identified by t-test analysis. This provided an extra degree of certainty that the features were significant across the entire data set.

Table 5.3. Numbers of statistically significant mass spectral features with p-values less than 0.01 and 0.001 which appeared at various times after intraperitoneal peanut challenge.

Time after i.p. challenge	Number of Significant Mass Spectral Features with Fold Changes $>\pm 1.5$	
	ANOVA & t-test p-value <0.01	ANOVA & t-test p-value <0.001
1 minute	30	12
10 minute	43 (Total of 73)	5 (Total of 17)
20 minute	59 (Total of 132)	11 (Total of 28)
30 minute	185 (Total of 317)	31 (Total of 59)
40 minute	501 (Total of 818)	149 (total of 208)

Volcano plots (Figure 5.9) were constructed for each time point plotting the t-test p values (as $-\log_{10}(\text{p-value})$) as a function of fold change (plotted as $-\log_2$ of fold change). This plot has the advantage of identifying those features which show very low p-values which are orders of magnitude lower than the normal “significant” cutoff. While volcano plots are useful in visualizing the magnitude and significance of change in the data, they do not identify chemical trends in the data.

An alternate method of visualizing these data was to plot the 3500 metabolomic features by LC retention time as a function of their m/z value. Those features which are significantly different from control samples are shown as black dots (Figures 5.10 and 5.11). These show chromatographic regions and mass spectral regions where metabolite features are significantly different from the control mice. Although these plots do not convey the magnitude or significance of change as well as the volcano plot, they do highlight chemical trends based on retention characteristics and molecular mass.

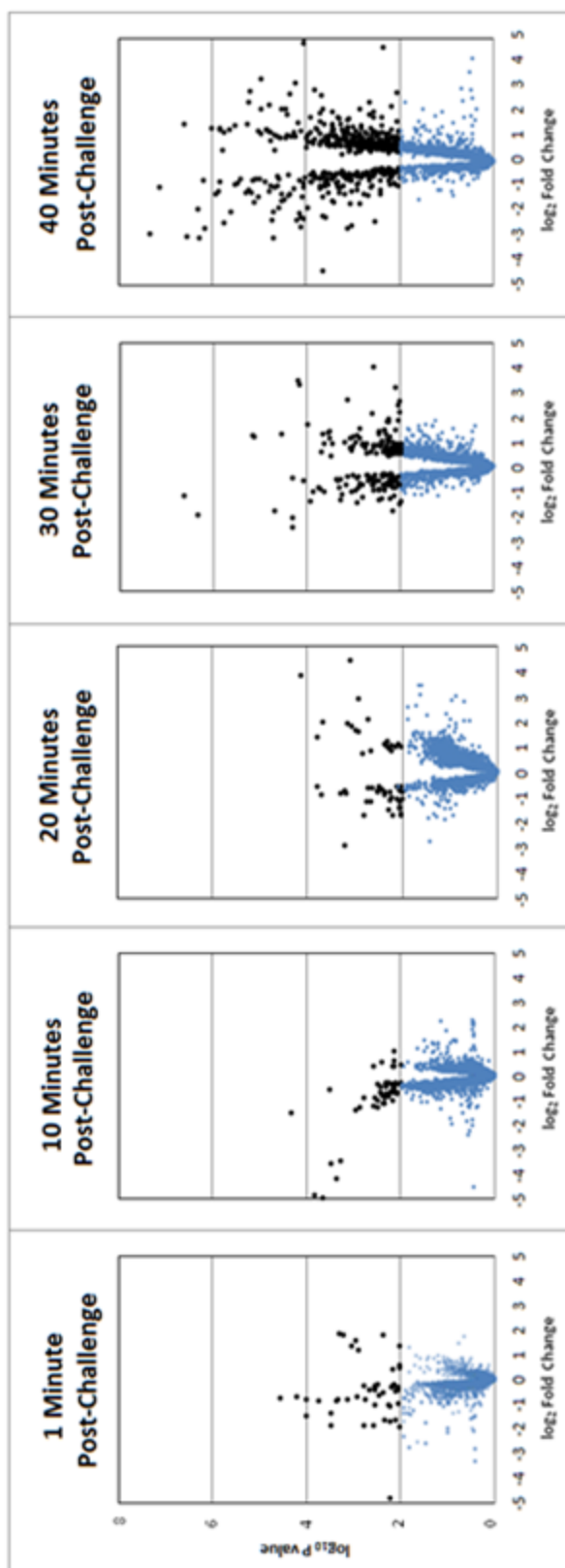


Figure 5.9. Volcano plot of metabolite features at various time stages from the second peanut challenge experiment comparing sensitized mice to mice treated with peanut only. Features appearing in black represent those with p-values <0.01. Each data plot contains ~3500 data points.

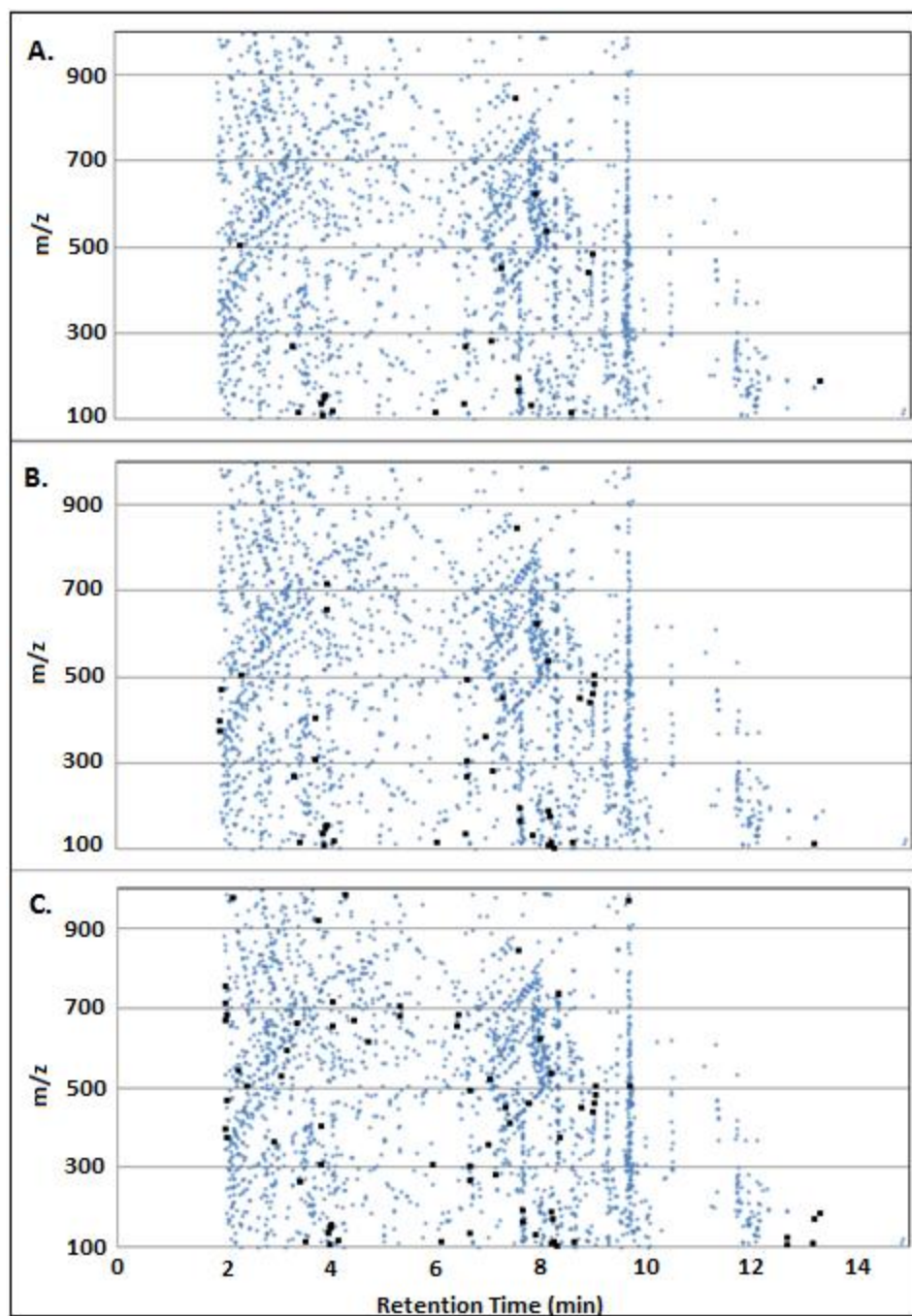


Figure 5.10. Plot of 3500 metabolite features observed in all samples plotted by retention time (minutes) versus m/z ratio. Features appearing in black are statistically significant ($p < 0.01$) pre-challenge (panel A), one-minute post-challenge (B) and 10 minutes post-challenge (C). Features from 20-40 minutes appear in Figure 5.11 (next page).

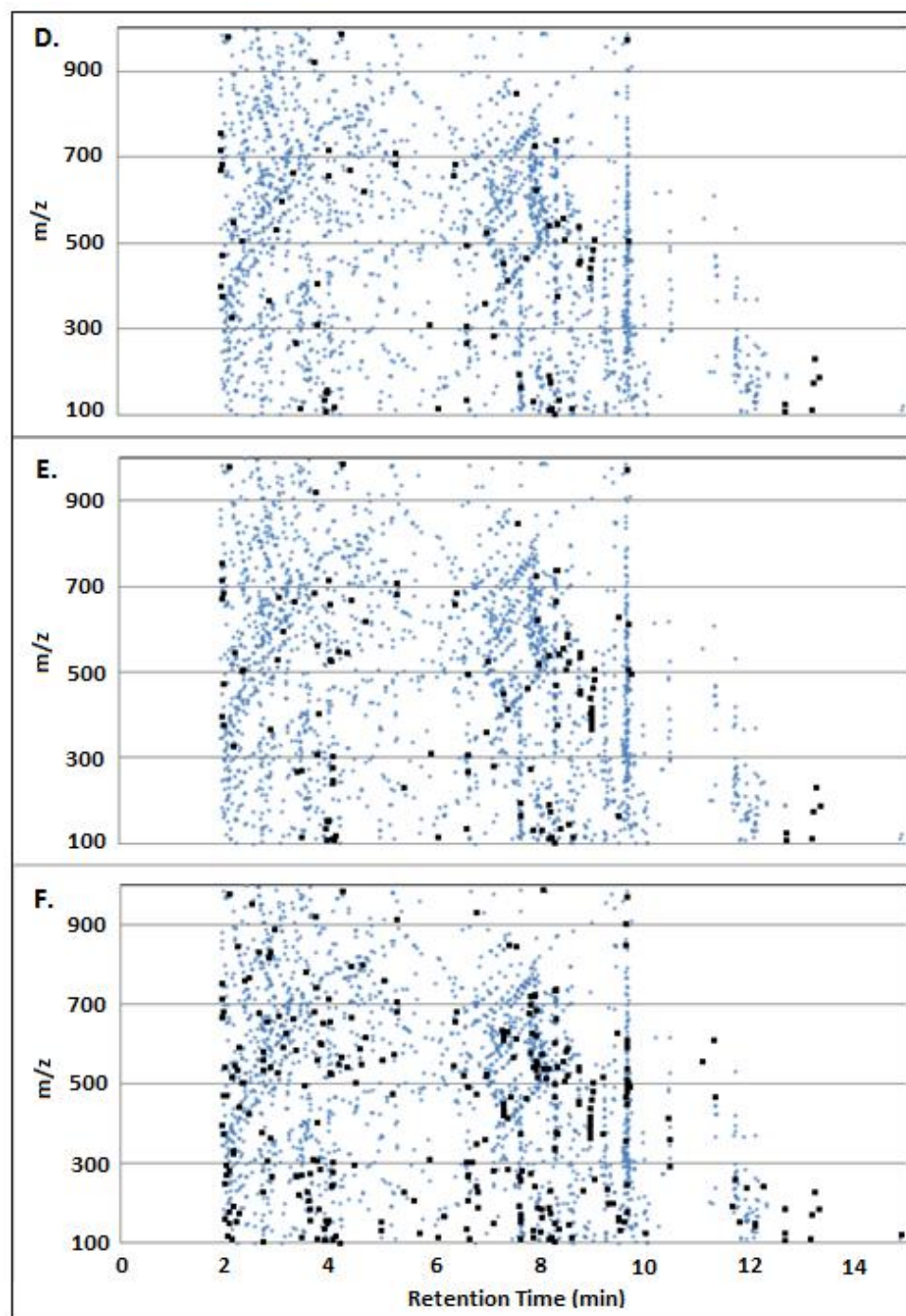


Figure 5.11. Plot of 3500 metabolite features observed in all samples plotted by retention time (minutes) versus m/z ratio. Features appearing in black are statistically significant ($p < 0.01$) 20 minutes post-challenge (panel D), 30 minutes post-challenge (E) and 40 minutes post-challenge (F).

5.3.6. Identification of Statistically Significant Metabolite Features in the Second Challenge Experiment

Of the 3500 metabolite features extracted and processed by XCMS and CAMERA, 30 features were found to be significant in the one-minute post-challenge samples with p-values less than 0.01. Of these 30 features, 12 had p-values less than 0.001. By the ten-minute point post-challenge, 73 features were found to be significant (p-value <0.01) with 17 having p-values less than 0.001.

The challenge at this point in the analysis was to determine the identity of these 73 metabolite features. Authentic chemical standards were shown to match 15 peaks in terms of their retention times and mass spectra. These species are shown as “green” entries in Table 5.3. Another group of compounds, shown as yellow in Table 5.3 were tentatively identified based on their mass spectral matches in databases such as METLIN (Scripps Institute for Metabolomics). Finally there were 15 unidentified compounds for which molecular formulae were derived from high mass resolution MS data and an additional eight features which are listed as “unknowns”.

Recently, (November 2012) a high-resolution quadrupole-time-of-flight mass spectrometer (Bruker maXis 4D) became available through the Biointerfaces Institute (McMaster University). This instrument is capable of MS/MS analyse at mass resolution of about 65,000 FWHM. Based on the retention time and MS data collected on the Bruker micrOTOF instrument, the maxis 4D instrument could be programmed with CID (collision-induced dissociation) experiments in order to obtain MS/MS data. From

analysis of these MS/MS spectra, 22 of the 73 features (~30%) were shown to be either unusual adduct peaks or in-source fragmentation peaks of parent molecules. An example spectrum is given in Figure 5.12 where an isomer of methylhistamine was found. These features were not identified by CAMERA. Thus, the list of analytes decreased from 73 to the 51 features which are listed in Table 5.3. Beyond the features appearing up to 10 minutes post-challenge, hundreds of other metabolite features were identified by 20 minutes post-challenge and later (appendix 4). Attempts to identify as many of these compounds by MS/MS in the limited amount of time available were made with the year-old sample remaining from the initial analyses on the lower resolution Bruker micrOTOF II.

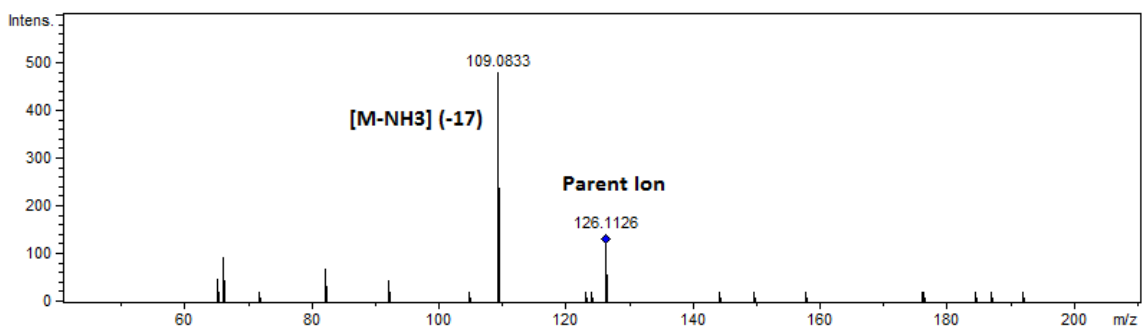


Figure 5.12. Positive mode MS/MS spectra of peak 126.113 with a CID energy of 10 eV. Although accurate mass measurements and fragmentation strongly indicates methylhistamine it cannot distinguish the position of the methyl group.

Table 5.4. Fifty-one metabolites found to be significantly altered in early stage PIA (by 10 minutes post challenge). Metabolites highlighted in green were identified by comparison to authentic chemical standards; metabolites in yellow were identified based on good matches between their mass spectra and mass spectra in databases; chemical formulae of metabolites in light red were assigned based on accurate mass and isotope ratio measurements. The remained are listed as unknowns.

m/z	RT (min)	P-values (ANOVA)	ID	m/z	RT (min)	P-values (ANOVA)	ID
(-)99.010	8.2	9.86E-05	Succinic anhydride	(+)382.148	6.6	1.66E-05	Met-Met-Thr
(+)104.107	8.2	1.40E-07	Choline	(+)399.271	2.0	8.34E-04	C ₁₈ H ₃₅ N ₆ O ₄
(-)110.025	4.5	7.84E-05	Cytosine	(-)405.268	3.8	2.53E-06	C ₂₄ H ₃₈ O ₅
(+)112.093	13.1	2.42E-14	Histamine	(+)414.595	7.3	9.26E-04	Unknown
(-)115.005	8.1	2.58E-04	Maleic acid	(+)441.215	8.9	6.21E-07	C ₂₀ H ₃₂ N ₄ O ₅ S
(+)116.071	8.9	6.00E-02	Proline	(+)452.132	8.7	6.77E-12	C ₂₂ H ₂₀ N ₄ O ₇
(+)126.022	9.2	3.87E-05	Taurine	(+)458.275	8.7	7.11E-12	C ₂₃ H ₄₀ NO ₈
(+)126.102	12.6	1.40E-13	Methylhistamine	(+)496.181	6.6	4.42E-05	lysoPC(16:0)
(+)132.077	9.5	4.04E-02	Creatine	(+)502.298	7.0	7.42E-06	lysoPE(20:4)
(+)137.047	3.9	2.56E-05	Hypoxanthine	(-)519.437	26.5	1.15E-02	C ₂₈ H ₅₉ N ₂ O ₆
(+)174.014	13.1	1.51E-16	C ₄ H ₄ N ₃ O ₅	(+)526.337	7.0	1.23E-04	C ₂₂ H ₄₉ N ₅ O ₇ P
(-)175.027	8.2	1.16E-04	Ascorbic acid	(+)531.342	3.0	1.85E-04	C ₂₄ H ₄₈ N ₆ O ₅ P
(-)181.052	3.6	2.63E-04	Homovanilic acid	(+)658.544	6.4	2.54E-04	Unknown
(-)191.021	8.2	4.59E-05	Citric acid	(+)658.549	4.0	5.44E-07	C ₄₀ H ₇₃ N ₃ O ₄
(+)218.139	8.7	4.38E-02	Propionylcarnitine	(+)665.049	3.3	2.74E-05	Unknown
(+)246.170	7.8	1.27E-02	2-Methyl-butylcarnitine	(+)670.426	4.4	1.22E-03	PE(29:1)
(+)269.102	6.6	2.02E-05	Inosine	(+)671.368	2.0	9.51E-05	Unknown
(-)274.074	6.6	5.40E-04	C ₁₄ H ₁₂ NO ₅	(+)682.543	5.2	7.91E-04	Unknown
(-)282.085	7.9	3.01E-04	Guanosine	(-)685.491	6.4	1.78E-03	Unknown
(+)282.125	8.6	4.16E-01	1-Methyladenosine	(-)709.426	5.2	2.80E-03	Unknown
(-)283.075	7.1	1.23E-06	Xanthosine	(-)717.447	4.0	2.24E-07	PG (32:2)
(-)309.281	3.8	8.16E-06	Eicosenoic acid	(+)738.565	8.3	2.98E-02	PC(23:5)
(-)311.294	5.9	9.41E-04	Arachidic acid	(+)740.462	8.3	1.56E-03	PC(23:4)
(-)357.110	6.6	7.67E-05	C ₁₈ H ₁₈ N ₂ O ₆	(+)757.396	2.0	1.09E-02	C ₃₃ H ₆₁ N ₂ O ₁₇
(-)367.284	2.9	1.44E-06	C ₂₀ H ₃₇ N ₃ O ₄	(+)982.032	2.1	8.83E-04	Unknown
(+)377.257	2.0	1.38E-03	C ₂₂ H ₃₅ NO ₄				

5.4. Discussion

5.4.1. Global Metabolite Profile in Mice Reflects Clinical Measurements and Observations

The assessment of PIA severity in mice is typically done by examination of clinical measurements such as core temperature decrease, rise in hematocrit levels as well as behavioral observations such as scratching, lethargy, and even seizures¹⁰⁵. In the two challenge experiments, behavioral symptoms of PIA (scratching, lethargy etc.) were observed in between the 10- and 20-minute time-points in the first experiment and between the 1- and 10-minute time-points in the second experiment. These observations correlate with the greatest changes in hematocrit levels and core body temperature. Not surprisingly, analysis of global metabolite profiles by OPLS-DA reveals that mice at the 20-minute time point were the most discernible from the starting profiles in the first challenge experiment and at the 10-minute point in the second experiment. Thus, significant changes found in the mouse metabolome parallel the clinical observations of an acute immunological attack.

This work is the first global analysis of metabolites involved in PIA and provides a large-scale discovery approach to the chemical features which are changing significantly with both the time progression of PIA and the severity of the anaphylaxis. The ability to clearly differentiate anaphylactic from non-anaphylactic mice and identify the stage of anaphylaxis presents significant opportunities to develop novel diagnostic tools which may provide new diagnostic procedures for early stages of PIA. The first goal of this part

of the work, was to assess the capabilities and utility of comprehensive metabolomics in peanut allergies has been addressed.

5.4.2. Metabolite Changes in Mice Reflective of Early Stage PIA

From both a diagnostic and critical care perspective, molecules which are released in the early stages of PIA are of special importance since these molecules are likely the key agents that are indicators of the first clinical symptoms of anaphylaxis¹⁰⁹. While metabolites released at this stage may not be the mediators which are the cause of PIA, these molecules may represent useful monitors of PIA.

Analysis of mice at the one-minute time point after challenge in the first experiment revealed 9 metabolite features that were elevated significantly or decreased significantly (as measured by fold change ± 1.5 with ANOVA and t-test p values < 0.01). These metabolites are listed in Table 5.1. At the one-minute time point of the second peanut challenge experiment revealed 30, features with p-values < 0.01 , and 12 features with p-values < 0.001 had emerged. By 10 minutes an additional 43 features (for a total of 73) with t-test and ANOVA values less than 0.01, 5 of which had p-values less than 0.001 for a total of 17. Attempts to identify these features through MS/MS experiments revealed that 22 of these total features were unusual adduct ions, such as the addition of multiple sodium ions or were in-source fragment ions such as the loss of the choline head-group in phosphatidylcholines (PC) and lysophosphatidylcholine (lysoPC) lipids.

These unusual adduct ions and fragments were “missed” by CAMERA. This work led to the final list of 51 metabolites (Table 5.3).

A number of metabolites released and/or elevated in the first 10 minutes after intraperitoneal peanut challenge were histamine and methylhistamine, known markers of mast cell degranulation¹¹⁰. Interestingly, a number of the other metabolites identified were epinephrine and ascorbic acid which are known to possess vaso-dilatory or vaso-constrictive properties¹¹¹. These compounds were released soon after challenge, likely in response to blood pressure changes induced by histamine. These molecules are not claimed to be mediators of PIA. However, their release provides additional evidence that PIA has occurred and that immediate changes at the molecular level are in fact happening at detectable levels in the serum of these animals.

Of the remaining identified molecules released or elevated in the early stages of PIA, a number of metabolites are of special interest. One metabolite, taurine also is known to effect blood pressure¹¹² in addition to its role as a component of many bile acids and as a neurotransmitter in the brain. Taurine has not been directly correlated to anaphylaxis but its wide ranging properties inspired the Jordana group to study the effects of taurine further. Although it is still in the preliminary stages, this work is yielding evidence that blocking taurine production in mice does ameliorate the severity of anaphylaxis.

Another interesting compound, choline, also has neuroactive properties and is an essential component of the phosphatidylcholine lipids which comprises a large percentage of the lipids in cell walls. Similarly, a large wide-spread change in phospholipids including phosphatidylcholines, phosphatidylethanolamines and lyso-phosphatidylcholines and is also observed. These changes are significant evidence of mast cell and basophil degranulation¹¹³. Biomarkers of anaphylaxis, the leukotrienes, and a confirmed mediator of PIA, platelet activating factor (PAF), are known to originate from scavenged cell wall remnants and other phosphocholines respectively¹¹⁴. Most phospholipid compounds have not been directly linked to anaphylaxis, however, their potential as biomarkers and their role in the chemical mechanisms of generating known mediators and other active compounds represent novel avenues of research which warrant further investigation.

5.4.3. Late Stage PIA Metabolic Changes

Although perhaps not as diagnostically important, metabolites that appear in late stages of PIA are probably important to achieve and understanding of the overall immunological response mechanism. Some of these metabolites such as the cystienyl-leukotrienes are known to be up to 100 times more potent than histamine¹¹⁵. By 20 minutes post challenge many new metabolite features appeared that were not observed in early stages of PIA. While the precise numbers of these later appearing features are undoubtedly fewer than what is initially revealed by statistical analysis,

there is no doubt that the number of metabolic features increases almost exponentially throughout the remainder of the anaphylactic attack as seen in Figures 5.7 and 5.8. Indeed by 40 minutes post challenge as many as 800 of the 3500 metabolites (~29%) have t-test p values of less than 0.01 and as many as 150 which have p values less than 0.001. The later included arachidic acid, leukotriene C₄ and LTB₄ which is a leukotriene-related arachidonic acid metabolite.

A great many of these metabolites cannot be identified due to a lack of standards and no matches with metabolite databases. There was also a profound increase in the numbers of phosphatidylcholines, lysophosphatidylcholines and phosphatidylethanolamines that were elucidated based on accurate mass measurements, MS/MS fragmentation patterns and isotope ratio measurements together with estimates based on LC retention observations. As stated in section 5.4.3 these lipids must arise from the activation of biochemical pathways during PIA and may represent novel biomarker and mediator candidates.

5.4.4. Special Challenges to Screening for PIA Mediators

While the identification of metabolites undergoing significant changes during PIA presents the opportunity for the discovery of potentially novel mediators (taurine) and confirmatory PIA molecules (leukotrienes, histamine, etc.), other metabolites such as arachidonic acid, a poly-unsaturated, 20 carbon fatty acid, and its saturated relative, arachidic acid, highlight challenges to the discovery of biologically relevant molecules

especially for food induced anaphylaxis. Arachidonic acid is an essential precursor to the leukotrienes and other eicosanoids¹¹⁶, many of which have known mediator function, meanwhile, arachidic acid is a relatively benign molecule. Both of these fatty acids are commonly found in peanut oil as a component of peanut oil¹¹⁷. While metabolomics may identify the increase in arachidic and arachidonic acid after intraperitoneal injection, it is incapable of predicting whether they originated from administration of peanut extract via intraperitoneal injection or from metabolism occurring due to the activation of the immune response which can synthesize and release these and related compounds.

A similar challenge also presents itself upon analysis of metabolism occurring in non-sensitized mice where the levels of metabolite are found to change although not in a manner which leads to easily identifiable trends. Another related challenge to identifying potential mediators which is illustrated in the work by Hu et al. arises due to the general increase of metabolic activity due to the mental and physical toll anaphylaxis exacts on the body¹⁰⁷. Like the study performed by Hu, a number of metabolites which are known to be completely unrelated to anaphylaxis are found to be altered after anaphylaxis has occurred such as glucose (as its Na⁺ adduct) which is observed to decrease after 30 minutes post challenge. These metabolite changes are hypothesized to be the result of down-stream effects from the PIA response and do not hold value for further study despite the noticeable changes which occur post-challenge.

5.5. Conclusions

The first goal of this work was to assess the capability and utility of a comprehensive metabolomics approach to determine whether PIA has occurred and to evaluate the degree of anaphylaxis being experienced by the mice. To this end OPLS-DA analysis has shown that a global metabolite analysis is indeed capable of differentiating anaphylactic subjects from healthy subjects. The second goal of this work was to determine whether a comprehensive metabolomics approach would be useful as a discovery tool to identify novel biomarker and mediator candidates. In this regard this work led to the discovery of a vast array of phospholipids that were released or increased during PIA, along with other metabolites such as taurine which have potential as biomarker candidates.

Further clinical and immunology-based studies will be required to determine whether the molecules identified in this approach are key biomolecules involved in this important immunological event. This analysis has demonstrated the huge potential of comprehensive metabolomics and LC-MS at medium mass resolution as a useful discovery platform for allergy research.

Chapter 6. Comprehensive Metabolomics of Pediatric Blood Serum Samples from Peanut Allergic Patients

6.1. Introduction

Animal models have proven to be invaluable for allergy research⁷; however, the quintessential test subjects will always be human patients since the overall goal is to develop clinical and therapeutic applications for humans. Working with human subjects presents a number of experimental difficulties which may complicate the results and their interpretation. Unlike animal-based anaphylaxis model studies where researchers can rigorously control the gender, age, diet, environment, and number of the subjects, human studies inherently involve a substantial degree of variability since subjects must be volunteers who, in addition to variables previously mentioned, may come from a variety of lifestyles and ethnic backgrounds.

Furthermore, experimental variables are compounded by ethical constraints; an example of such a constraint is that a sensitized animal such as a mouse may be challenged with a dose of a peanut sample far exceeding the amount required to induce full-blown anaphylaxis. A human challenge experiment on the other hand, must use much smaller dosages and must be terminated as soon as the first clinical symptoms of an allergic reaction arise³⁰.

**Disclaimer: All work described in this chapter was approved by the Research Ethics Board of McMaster University. Human samples were collected as part of an on-going allergen study led by Dr. Susan Waserman, Dept. of Medicine, McMaster University; human serum samples were extracted by Joshua Kong.*

Since PIA is not fully induced in human subjects, PIA mediators may not be released in sufficient quantities for detection. For this reason known biomarkers such as the leukotrienes are unreliable for diagnosis in humans²⁸.

In light of the positive metabolomic results found in mice described in Chapters 4 and 5, an unplanned but welcome opportunity to apply comprehensive metabolomics analysis to a small subset of human serum samples arose serendipitously. Nine peanut-allergic children had participated in a peanut challenge experiment as part of a larger allergen study conducted at the McMaster Children's Hospital under the supervision of Dr. Susan Wasserman. Very small volumes of serum from these children (~10µL each) were provided to us for metabolomic studies. The original goal of the Wasserman led study was to establish the degree of tolerance or threshold levels to peanuts for these children.

For this metabolomic study, the blood from nine children with known hypersensitivity to peanuts was collected before the oral peanut challenge. Then the patients were challenged with an oral dose of peanuts. If the child complained of discomfort or symptoms such as itchiness, breathing difficulty, etc., a second blood sample was taken and the challenge experiment was terminated. For patients not responding to the initial dose after 20 minutes, another, larger dose of peanuts was given. This sequence was repeated every twenty minutes until a response was observed.

These symptoms occurred anywhere from 10 minutes to 2 hours after the initial dose of peanuts had been administered.

Although the experimental design was not optimal for metabolomic studies, the offer to analyze nine of these samples was an extraordinary opportunity. Since pre-challenge sample and post-challenge sample were collected from the same patient, each patient acted as his/her own control. In other words, the pre-challenge serum sample reflected the subject's initial metabolic state which of course would be different from another subject. By comparing this pre-challenge sample to the post-challenge sample from the same patient, the metabolite variation between subjects are minimized. While unintended, this experimental design feature de-emphasizes metabolites which were unique to the subject from sources such as diet, lifestyle etc. and emphasizes metabolite changes which occur solely due to the oral challenge with peanuts. Despite the small number of total subjects, this analysis was an ideal opportunity to determine whether a larger scale study would be warranted. The specific goal of this work was to assess the capability of comprehensive metabolomics for the discovery of metabolites that may be diagnostic biomarkers or mediators of peanut-induced anaphylaxis in humans and to compare these data to the mouse data discussed previously.

After sample collection, the blood was allowed to clot and the clear serum was removed and stored at -80°C. Samples were extracted as outlined in Chapter 2 and

analyzed by LC-ESI-TOF-MS in both positive and negative ionization modes with the dual column (ZIC-RP Amide) method developed in Chapter 3.

6.2. Results

Pre-challenge and post-challenge blood serum samples from 9 peanut allergic children were analyzed in order to compare pre-challenge metabolite levels to post-challenge levels. This analysis yielded a total of 5500 extracted and aligned metabolite features, many of which only appeared in individual samples or in the paired pre-challenge and post-challenge sets from a single child. Global multivariate analysis of all 5500 metabolite features using PCA analysis (unsupervised method) and by OPLS-DA (supervised method) show a clearly defined separation of pre-challenge and post-challenge samples (figures 6.1 and 6.2, respectfully). OPLS-DA gave regression and goodness of fit scores of 0.55 and 0.94 respectively indicative of a very robust predictive model.

Out of the 5500 metabolite features observed in all samples, approximately 2100 unique metabolite features were found in at least 6 of the 9 subjects with an average biological variability of ~50%. Of these 2100 common features approximately 200 features appeared only in the post-challenge samples. This is an astonishing number of new, post-challenge features, many of which were among the largest peaks observed in the post-challenge chromatograms. In addition, 70 features in the post-challenge data set showed significantly increased levels compared to pre-challenge levels ($p < 0.01$)

together with an additional 43 features were found to have decreased significantly compared to pre-challenge levels. Finally, 15 features were found to have decrease to such a degree that they were not detected in the post-challenge samples. Table 6.1 lists the identified metabolites which were observed to significantly increase or decrease post-challenge or only appear in the post-challenge samples.

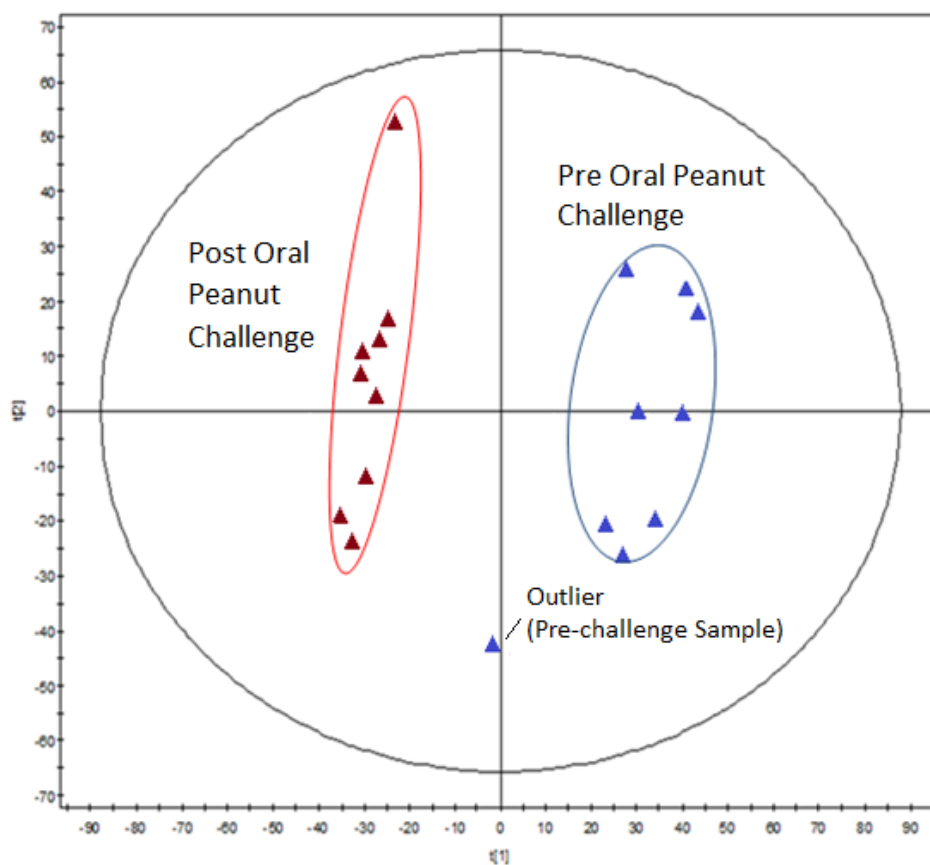


Figure 6.1. Principal component analysis (PCA) score plot of blood serum samples from 9 children known to have peanut allergy before and after oral peanut challenge.

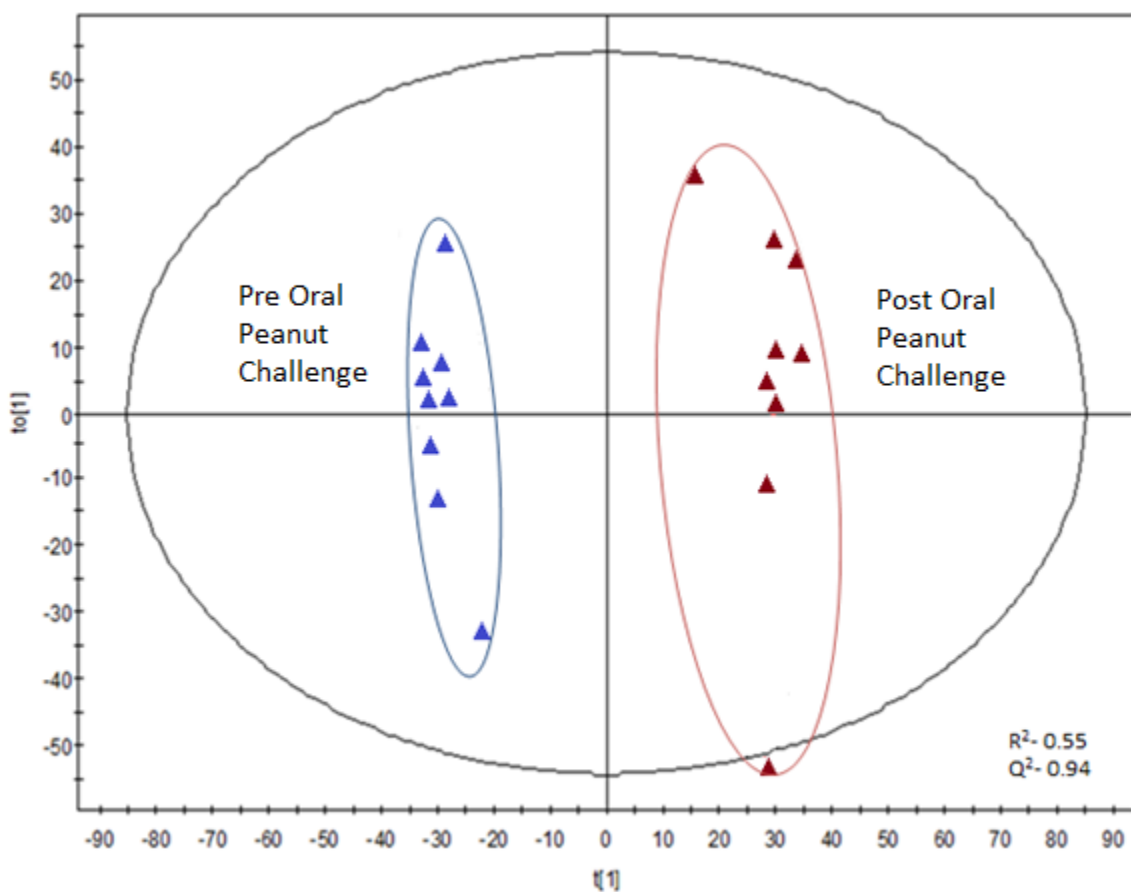


Figure 6.2. Orthogonal partial least squares-discriminate analysis (OPLS-DA) score plot of blood serum samples from children with known peanut allergy pre-challenge and post-oral peanut challenge. Note using a priori knowledge of the samples, regression analysis can be applied to the PCA model and a quantitative prediction model can be generated. A very high Q^2 value (0.94) indicates that the model is very robust.

Table 6.1. Metabolites observed to increase or decrease in serum samples obtained from children with peanut allergies after an oral peanut challenge compared to their pre-challenge levels. Metabolite features appearing in green have been identified by comparison to authentic chemical standards; metabolites appearing in yellow were identified based on good matches between their mass spectra and mass spectra in databases; chemical formulae of metabolites in red were assigned based on accurate mass and isotope ratio measurements. For features which did not appear in pre-challenge samples the average fold change was estimated by dividing the S/N of the peak by the quantitation limit (S/N=10).

m/z	Identification	Retention Time (min)	Average Fold Change	t-test
(+)110.036	C ₄ H ₄ N ₃ O	4.1	0.43	1.4E-04
(-)124.007	Taurine	9.3	0.54	2.2E-05
(+)126.023	Taurine	9.3	0.55	1.2E-05
(-)151.025	Xanthine	4.3	0.48	8.9E-05
(+)153.043	Xanthine	4.2	0.48	2.1E-04
(-)154.049	C ₅ H ₆ N ₄ O ₂	2.8	15	9.2E-04
(-)161.037	C ₆ H ₉ O ₅	2.5	8	5.8E-04
(-)175.075	C ₁₁ H ₁₁ O ₂	10.3	0.57	1.0E-02
(+)231.087	C ₆ H ₁₁ N ₆ O ₄	4.1	2.49	6.6E-04
(-)232.027	Dopamine Sulfate	3.4	700	1.3E-03
(-)233.014	Phenylglycol-3-O-sulfate	4.5	10	3.7E-04
(-)246.991	C ₄ H ₇ O ₁₂	3.9	5	1.3E-03
(+)253.133	C ₁₆ H ₁₇ N ₂ O	4.2	2	2.6E-04
(+)274.194	Val-Arg	11.9	0.48	4.2E-04
(+)275.121	C ₇ H ₁₅ N ₈ O ₄	4.2	4	1.7E-04
(+)309.238	C ₁₇ H ₃₄ O ₃ Na	2.0	10	7.9E-04
(+)311.140	Phe-Phe	6.9	0.31	6.4E-05
(+)313.158	Phe-Phe	6.8	0.31	4.1E-05
(+)314.184	C ₁₃ H ₂₄ N ₅ O ₄	4.5	3	5.2E-05
(+)335.114	C ₁₀ H ₂₁ N ₆ O ₃ P ₂	4.5	3	1.1E-04
(+)362.226	C ₁₂ H ₂₈ N ₉ O ₄	3.6	30	2.9E-06
(+)377.264	C ₂₀ H ₃₃ N ₄ O ₃	2.1	10	1.8E-07
(+)379.253	Neuroprostane	3.5	40	8.9E-06
(+)388.260	C ₂₂ H ₃₄ N ₃ O ₃	2.0	15	5.6E-06
(+)401.266	C ₂₃ H ₃₈ O ₄ (Na ⁺)	4.0	6	3.2E-06
(+)402.237	C ₁₄ H ₃₆ N ₅ O ₆ S	5.6	3	3.0E-05
(+)406.253	C ₁₄ H ₃₂ N ₉ O ₅	4.5	20	1.9E-06
(+)421.285	C ₂₀ H ₄₂ N ₂ O ₅ P	2.1	60	2.0E-06
(+)452.305	C ₁₈ H ₄₂ N ₇ O ₄ S	3.2	9	2.0E-06

(-)455.232	$C_{24}H_{32}N_4O_5$	3.7	3	1.0E-02
(+)465.310	PA(20:1)	2.9	400	1.2E-06
(+)466.331	PE(18:0)	2.9	7	3.5E-06
(+)467.305	$C_{16}H_{39}N_{10}O_6$	5.8	20	1.4E-06
(+)476.318	LysoPC(O-16:3)	2.2	35	3.1E-06
(+)482.315	LysoPC(O-16:0)	5.5	24000	3.1E-06
(+)511.331	$C_{18}H_{43}N_{10}O_7$	6.7	15	3.3E-07
(+)518.340	LysoPC(18:3)	4.5	40	2.1E-06
(+)520.342	LysoPC(18:2)	2.3	150	2.8E-06
(+)524.343	LysoPC(18:0)	2.8	2500	1.1E-05
(+)539.270	$C_{20}H_{40}N_6O_9P$	2.4	4	2.3E-04
(+)540.354	LysoPS(20:0)	5.1	50	2.3E-06
(+)555.356	PG(21:0)	7.1	10	2.3E-07
(+)562.364	LysoPE(24:2)	5.8	120	1.5E-06
(+)564.372	LysoPE(24:1)	2.5	50	3.2E-06
(+)566.413	LysoPE(24:0)	2.5	10	2.8E-06
(+)580.420	LysoPC(22:0)	2.0	0.38	1.0E-02
(-)581.294	$C_{31}H_{42}N_4O_5P$	2.9	15	1.0E-05
(+)606.391	LysoPC(24:1)	6.6	20	8.5E-07
(+)608.403	LysoPC(24:0)	2.7	65	4.0E-06
(-)625.323	$C_{33}H_{46}N_4O_6P$	3.2	60	7.5E-06
(-)635.352	$C_{23}H_{51}N_6O_{14}$	3.1	5	1.9E-06
(+)659.505	LysoPA(P-34:1)	2.5	0.33	2.5E-03
(-)669.344	PI(22:0)	3.0	15	1.0E-05
(-)679.372	$C_{31}H_{52}N_8O_7P$	3.8	14.5	3.5E-06
(+)693.455	LysoPA(36:6)	2.0	40	3.7E-06
(+)712.509	LysoPE(34:4)	2.2	0.42	5.9E-04
(-)713.373	$C_{26}H_{54}N_{10}O_{11}P$	3.4	10	3.6E-06
(-)723.400	PI(26:1)	3.3	20	2.3E-06
(-)740.391	$C_{25}H_{59}N_9O_{14}P$	3.3	150	1.2E-06

Figure 6.3 shows the fold change of all 2100 mass spectral features after challenge as a function of mass-to-charge ratio. For those features which did not appear in pre-challenge (or post-challenge) samples, the fold change was estimated by dividing the S/N ratio of the peak in the post challenge chromatogram by 10 (the S/N quantitation limit). Figure 6.4 shows the fold change post-challenge as a function of mass-to-charge ratio for those metabolites which had p values less than 0.01.

Figure 6.5 displays a volcano plot showing the log of the net fold change of all 2100 metabolite features as a function of the $-\log$ of the t-test p value. Figure 6.6 shows the retention times of all 2100 metabolite features as a function of their m/z ratios. Table 6.2 summarizes the numbers of features appearing only in post-challenge samples, only in pre-challenge samples, and by increase/decrease grouped by m/z range. Finally, Table 6.3 summarizes the number of features changing by degree of fold change range, grouped in three m/z ranges.

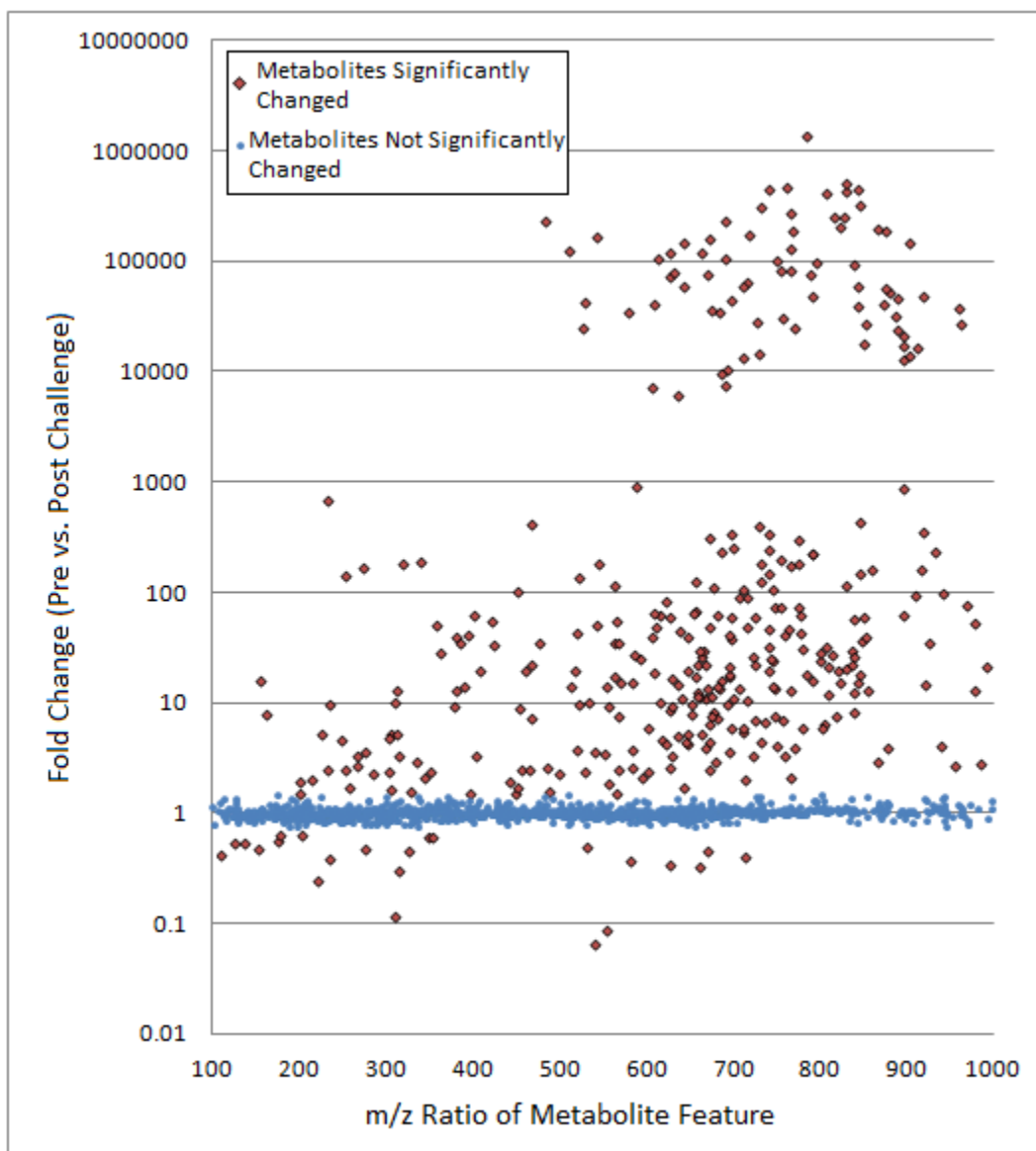


Figure 6.3. Plot of fold change (post-challenge vs. pre-challenge) for 2100 metabolite features in human serum as a function of mass-to-charge ratio. Note, of the total observed features, approximately 200 were only observed in post-challenge samples.

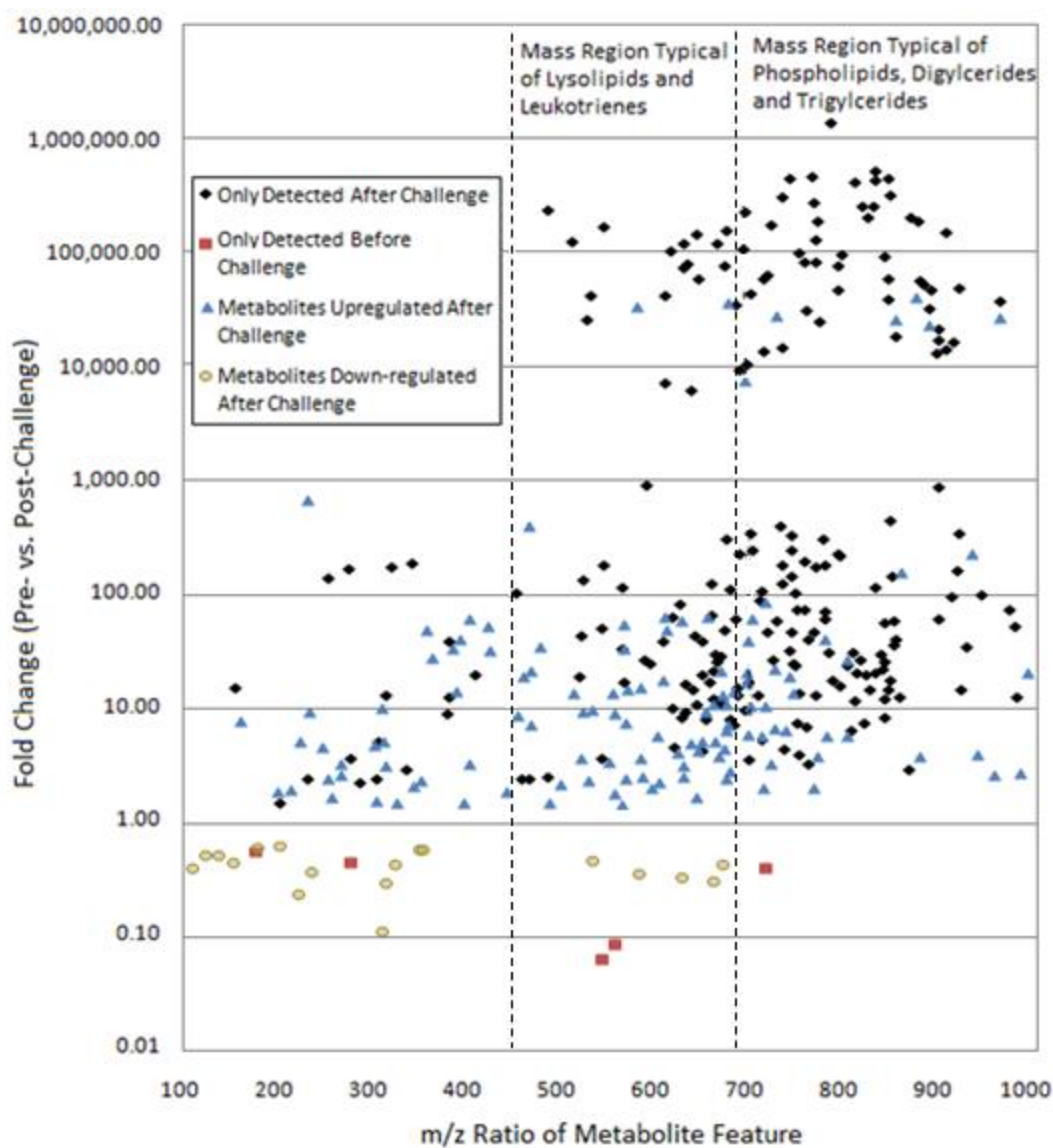


Figure 6.4. Plot of fold change (post-challenge vs. pre-challenge) for metabolite features found to be significantly different in human serum ($p < 0.01$ i.e., red diamonds-shaped points in Figure 6.3) plotted as a function of the mass-to-charge ratio of the metabolite feature. For metabolites only appearing in post-challenge samples the average fold change was estimated by dividing the S/N of the peak by the quantitation limit ($S/N=10$).

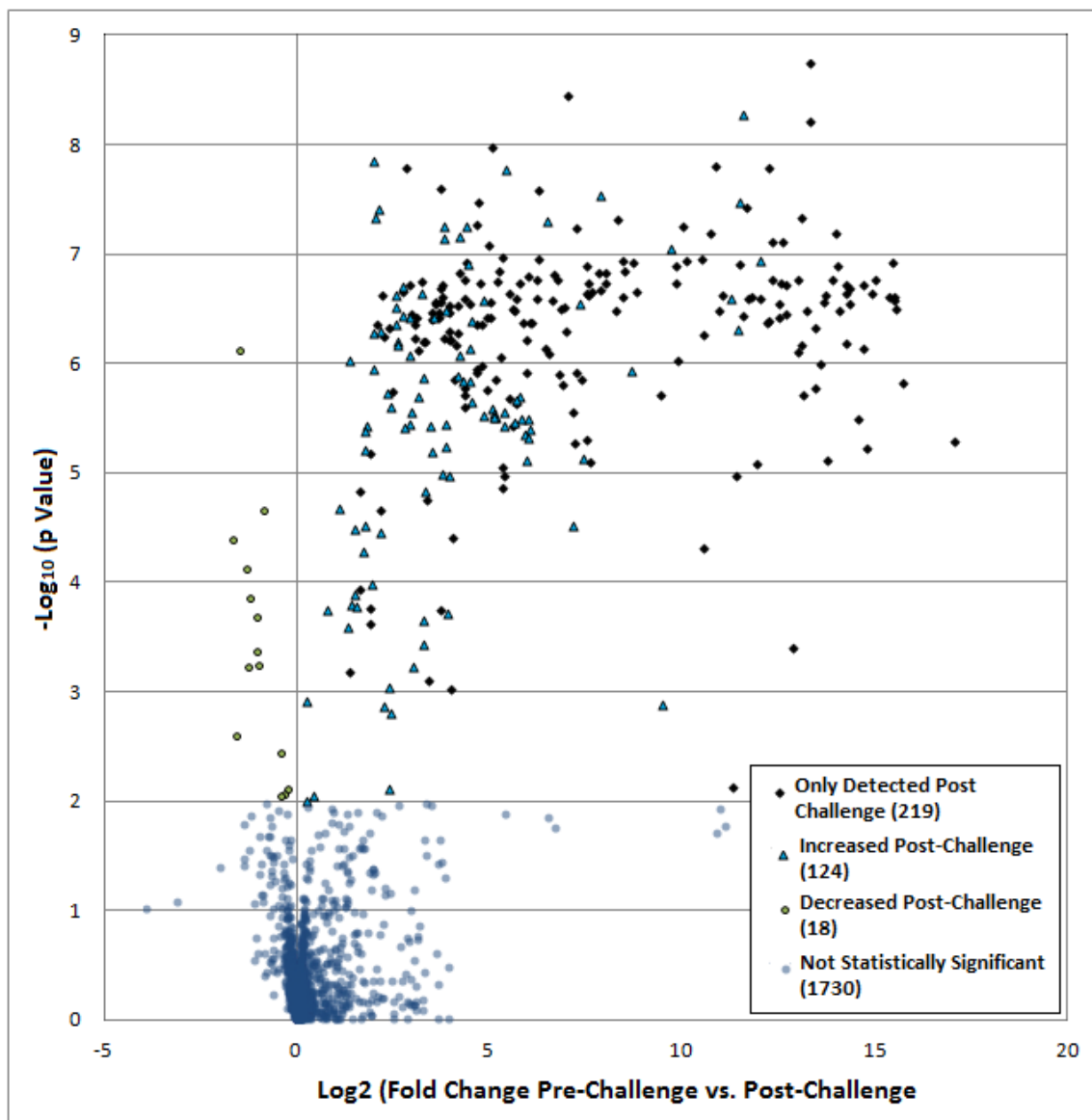


Figure 6.5. Volcano plot of approximately 2100 metabolite features observed in human challenge samples. Note, very few features (47) appeared between 3-5 on the $-\log_{10} p$ Value scale (p between 10^{-3} - 10^{-5}) compared to the number of features (314) appearing above 5 (p values $<10^{-5}$). For metabolites only appearing in post-challenge samples the average fold change was estimated by dividing the S/N of the peak by the quantitation limit (S/N=10).

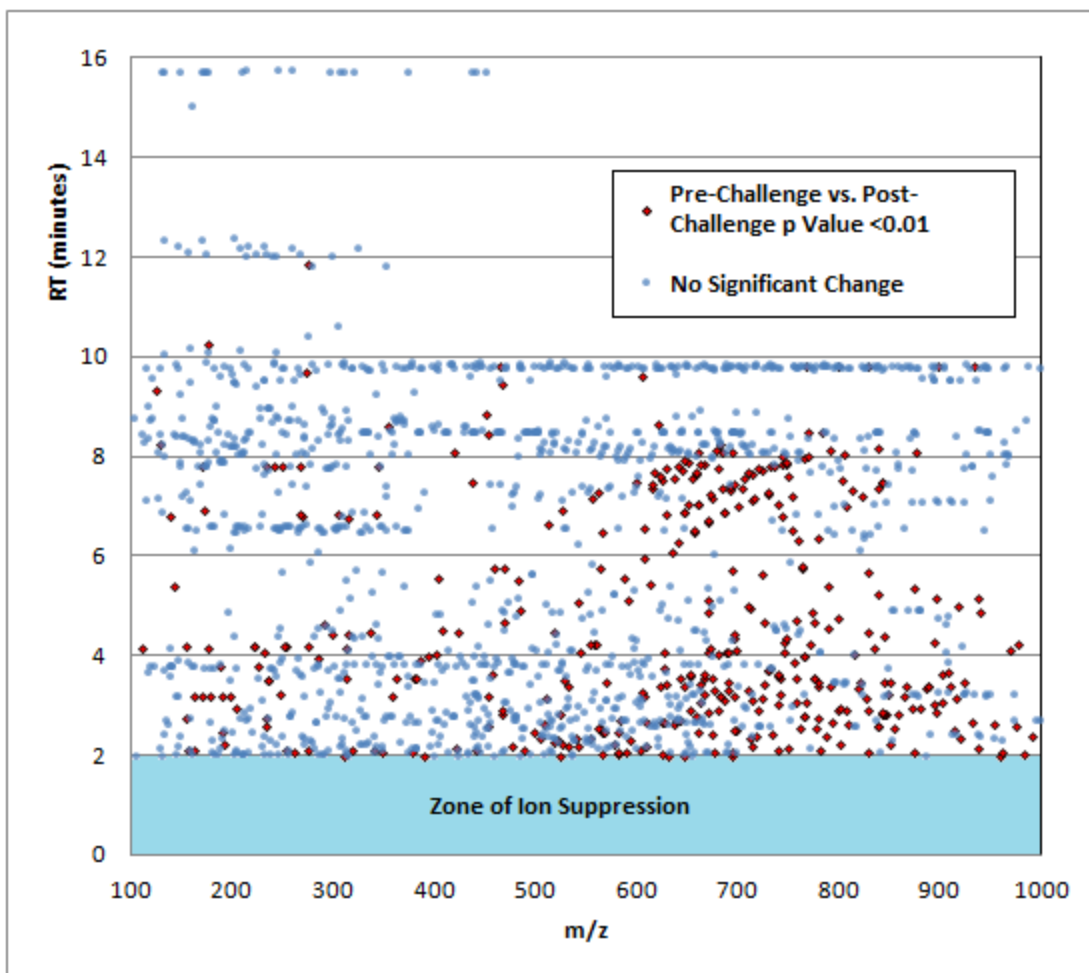


Figure 6.6. Chromatographic profile of the 2100 metabolomic features found in at least 5 subjects plotted as retention time versus m/z ratio. Features which had undergone significant change are highlighted in red. The zone from 0-2 minutes ends at $k' = \sim 0.7$ and is a zone where ion suppression is known to occur.

Table 6.2. Numbers of metabolite features which showed statistically significant changes in levels ($p < 0.01$) in either pre-challenge or post-challenge serum samples collected from children who are allergic to peanuts following oral challenge with peanuts. The metabolites are arranged in one of three groups according to their m/z range.

	# Metabolite Features m/z 100-450	# Metabolite Features m/z 450-700	# Metabolite Features m/z 700-1000	Total # Metabolite Features
Metabolites with increased levels post-challenge vs. pre-challenge	31	65	28	124
Metabolites with decreased levels post-challenge vs. pre-challenge	13	5	0	18
Metabolites only detected post-challenge	17	80	122	219
Metabolites only detected pre-challenge	2	2	1	5
Total # Metabolite Features	63	152	151	366

Table 6.3. Numbers of metabolite features which showed statistically significant changes in levels ($p < 0.01$) in either pre-challenge or post-challenge serum samples collected from children who are allergic to peanuts following oral challenge with peanuts. The data are arranged according to the degree of fold change (post-challenge relative to pre-challenge) in one of three m/z ranges.

Fold Change	# components m/z 100-450	# components m/z 450-700	# components m/z 700-1000	Total
<0.7	15	7	23	45
1.5-10	31	46	10	87
10-100	10	40	46	96
100-1000	7	51	21	79
1000-10000	0	3	0	3
>10000	0	5	51	56
Total	63	152	151	366

6.3. Discussion

6.3.1. Differentiation of Pre-Challenge Metabolome from Post-Challenge Metabolome

The diagnostic reliability of known biomarkers of allergic response (such as histamine) is rather low. A key focus of this work was to determine whether comprehensive metabolite profiling of the serum of peanut-allergic children could provide insights into those molecules involved in the adverse reactions to peanuts experienced by these children. These molecules could serve as diagnostic biomarkers of allergic response. Analysis of both the unsupervised PCA score plot and the supervised OPLS-DA score plot revealed that the post-challenge serum metabolomes of these children were clearly differentiated from their pre-challenge metabolomes. Both the R^2 and Q^2 scores (0.55 and 0.94 respectively) of the OPLS-DA model were very high indicative of a very robust model. This high Q^2 score was likely driven by the fact that 366 metabolomic features showed significant change (Table 6.2). Of these, there were 219 metabolite features which were only observed post-challenge. Moreover, a total of 138 features showed fold changes greater than 100 (Table 6.3). While many of these features may have arose from the digestion of the peanuts administered in the oral challenge experiment, the overall degree of metabolomic change is quite extraordinary.

In addition to the multivariate analyses, it was observed that huge increases in features with m/z ratios typical of lipids were found in post-challenge samples. A simple visual inspection of the averaged mass spectra intensity found in the retention region

where lysoPC and LysoPE lipids were identified by MS/MS (Figure 6.7) shows a massive intensity increase (>100 fold change) in a number of lysoPCs and LysoPEs. An example MS/MS spectra is given in Figure 6.8. Interestingly, a number of these lyso lipids which were confirmed by MS/MS were found to have the same length of fatty acid chains (24 carbons with 0 to 2 degrees of unsaturation) and were highly elevated compared to the pre-challenge levels *in all nine subjects.* The relative MS intensity of these peaks is shown in Figure 6.9. Additionally, a number of lysoPCs with carbon chain lengths of 18 with 0-3 degrees of unsaturation begin to appear in post challenge samples with S/N ratios greater than 100 also in all nine subjects. Indeed, one lysoPC (lysoPC(18:2)) changes from undetected in pre-challenge samples to a signal intensity greater than 1000 above the level of noise. While these specific compounds show a relative standard deviation in post-challenge samples of approximately 50%, the enormous fold change more than compensates for this biological variation.

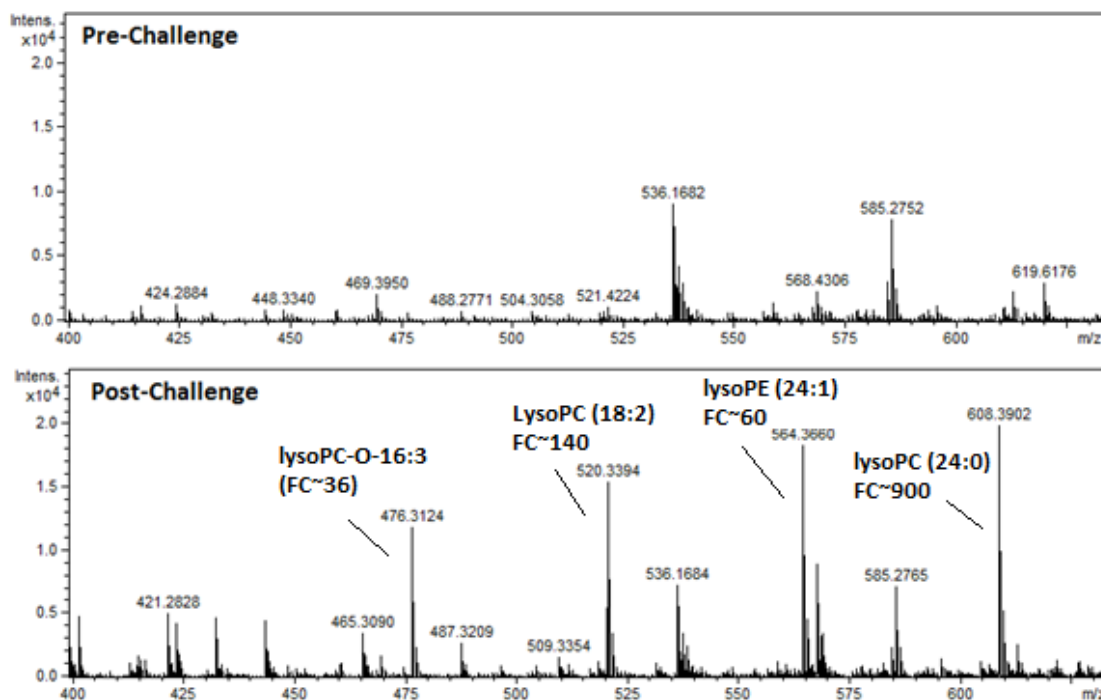


Figure 6.7. Averaged mass spectra of lyso lipid mass region in chromatograms over 2-5 minutes. Post-challenge samples show large increase in lipids compared to pre-challenge.

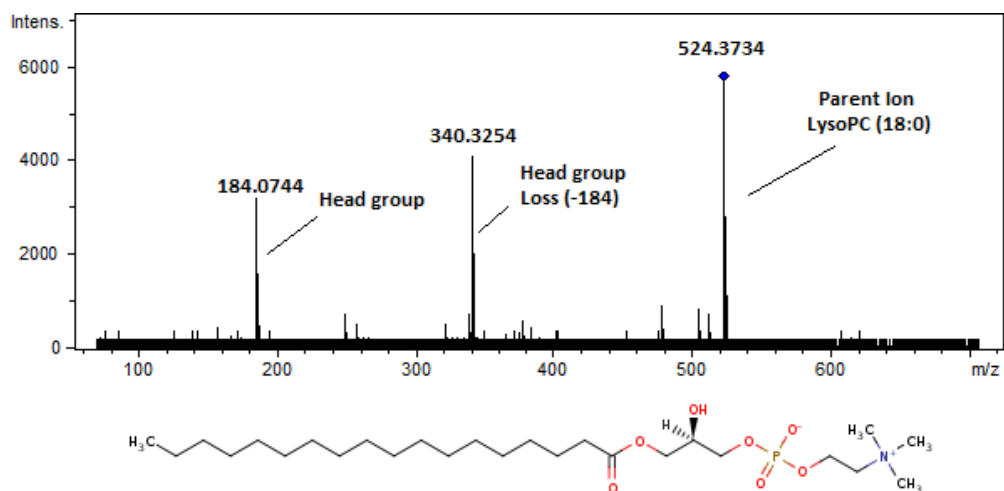


Figure 6.8. MS/MS spectrum (positive mode) of 524.373 peak which due to observed losses is confirmed to be lyso-phosphatidylcholine(18:0). Spectrum taken with a CID collision energy of 25eV.

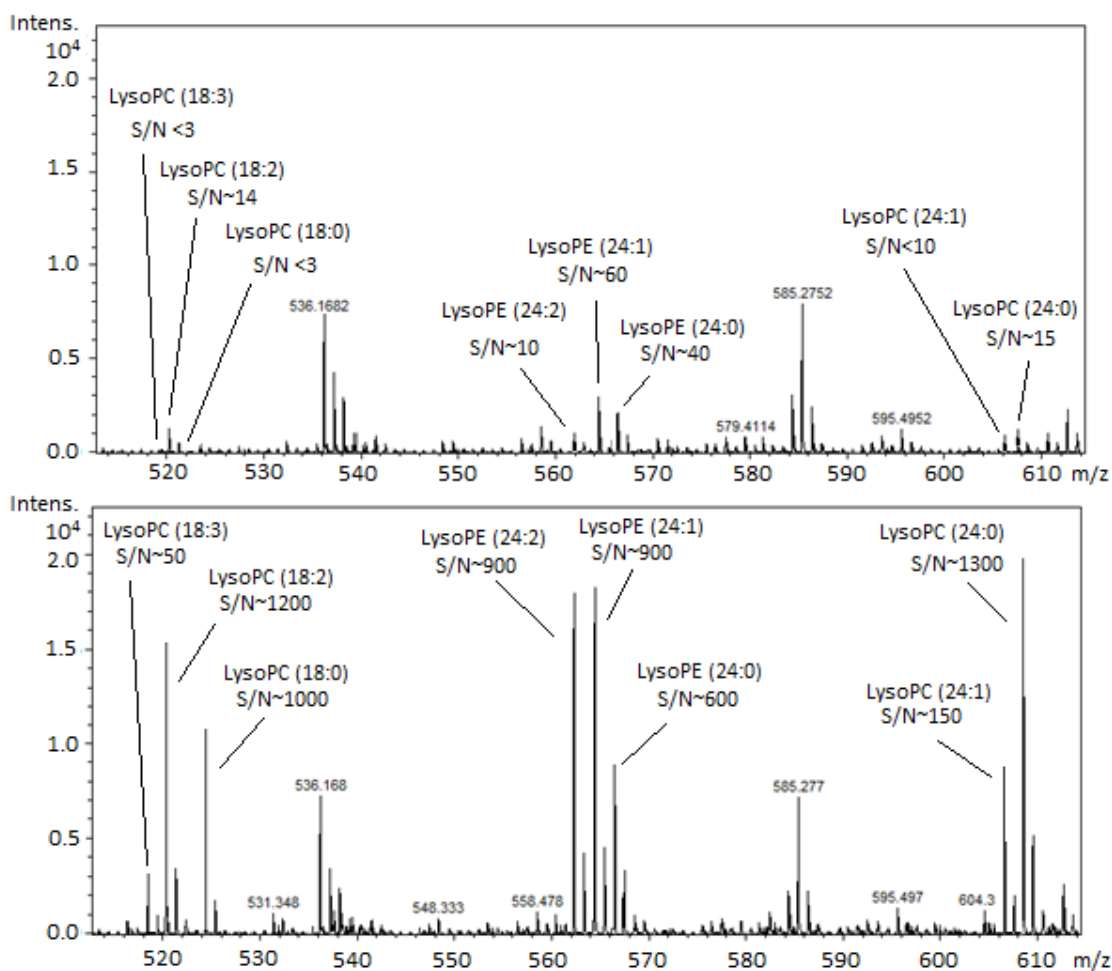


Figure 6.9. Positive ionization mass spectra from LC-MS analyses of pre-challenge sample (top) and its corresponding post-challenge sample (bottom) showing signal intensities of five lysoPCs and three lysoPEs. The chemical identity of these compounds were confirmed by MS/MS CID experiments.

Even more encouraging, these same lipid classes albeit with different fatty acid compositions increased significantly in mice post-challenge although not to the same magnitude as seen in these human samples. These phospholipid types are not commonly found in raw peanuts or peanut products (~98% triacylglycerols and diacylglycerols)^{31,32} meaning that the appearance of these phospholipids due to the

ingestion of peanuts is very unlikely. These lipids may have arisen from the breakdown and degranulation of mast cells and basophils.

These subsets of specific lipids provide a suite of compounds which have enormous potential to be used as early markers of an allergic reaction to peanuts. The huge intensity increases of certain lipids and lyso-lipids post-challenge were observed in each of the nine human subjects in this small group. Clearly, additional work is needed with a larger set of allergic volunteers however if this response were characteristic of peanut allergic response, it would be easy to develop a sensitive diagnostic testing procedure with a targeted analytical method.

The small volume of serum available from each participant (10 μ L per sample) in this study was sufficient for only a limited number of MS/MS experiments to identify the types of lipids in these samples. Nonetheless 8 specific lyso-phospholipids were identified by MS/MS. Methods specific to these lipids which do not require chromatography (e.g., direct infusion MS) may suffice for rapid screening of these samples. It is clear that further experiments are warranted with a more rigorous experimental design before the full potential of these lipids can be fully assessed as diagnostic markers; however, these initial results are extremely encouraging and provide ample justification for future investigations on a larger number of children.

In addition to the substantial increase in a number of lipids, two polar molecules of note were observed to decrease in post-challenge samples compared to their pre-

challenge levels, taurine and xanthine. Taurine was observed to increase in post-challenge mice in contrast to the results observed in the human samples. It is possible that taurine levels increased in the children quickly after the initial peanut dose was administered and gradually decreased as the experiment proceeded. To test this hypothesis, a time-based challenge experiment in peanut-allergic children would be required. The second polar metabolite was xanthine, the immediate precursor to uric acid. Evidence presented in Chapter 4 demonstrated that xanthine and other uric acid precursors had decreased in sensitized mice compared to non-sensitized mice. This decrease in uric acid precursors may provide further evidence supporting the role of uric acid in the dysregulation of the immune system leading to the continued persistence of this allergy type.

6.4. Conclusions

The work presented in this chapter is the first comprehensive metabolomic study that profiled peanut-allergic children prior to and after an oral peanut challenge. Despite the limited number of samples and the small volumes of serum available, profound changes in their metabolite profiles were observed. At least 366 metabolites were found to be significantly altered in post-challenge samples. Among these metabolites 147 were only detected after the onset of clinical symptoms. Of the metabolites increasing or appearing post-challenge, the fold change of a number of lysophospholipids were observed to be among the largest. Eight specific lysoPC and lysoPE

lipids which possessed similar fatty-acid compositions were identified by tandem MS and accurate mass measurement. While these eight lipids were but a few of the observed lipids increasing, these lipids may provide a novel suite of molecules for use as a highly sensitive, targeted diagnostic test for peanut induced allergic reaction. Based on these results, a further study with a larger number of samples is clearly warranted to validate these molecules as biomarkers. Further study with larger serum quantities available may lead to the identification of other, related lipids. This study also identified two polar molecules, taurine and xanthine, previously identified in mouse studies, as being significantly decreased post-challenge in these children.

Chapter 7. Conclusions and Future Directions

7.1. Conclusions

The main focus of the work presented in this thesis centered on the application of comprehensive metabolomics for the identification of key metabolites involved in the development of peanut allergy and peanut-induced anaphylaxis. This work is the first comprehensive assessment of metabolites in peanut allergy research. To date, much of the research on peanut allergies has focused on the role of the immune system and the proteins in peanuts believed to be responsible for hypersensitivity to peanuts; almost no resources have been spent on studying peanut allergy at the molecular or metabolite level. Work described herein has provided the first evidence supporting the power of comprehensive metabolomics as a diagnostic and discovery tool for allergy research.

This thesis begins with the development of a novel methodology for comprehensive analysis of serum metabolome using liquid chromatography-electrospray ionization-time of flight mass spectrometry (Chapter 3). A major analytical challenge in metabolomics is the need to analyze a wide range of chemical species from highly polar and ionic compounds to highly non-polar species such as lipids. If an analysis is to be truly comprehensive, the analysis must cover the wide array of chemically diverse metabolites ideally in a single analytical injection. To address this problem, the tandem coupling of pairs of LC columns was explored using standards then serum samples with a goal of retaining the broadest range of metabolites in a single

injection while at the same time, reducing the impacts of ion suppression commonly observed in electrospray ionization. Different column combinations were found to be able to separate more components in the tandem mode than through the use of either column. This unique approach, which to the best of our knowledge has never been used prior to this work, greatly expanded coverage of the metabolome within a single chromatographic analysis. The developed methodology addressed the first two stated objectives of this thesis which were to investigate a variety of liquid chromatography columns and column combinations for use in metabolomics analysis and to develop and validate liquid chromatography-mass spectrometry methods which would be appropriate for the simultaneous retention of a wide range of polar and non-polar metabolites with minimal ion suppression. This methodology was used in a metabolomic study of blood serum samples from mice and human.

Chapter 4 applied these analytical methods to the study of the metabolome of mice undergoing sensitization to peanuts using cholera toxin as an adjuvant. This work revealed a significant perturbation in purine metabolism in mice undergoing sensitization; uric acid was hypothesized as the important purine. This hypothesis was tested by members of the Dr. Manel Jordana research group. Their work confirmed that uric acid, plays a significant role in inducing peanut hypersensitivity in mice. As a result of this comprehensive metabolomics study, the Jordana group has recently demonstrated in an alternative mouse sensitization model that uric acid is a significant player in that model as well. This application of comprehensive metabolomics as a

discovery tool to study food allergy development is the first of its kind. This work addresses a key knowledge gap in our understanding of allergy development and fulfills the thesis objectives to utilize comprehensive metabolomics by LC-MS to discover metabolite pathways with cause sensitization to peanuts. This work also partially addresses the thesis objective to assess comprehensive metabolomics as a diagnostic tool for peanut allergy.

Next, this approach was applied in a metabolomic study of mice undergoing peanut-induced anaphylaxis (Chapter 5). This work demonstrated that comprehensive metabolomics is not only capable of differentiating mice undergoing anaphylaxis from non-anaphylactic mice, but is also useful in monitoring the development of anaphylaxis in these mice. This work also revealed that during anaphylaxis there was a substantial increase in taurine together with a number of phospholipids and lysophospholipids. Both findings are new and have not been previously correlated with peanut-induced anaphylaxis. As a result of these findings, the Jordana lab has begun experiments to assess the effects of taurine regarding its role as an anaphylactic mediator. Preliminary findings suggest that blocking taurine production leads to better clinical outcomes.

As the thesis work was nearing completion, a serendipitous opportunity arose to examine blood serum samples from nine peanut allergic children who were participating in a peanut challenge experiment as part of another study. We were able to obtain about 10 μ L of serum before the oral peanut challenge and another 10 μ L of serum taken

upon the first indication of allergy symptoms. Comprehensive metabolomics analyses identified massive changes in the metabolite profiles of these children following the oral peanut challenge. While full identification of metabolites was precluded due to the small amount of sample, dramatic changes in the levels of a number of lyso-phosphatidylcholines, lyso-phosphatidylethanolamines and other high molecular mass lipids were observed. Many of these lipids showed enormous increases (10^3 - 10^6 -fold increases) in all children studied. This is an extraordinary observation. While some of these lipid increases were no doubt due to the ingestion of peanuts, many of the phospholipid increases are likely not from digestion. This suite of lipids has the potential to serve as a unique set of biomarkers which can aid in the diagnosis of peanut allergy. These exciting results mandate that a larger study of peanut-allergic children is needed and that a time-course of lipid increases be determined. This discovery could be a significant breakthrough in peanut allergy research. The work presented in chapters 5 and 6 addressed the objectives of this thesis regarding the assessment of comprehensive metabolomics as a biomarker and mediator discovery tool and to assess the metabolomic changes occurring in children after an oral peanut challenge. These chapters also complement work done in chapter 4 to fulfill the thesis objective to assess comprehensive metabolomics as a diagnostic tool for peanut allergy.

In summary, the work presented in this thesis has documented the successful development of a novel chromatography approach which has been applied to blood serum samples for comprehensive metabolomic studies. This analytical strategy has

been applied to the study of mice undergoing sensitization to peanuts; the purine degradation pathway, previously uncorrelated to peanut allergy, and the end product uric acid, has since been proven to be essential for sensitization. Taurine and a number of phospholipids showed increases in mice and in humans undergoing allergic reactions which represent novel mediator and biomarker candidates. Finally, the results of the work presented in this thesis have provided many new directions for future research in peanut allergies.

7.2. Future Directions

The work presented in this thesis represents a significant advancement in our knowledge regarding peanut allergies and peanut-induced anaphylaxis at the molecular level. Several new directions may be taken in future studies which spring-board from the work presented.

One avenue for further study would be a time-series analysis of the lipids which show significant increases during peanut-induced anaphylaxis. Platelet-activating factor, a mediator of PIA, is a phosphatidylcholine-based lipid synthesized by cells such as basophils primarily through lipid remodeling of phosphatidylcholines upon activation from inflammatory agents. By better understanding the bio-synthetic pathways of PAF and related lipids under inflammatory conditions, potential therapeutic targets may be discovered which may prevent PIA from occurring. This work expands upon the findings

in this thesis in both mice and children where some phospholipids were significantly increased during anaphylaxis.

Another potentially fruitful avenue of research arising is the investigation of the role of taurine in the on-set of PIA. In both mouse and human patients taurine was found to be dysregulated after peanut challenge. This molecule may represent a novel diagnostic target for the rapid diagnosis of peanut allergy. Preliminary stages, initial results from the Jordana group indicate that treatment of sensitized mice with β -alanine, a compound known to block taurine production, produces more favorable clinical out-comes after peanut challenge.

The discovery of metabolic pathways that are affected during sensitization or allergen challenge is the holy grail in allergy research. The purine degradation pathway was identified as such a candidate. This discovery opens the door for the development and elucidation of new sensitization protocols which do not require the use of adjuvants. One such model under development in the Jordana lab involves the stressing of exposed skin which in turn causes DAMP responses known to increase uric acid levels. By further understanding the role of uric acid and purine degradation in the sensitization process, new insights into how peanut allergies originate may arise.

The use of metabolomic analysis in pediatric studies (such as the study in Chapter 6) should be explored. The probability of discovery of biomarker candidates of peanut-induced anaphylaxis is very high indeed. Proposed future work for human

studies will involve both the expansion of the number of children recruited for study in addition to the incorporation of age/gender matched control groups. Metabolomic changes should be monitored as a function of time at a fixed dose of peanut. Attention needs to be paid to the experimental design aspects of these experiments to increase the robustness of the analysis for yielding biomarker candidates with good potential in the clinic.

Another avenue for future research would be to investigate the role of gut microbiota in promoting tolerance to peanut via the study of mice bred in a sterile, germ-free facility. Preliminary data from the Jordana group has indicated that mice bred and housed in a germ-free environment can be sensitized to peanut without the use of an adjuvant or other immune system stressor. This result strongly suggests that a profound dysregulation of the immune system is taking place in mice without gut flora. Comprehensive metabolomic studies would enable the identification of those metabolites which are dysregulated in germ-free mice. This in turn, may suggest possible roles for gut flora in the maintenance of homeostasis or tolerance towards peanuts.

Section 8. References

- (1) Patti, G. J.; Yanes, O.; Siuzdak, G. *Nature Reviews. Mol. Cell Biol.* **2012**, *13*, 263–9.
- (2) Pauling, L.; Robinson, A.; Teranishi, R.; Cary, P. *PNAS* **1971**, *68*, 2374–2376.
- (3) Oliver, S. G.; Winson, M. K.; Kell, D. B.; Baganz, F. *Trends in Biotechnol.* **1998**, *16*, 373–378.
- (4) Nicholson, J. K.; Lindon, J. C.; Holmes, E. *Xenobiotica* **1999**, *29*, 1181–1189.
- (5) Fiehn, O. *Comp. Funct. Genom.* **2001**, *2*, 155–168.
- (6) Reaves, M. L.; Rabinowitz, J. D. *Current Opin. Biotechnol.* **2011**, *22*, 17–25.
- (7) Brindle, J. T.; Antti, H.; Holmes, E.; Tranter, G.; Nicholson, J. K.; Bethell, H. W. L.; Clarke, S.; Schofield, P. M.; McKilligin, E.; Mosedale, D. E.; Grainger, D. J. *Nature Medicine* **2002**, *8*, 1439–1444.
- (8) Kirschenlohr, H. L.; Griffin, J. L.; Clarke, S. C.; Rhydwen, R.; Grace, A. A.; Schofield, P. M.; Brindle, K. M.; Metcalfe, J. C. *Nature Medicine* **2006**, *12*, 705–711.
- (9) Manna, S. K.; Patterson, A. D.; Yang, Q.; Krausz, K. W.; Idle, J. R.; Fornace, A. J.; Gonzalez, F. J. *J. Proteom. Res.* **2011**, *10*, 4120–4133.
- (10) Cheng, L. L.; Burns, M. a; Taylor, J. L.; He, W.; Halpern, E. F.; McDougal, W. S.; Wu, C.-L. *Cancer Research* **2005**, *65*, 3030–3034.
- (11) Chun, E.; Chan, Y.; Koh, P. K.; Mal, M.; Cheah, P. Y.; Eu, K. W.; Backshall, A.; Cavill, R.; Nicholson, J. K.; Keun, H. C. *J. Proteom. Res.* **2009**, 352–361.
- (12) Lanz, C.; Patterson, A. D.; Slavík, J.; Krausz, K. W.; Ledermann, M.; Gonzalez, F. J.; Idle, J. R. *Radiation Research* **2009**, *172*, 198–212.
- (13) Johnson, C. H.; Patterson, A. D.; Krausz, K. W.; Lanz, C.; Kang, D. W.; Luecke, H.; Gonzalez, F. J.; Idle, J. R. *Radiation Research* **2011**, *175*, 473–484.
- (14) Ptolemy, A. S.; Rifai, N. *Scandinavian J. Clin. Lab. Invest.* **2010**, *242*, 6–14.
- (15) Johnson, C. H.; Gonzalez, F. J. *J. Cell. Physiol.* **2012**, *227*, 2975–2981.

- (16) Dunn, W. B.; Erban, A.; Weber, R. J. M.; Creek, D. J.; Brown, M.; Breitling, R.; Hankemeier, T.; Goodacre, R.; Neumann, S.; Kopka, J.; Viant, M. R. *Metabolomics* **2012**.
- (17) Sumner, L. W.; Amberg, A.; Barrett, D.; Beale, M. H.; Beger, R.; Daykin, C. a.; Fan, T. W.-M.; Fiehn, O.; Goodacre, R.; Griffin, J. L.; Hankemeier, T.; Hardy, N.; Harnly, J.; Higashi, R.; Kopka, J.; Lane, A. N.; Lindon, J. C.; Marriott, P.; Nicholls, A. W.; Reily, M. D.; Thaden, J. J.; Viant, M. R. *Metabolomics* **2007**, *3*, 211–221.
- (18) Bennett, B. D.; Kimball, E. H.; Gao, M.; Osterhout, R.; Van Dien, S. J.; Rabinowitz, J. D. *Nature Chem. Biol.* **2009**, *5*, 593–599.
- (19) Yanes, O.; Tautenhahn, R.; Patti, G. J.; Siuzdak, G. *Anal. Chem.* **2011**, *83*, 2152–2161.
- (20) Koulman, A.; Lane, G. a; Harrison, S. J.; Volmer, D. a *Anal. and Bioanal. Chem.* **2009**, *394*, 663–670.
- (21) Goodsaid, F. M.; Frueh, F. W.; Mattes, W. *Toxicology* **2008**, *245*, 219–223.
- (22) Weckwerth, W.; Fiehn, O. *Current Opin. Biotechnol.* **2002**, *13*, 156–160.
- (23) Chen, J.; Wang, W.; Lv, S.; Yin, P.; Zhao, X.; Lu, X.; Zhang, F.; Xu, G. *Anal Chim Acta* **2009**, *650*, 3–9.
- (24) Patti, G. J.; Yanes, O.; Shriver, L. P.; Courade, J.-P.; Tautenhahn, R.; Manchester, M.; Siuzdak, G. *Nature Chem Bio* **2012**, *8*, 232–234.
- (25) Dang, L.; White, D. W.; Gross, S.; Bennett, B. D.; Bittinger, M. a; Driggers, E. M.; Fantin, V. R.; Jang, H. G.; Jin, S.; Keenan, M. C.; Marks, K. M.; Prins, R. M.; Ward, P. S.; Yen, K. E.; Liao, L. M.; Rabinowitz, J. D.; Cantley, L. C.; Thompson, C. B.; Vander Heiden, M. G.; Su, S. M. *Nature* **2009**, *462*, 739–744.
- (26) Becker, S.; Kortz, L.; Helmschrodt, C.; Thiery, J.; Ceglarek, U. *J. Chrom. B*, **2012**, *883-884*, 68–75.
- (27) Fiehn, O. *Plant Molecular Biology* **2002**, *48*, 155–171.
- (28) Denery, J. R.; Nunes, A. A. K.; Dickerson, T. J. *Anal Chem.* **2011**, 1040–1047.
- (29) Theodoridis, G.; Gika, H. G.; Wilson, I. D. *Mass Spectrom Rev* **2011**, *30*, 884–906.

- (30) Want, E. J.; Nordström, A.; Morita, H.; Siuzdak, G. *J Proteome Res* **2007**, *6*, 459–468.
- (31) Lei, Z.; Huhman, D. V.; Sumner, L. W. *J Biol Chem* **2011**, *286*, 25435–25442.
- (32) Zhou, B.; Xiao, J. F.; Tuli, L.; Ressom, H. W. *Molecular Biosys* **2012**, *8*, 470–481.
- (33) Chapman, S. *Physical Rreview* **1937**, *52*, 184.
- (34) Iribarne, J. V. *J Chem Phys* **1976**, *64*, 2287.
- (35) Dole, M. *J Chem Phys* **1968**, *49*, 2240.
- (36) Lv, H.; Palacios, G.; Hartil, K.; Kurland, I. J. *J Proteome Res* **2011**, *10*, 2104–2112.
- (37) Zhang, A.; Sun, H.; Wang, P.; Han, Y.; Wang, X. *Analyst* **2012**, *137*, 293–300.
- (38) Chalcraft, K. R.; Lee, R.; Mills, C.; Britz-Mckibbin, P. *Anal Chem.* **2009**, *81*, 2506–2515.
- (39) Chalcraft, K. R.; Britz-McKibbin, P. *Anal Chem.* **2009**, *81*, 307–314.
- (40) Croley, T. R.; White, K. D.; Callahan, J. H.; Musser, S. M. *JASMS* **2012**, 1569–1578.
- (41) Patti, G. J. *J Sep Sci.* **2011**, *34*, 3460–3469.
- (42) Castro-Puyana, M.; García-Cañas, V.; Simó, C.; Cifuentes, A. *Electrophoresis* **2012**, *33*, 147–67.
- (43) Andrés, A.; Téllez, A.; Rosés, M.; Bosch, E. *J Chromatogr. A* **2012**, *1247*, 71–80.
- (44) Nikitas, P.; Pappa-Louisi, a; Tsoumachides, S.; Jouyban, A, *J Chromatogr. A* **2012**, *1251*, 134–140.
- (45) Alpert, A. J. *J Chromatogr* **1990**, *499*, 177–196.
- (46) Kawachi, Y.; Ikegami, T.; Takubo, H.; Ikegami, Y.; Miyamoto, M.; Tanaka, N. *J Chromatogr. A* **2011**, *1218*, 5903–5919.
- (47) Callahan, D. L.; De Souza, D.; Bacic, A.; Roessner, U. *J Sep Sci.* **2009**, *32*, 2273–2280.

- (48) Zhang, T.; Creek, D. J.; Barrett, M. P.; Blackburn, G.; Watson, D. G. *Anal Chem.* **2012**, *84*, 1994–2001.
- (49) Boysen, R. I.; Yang, Y.; Chowdhury, J.; Matyska, M. T.; Pesek, J. J.; Hearn, M. T. W. *J Chromatogr. A* **2011**, *1218*, 8021–8026.
- (50) Finkelman, F. D. *JACI* **2007**, *120*, 506–515
- (51) Perrier, C.; Thierry, a-C.; Mercenier, A.; Corthésy, B. *Clinical and Experimental allergy : J Brit Soc Allergy Clin Immun.* **2010**, *40*, 153–162.
- (52) Strait, R. T.; Morris, S. C.; Yang, M.; Qu, X.-W.; Finkelman, F. D. *Journal of Allergy and Clin Immun.* **2002**, *109*, 658–668.
- (53) Oettgen, H. C.; Martin, T. R.; Wynshaw-Boris, A.; Deng, C.; Drazen, J. M.; Leder, P. *Nature* **1994**, *370*, 367–370.
- (54) Boden, S. R.; Wesley Burks, a *Immunol Rev.* **2011**, *242*, 247–257.
- (55) Bk, W.; Yee, A.; Jelley, D.; Ziegler, M.; Jb, Z.; Jelley, D.; Ziegler, M. *Pediatr Allergy Immunol.* **2007**, 231–239.
- (56) Arias, K.; Baig, M.; Colangelo, M.; Chu, D.; Walker, T.; Goncharova, S.; Coyle, A.; Vadas, P.; Wasserman, S.; Jordana, M. *JACI* **2009**, *124*, 307–14,
- (57) Sun, J.; Arias, K.; Alvarez, D.; Fattouh, R.; Walker, T.; Goncharova, S.; Kim, B.; Wasserman, S.; Reed, J.; Coyle, A. J.; Jordana, M. *J Immun.* **2007**, *179*, 6696–6703.
- (58) Bruce, S. J.; Tavazzi, I.; Parisod, V.; Rezzi, S.; Kochhar, S.; Guy, P. *Anal Chem.* **2009**, *81*, 3285–3296.
- (59) Theodoridis, G.; Gika, H. G.; Wilson, I. D. *TrAC Trend Anal Chem* **2008**, *27*, 251–260.
- (60) Issaq, H. J.; Van, Q. N.; Waybright, T. J.; Muschik, G. M.; Veenstra, T. D. *J Sep Sci.i* **2009**, *32*, 2183–2199.
- (61) Jankevics, A.; Merlo, M. E.; De Vries, M.; Vonk, R. J.; Takano, E.; Breitling, R. *Metabolomics* **2012**, *8*, 29–36.
- (62) Theodoridis, G. a; Gika, H. G.; Want, E. J.; Wilson, I. D. *Anal Chim Acta* **2012**, *711*, 7–16.

- (63) Wang, X.; Sun, H.; Zhang, A.; Wang, P.; Han, Y. *J Sep Sci.* **2011**, *34*, 3451–3459.
- (64) Gilar, M.; Olivova, P.; Daly, A. E.; Gebler, J. C. *Anal Chem* **2005**, *77*, 6426–6434.
- (65) Gray, M. J.; Sweeney, A. P.; Dennis, G. R.; Slonecker, P. J.; Shalliker, R. A. *Analyst* **2003**, *128*, 598.
- (66) Jandera, P. *J Sep Sci.* **2008**, *31*, 1421–1437.
- (67) Liu, Y.; Guo, Z.; Feng, J.; Xue, X.; Zhang, F.; Xu, Q.; Liang, X. *J Sep Sci.* **2009**, *32*, 2871–2876.
- (68) Parrilla Vázquez, P.; Martínez Galera, M.; Serrano Guirado, a; Parrilla Vázquez, M. M. *Anal Chim Acta* **2010**, *666*, 38–44.
- (69) Shaaban, H.; Górecki, T. *Anal Chim Acta* **2011**, *702*, 136–143.
- (70) Galera, M. M.; Vázquez, P. P.; Vázquez, M. D. M. P.; García, M. D. G.; Amate, C. F. *J Sep Sci.* **2011**, 1796–1804.
- (71) Zhao, Y.; Kong, R. P. W.; Li, G.; Lam, M. P. Y.; Law, C. H.; Lee, S. M. Y.; Lam, H. C.; Chu, I. K. *J Sep Sci.* **2012**, *35*, 1755–1763.
- (72) Louw, S.; Pereira, A. S.; Lynen, F.; Hanna-Brown, M.; Sandra, P. *J Chromatogr. A* **2008**, *1208*, 90–94.
- (73) Liu, X.; Pohl, C.; Woodruff, A.; Chen, J. *J Chromatogr. A* **2011**, *1218*, 3407–3412.
- (74) Liu, X.; Pohl, C. *J Sep Sci.* **2010**, *33*, 779–786.
- (75) Pesek, J. J.; Matyska, M. T.; Fischer, S. M.; Sana, T. R. *J Chromatogr. A* **2008**, *1204*, 48–55.
- (76) Herrero, M.; Cacciola, F.; Donato, P.; Giuffrida, D.; Dugo, G.; Dugo, P.; Mondello, L. *J Chromatogr. A* **2008**, *1188*, 208–215.
- (77) Gray, M. J.; Slonecker, P. J.; Dennis, G.; Shalliker, R. *J Chromatogr. A* **2005**, *1096*, 92–100.
- (78) Sandra, P.; Vanhoenacker, G. *J Sep Sci.* **2007**, *30*, 241–244.
- (79) Peters, F. T.; Remane, D. *Anal Bioanal Chem.* **2012**, *403*, 2155–2172.

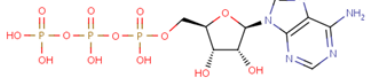
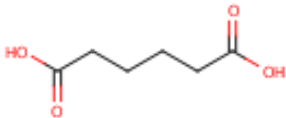
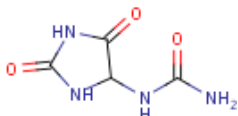
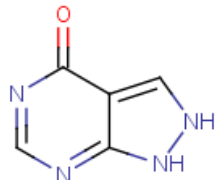
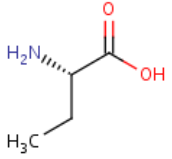
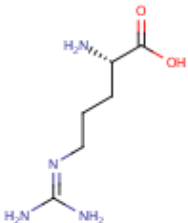
- (80) a, J.; Trygg, J.; Gullberg, J.; Johansson, A. I.; Jonsson, P.; Antti, H.; Marklund, S. L.; Moritz, T. *Anal Chem.* **2005**, *77*, 8086–8094.
- (81) Roy, S. M.; Anderle, M.; Lin, H.; Becker, C. H. *Int. J Mass Spectrom.* **2004**, *238*, 163–171.
- (82) Wedge, D. C.; Allwood, J. W.; Dunn, W.; Vaughan, A. A.; Simpson, K.; Brown, M.; Priest, L.; Blackhall, F. H.; Whetton, A. D.; Dive, C.; Goodacre, R. *Anal Chem.* **2011**, 6689–6697.
- (83) Enke, C. G. *Anal Chem.* **1997**, *69*, 4885–4893.
- (84) Liang, H. R.; Foltz, R. L.; Meng, M.; Bennett, P. *Rapid Commun Mass Spectrom.* **2003**, *17*, 2815–2821.
- (85) Remane, D.; Meyer, M. R.; Wissenbach, D. K.; Maurer, H. H. *Rapid Commun Mass Spectrom.* **2010**, 3103–3108.
- (86) Bajad, S. U.; Lu, W.; Kimball, E. H.; Yuan, J.; Peterson, C.; Rabinowitz, J. D. *J Chromatogr. A* **2006**, *1125*, 76–88.
- (87) Skolnick, H. S.; Conover-Walker, M. K.; Koerner, C. B.; Sampson, H. a; Burks, W.; Wood, R. *JACI* **2001**, *107*, 367–74.
- (88) Finkelman, F. D. *Curr Opin Immunol.* **2010**, *22*, 783–788.
- (89) Brandt, E. B.; Strait, R. T.; Hershko, D.; Wang, Q.; Muntel, E. E.; Scribner, T. a; Zimmermann, N.; Finkelman, F. D.; Rothenberg, M. E. *J Clin Investig.* **2003**, *112*, 1666–1677.
- (90) Birmingham, N. P.; Parvataneni, S.; Hassan, H. M. A.; Harkema, J.; Samineni, S.; Navuluri, L.; Kelly, C. J.; Gangur, V. *Internat Archives of Allergy and Immunol.* **2007**, *144*, 203–210.
- (91) Dearman, R. J.; Kimber, I. *Clinical and experimental allergy : J Brit Soc Allergy Clin Immunol.* **2009**, *39*, 458–468.
- (92) Lavelle, E. C.; Jarnicki, A.; Mcneela, E.; Armstrong, M. E.; Higgins, S. C.; Leavy, O.; Mills, K. H. G. *J. Leukocyte Biol.* **2004**, *75*, 756–763.
- (93) Bharati, K.; Ganguly, N. K. *Ind J Med Res.* **2011**, *133*, 179–187.

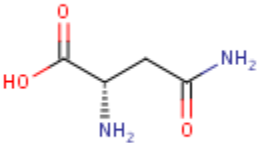
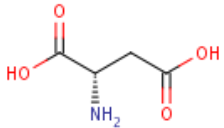
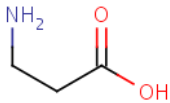
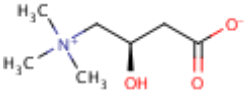
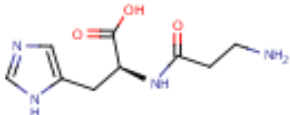
- (94) Dunn, W. B.; Broadhurst, D.; Begley, P.; Zelena, E.; Francis-McIntyre, S.; Anderson, N.; Brown, M.; Knowles, J. D.; Halsall, A.; Haselden, J. N.; Nicholls, A. W.; Wilson, I. D.; Kell, D. B.; Goodacre, R. *Nature Protocols* **2011**, *6*, 1060–1083.
- (95) Jones, O. a H.; Spurgeon, D. J.; Svendsen, C.; Griffin, J. L. *Chemosphere* **2008**, *71*, 601–609.
- (96) Willart, M. a M.; Lambrecht, B. N. *Clinical and experimental allergy : J Brit Soc Allergy Clin Immun.* **2009**, *39*, 12–19.
- (97) García Puig, J.; Mateos, F. *PWS* **1994**, *16*, 40–54.
- (98) Kool, M.; Willart, M. a M.; Van Nimwegen, M.; Bergen, I.; Pouliot, P.; Virchow, J. C.; Rogers, N.; Osorio, F.; Reis e Sousa, C.; Reis E Sousa, C.; Hammad, H.; Lambrecht, B. N. *Immunity* **2011**, *34*, 527–540.
- (99) Sicherer, S. H. *JACI* **2011**, *127*, 594–602.
- (100) Sicherer, S. H.; Sampson, H. *JACI* **2010**, *125*, S116–125.
- (101) Sampson, H. a; Muñoz-Furlong, A.; Campbell, R. L.; Adkinson, N. F.; Bock, S. A.; Branum, A.; Brown, S. G. a; Camargo, C. a; Cydulka, R.; Galli, S. J.; Gidudu, J.; Gruchalla, R. S.; Harlor, A. D.; Hepner, D. L.; Lewis, L. M.; Lieberman, P. L.; Metcalfe, D. D.; O’Connor, R.; Muraro, A.; Rudman, A.; Schmitt, C.; Scherrer, D.; Simons, F. E. R.; Thomas, S.; Wood, J. P.; Decker, W. W. *JACI* **2006**, *117*, 391–397.
- (102) Sicherer, S. H.; Muñoz-Furlong, A.; Sampson, H. *JACI* **2003**, *112*, 1203–1207.
- (103) Varshney, P.; Jones, S. M.; Scurlock, A. M.; Perry, T. T.; Kemper, A.; Steele, P.; Hiegel, A.; Kamilaris, J.; Carlisle, S.; Yue, X.; Kulis, M.; Pons, L.; Vickery, B.; Burks, a W. *JACI* **2011**, *127*, 654–660.
- (104) Bock, S. a; Muñoz-Furlong, a; Sampson, H. *JACI* **2001**, *107*, 191–3.
- (105) Arias, K.; Chu, D. K.; Flader, K.; Botelho, F.; Walker, T.; Arias, N.; Humbles, A. a; Coyle, A. J.; Oettgen, H. C.; Chang, H.-D.; Van Rooijen, N.; Wasserman, S.; Jordana, M. *JACI* **2011**, *127*, 1552–1561
- (106) Keet, C. *Pediatric Clinics of North America* **2011**, *58*, 377–388
- (107) Hu, X.; Wu, G.-P.; Zhang, M.-H.; Pan, S.-Q.; Wang, R.-R.; Ouyang, J.-H.; Liu, J.-G.; Chen, Z.-Y.; Tian, H.; Liu, D.-B. *Anal Bioanal Chem.* **2012**.

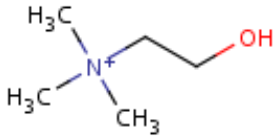
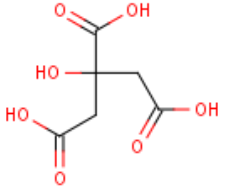
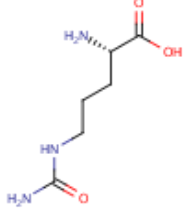
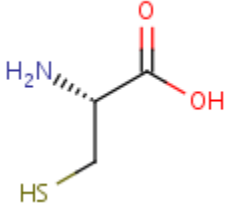
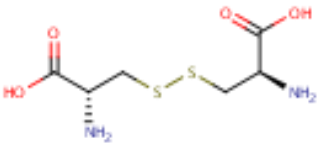
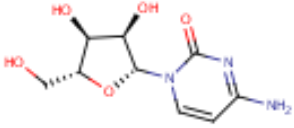
- (108) Fiehn, O. *Comparative and functional genomics* **2001**, *2*, 155–168.
- (109) Berni Canani, R.; Di Costanzo, M.; Troncone, R. *Nutrition* **2011**, *27*, 983–987.
- (110) Amin, K. *Respiratory Med.* **2012**, *106*, 9–14.
- (111) Grossmann, M.; Dobrev, D.; Himmel, H. M.; Ravens, U.; Kirch, W. *Hypertension* **2001**, *37*, 949–954.
- (112) Abe, M.; Tokunaga, T.; Yamada, K.; Furukawa, T. *Neuropharmacology* **1988**, *27*, 309–318.
- (113) Grosman, N. *Int Immunopharm.* **2001**, *1*, 1321–1329.
- (114) Weller, P. F.; Dvorak, a M. *JACI* **1994**, *94*, 1151–1156.
- (115) Laidlaw, T. M.; Boyce, J. *J Brit Soc Allergy Clin Immun.* **2012**, *42*, 1313–1320.
- (116) Bozza, P. T.; Magalhães, K. G.; Weller, P. F. *Biochim Biophys Acta* **2009**, *1791*, 540–551.
- (117) Sanders, T. H. *J Amer Oil Chem Soc.* **1980**, *9*, 12–15.

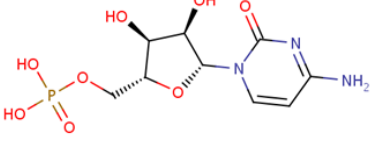
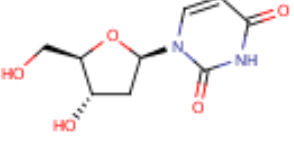
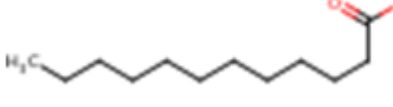
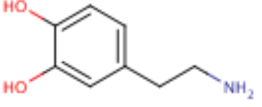
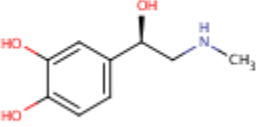
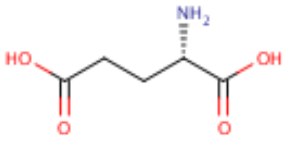
Appendix 1. Listing of Chemical Standards Used for Method Development. Retention times are given for LC gradient used for blood serum analysis of peanut allergy (Section 2.4)

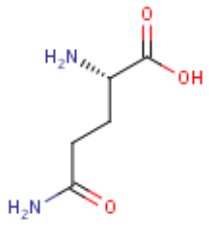
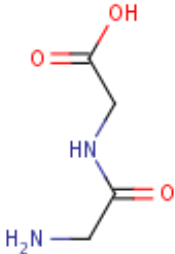
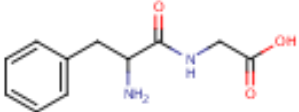
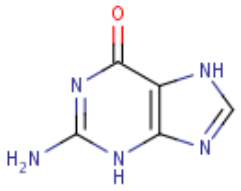
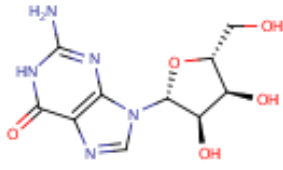
Name	Monoisotopic Mass and Formula	RT	Metabolite Class	Chemical Structure
Acetylcarnitine	203.116 C ₉ H ₁₇ NO ₄	9.7	Acyl Carnitine	
Acetylcholine	146.118 C ₇ H ₁₆ NO ₂	7.9	Choline	
Adenine	135.054 C ₅ H ₅ N ₅	3.3	Purine	
Adenosine	267.097 C ₁₀ H ₁₃ N ₅ O ₄	3.3	Nucleoside	
Adenosine Monophosphate	347.063 C ₁₀ H ₁₄ N ₅ O ₇ P	4.3	Nucleotide	
Adenosine Diphosphate	427.029 C ₁₀ H ₁₅ N ₅ O ₁₀ P ₂	4.5	Nucleotide	

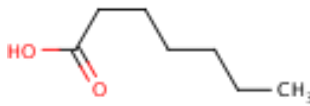
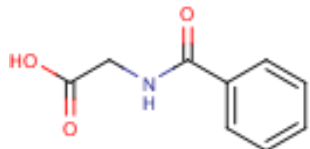
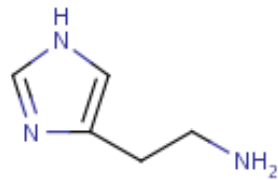
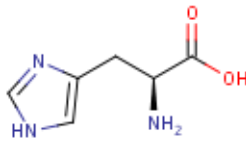
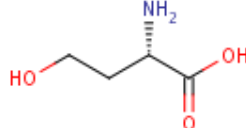
Adenosine Triphosphate	506.996 $C_{10}H_{16}N_5O_{13}P_3$	4.6	Nucleotide	
Adipic Acid	146.057 $C_6H_{10}O_4$	2.1	Organic Acid	
Alanine	89.047 $C_3H_7NO_2$	8.1	Amino Acid	
Allantoin	158.044 $C_4H_6N_4O_3$	10.1	Purine	
Allopurinol	136.039 $C_5H_4N_4O$	2.5	Purine	
2-Aminobutyric Acid	103.063 $C_4H_{10}N_2O_2$	9.1	Amino Acid	
Arginine	174.111 $C_6H_{14}N_4O_2$	11.9	Amino Acid	

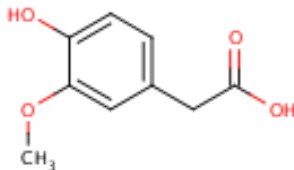
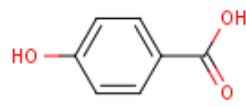
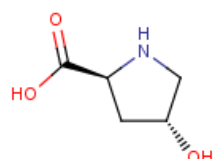
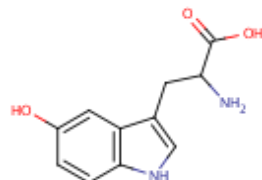
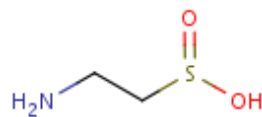
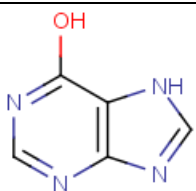
Asparagine	132.053 C ₄ H ₈ N ₂ O ₃	9.8	Amino Acid	
Aspartic Acid	133.038 C ₄ H ₇ NO ₄	10.2	Amino Acid	
B-Alanine	89.047 C ₃ H ₇ NO ₂	9.0	Amino Acid	
Caffeine	194.080 C ₈ H ₁₀ N ₄ O ₂	4.3	Purine	
Carnitine	161.105 C ₇ H ₁₅ NO ₃	10.0	Carnitine	
Carnosine	226.107 C ₉ H ₁₄ N ₄ O ₃	8.6	Amino Acid	

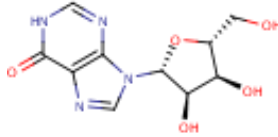
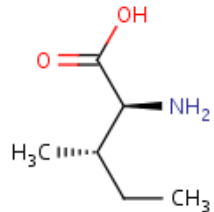
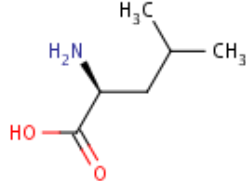
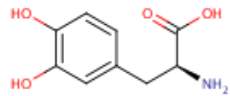
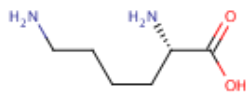
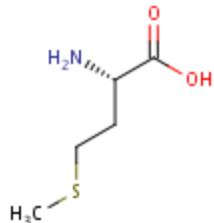
Choline	104.107 C ₅ H ₁₄ NO	8.5	Choline	
Citric Acid	192.027 C ₆ H ₈ O ₇	8.2	Organic Acid	
Citrulline	175.096 C ₆ H ₁₃ N ₃ O ₃	10.0	Amino Acid	
Cysteine	121.019 C ₃ H ₇ NO ₂ S	5.1	Amino Acid	
Cystine	240.024 C ₆ H ₁₂ N ₂ O ₄ S ₂	4.8	Amino Acid	
Cytidine	243.086 C ₉ H ₁₃ N ₃ O ₅	7.6	Nucleoside	

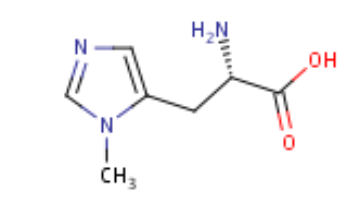
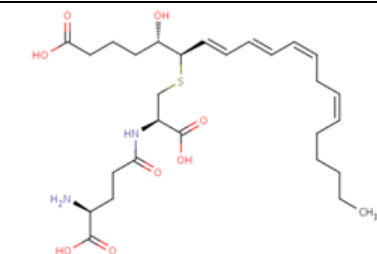
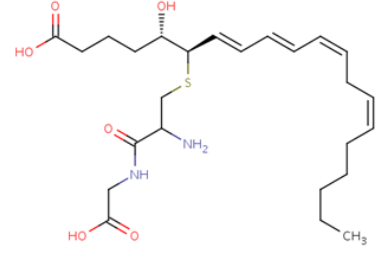
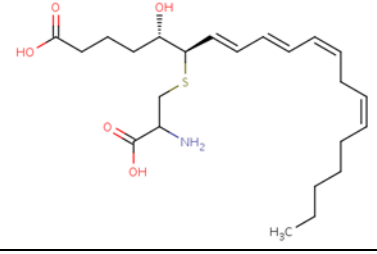
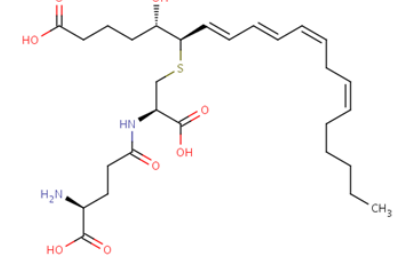
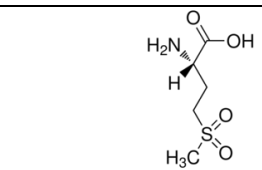
Cytidine Monophosphate	323.052 C ₉ H ₁₄ N ₃ O ₈ P	4.5	Nucleotide	
Deoxyuridine	228.075 C ₉ H ₁₂ N ₂ O ₅	5.1	Nucleoside	
Dodecanoic Acid	200.177 C ₁₂ H ₂₄ O ₂	2.3	Fatty Acid	
Dopamine	153.079 C ₈ H ₁₁ NO ₂	11.2	Biogenic Amine	
Epinephrine	183.089 C ₉ H ₁₃ NO ₃	8.3	Catechol	
Glutamic Acid	147.053 C ₅ H ₉ NO ₄	9.4	Amino Acid	

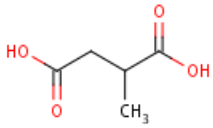
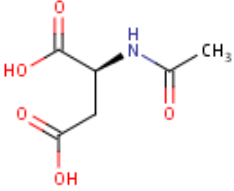
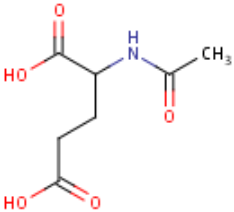
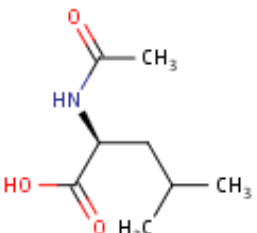
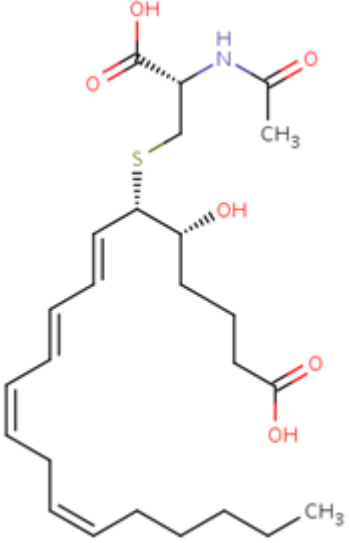
Glutamine	146.069 $C_5H_{10}N_2O_3$	9.6	Amino Acid	 The chemical structure of glutamine is shown. It consists of a central carbon atom bonded to a hydrogen atom (not explicitly shown), an amino group (H ₂ N), a carboxyl group (COOH), and a side chain consisting of two methylene groups and another amino group (CH ₂ CH ₂ NH ₂).
Glycyl-Glycine	132.053 $C_4H_8N_2O_3$	10.6	Peptide	 The chemical structure of glycyl-glycine is shown. It consists of two glycine residues linked by a peptide bond. The first glycine is at the N-terminus, and the second is at the C-terminus.
Glycyl-Phenylalanine	222.100 $C_{11}H_{14}N_2O_3$	8.6	Peptide	 The chemical structure of glycyl-phenylalanine is shown. It consists of a phenylalanine residue and a glycine residue linked by a peptide bond. The phenylalanine is at the N-terminus, and the glycine is at the C-terminus.
Guanine	151.049 $C_5H_5N_5O$	7.3	Purine	 The chemical structure of guanine is shown. It is a purine base consisting of a fused bicyclic ring system (a six-membered ring fused to a five-membered ring) with a carbonyl group and an amino group.
Guanosine	283.092 $C_{10}H_{13}N_5O_5$	7.9	Nucleoside	 The chemical structure of guanosine is shown. It consists of a guanine base linked to a ribose sugar via a glycosidic bond. The ribose sugar is in its cyclic form.

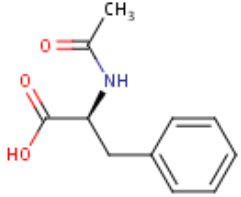
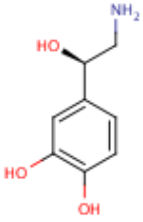
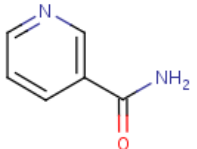
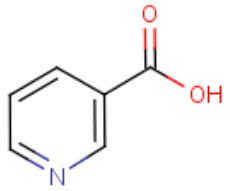
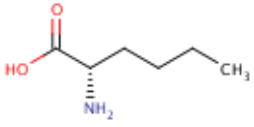
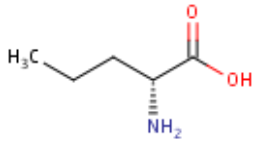
Heptanoic Acid	130.0994 C ₇ H ₁₄ O ₂	2.0	Fatty Acid	
Hippuric Acid	179.058 C ₉ H ₉ NO ₃	2.5	Amino Acid	
Histamine	111.080 C ₅ H ₉ N ₃	13.6	Biogenic Amine	
Histidine	155.069 C ₆ H ₉ N ₃ O ₂	11.6	Amino Acid	
Homoserine	119.058 C ₄ H ₉ NO ₃	9.6	Amino Acid	

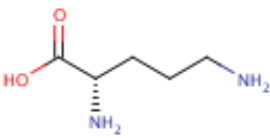
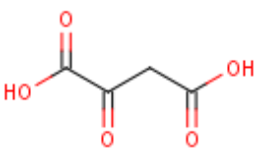
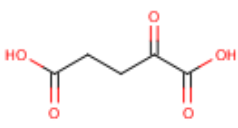
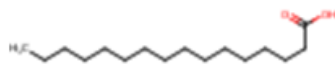
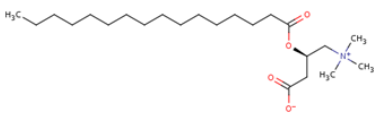
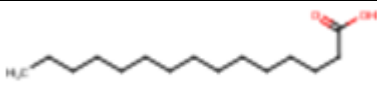
Homovanillic Acid	182.058 C ₉ H ₁₀ O ₄	2.0	Organic Acid	
4-Hydroxybenzoic Acid	138.032 C ₇ H ₆ O ₃	3.3	Organic Acid	
4-Hydroxyproline	131.058 C ₅ H ₉ NO ₃	9.3	Amino Acid	
5-Hydroxytryptophan	220.085 C ₁₁ H ₁₂ N ₂ O ₃	9.0	Amino Acid	
Hypotaurine	109.020 C ₂ H ₇ NO ₂ S	3.9	Sulfonic Acid	
Hypoxanthine	136.039 C ₅ H ₄ N ₄ O	4.0	Purine	

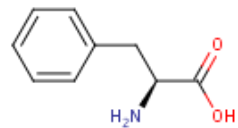
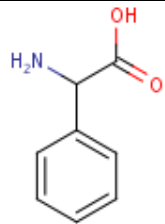
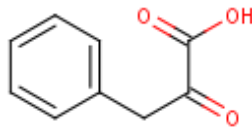
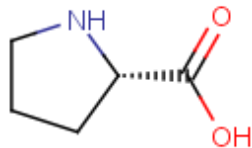
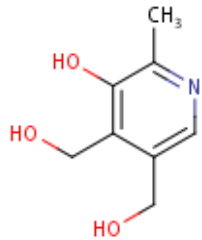
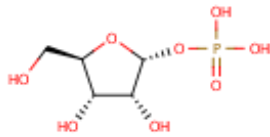
Inosine	268.081 $C_{10}H_{12}N_4O_5$	6.6	Nucleoside	
Isoleucine	131.095 $C_6H_{13}NO_2$	8.0	Amino Acid	
Leucine	131.095 $C_6H_{13}NO_2$	7.8	Amino Acid	
Levodopa	197.069 $C_9H_{11}NO_4$	8.7	Amino Acid	
Lysine	146.105 $C_6H_{14}N_2O_2$	12.1	Amino Acid	
Methionine	149.051 $C_5H_{11}NO_2S$	8.5	Amino Acid	

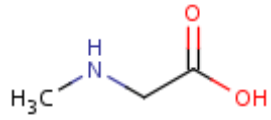
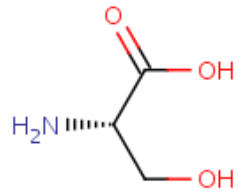
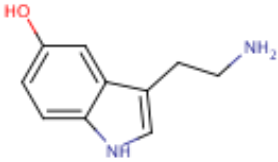
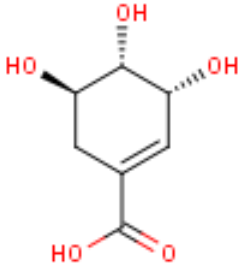
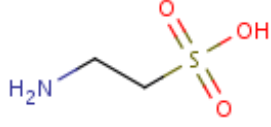
3-Methylhistidine	191.085 $C_7H_{11}N_3O_2$	12.6	Amino Acid	
Leukotriene C ₄	625.303 $C_{30}H_{47}N_3O_9S$	7.9	Cystienyl-leukotriene	
Leukotriene D ₄	496.261 $C_{25}H_{40}N_2O_6S$	8.1	Cystienyl-leukotriene	
Leukotriene E ₄	439.239 $C_{23}H_{37}NO_5S$	8.3	Cystienyl-leukotriene	
Leukotriene F ₄	568.282 $C_{30}H_{45}N_3O_9S$	8.4	Cystienyl-leukotriene	
Methionine Sulfone	181.040 $C_5H_{11}NO_4S$	8.9	Amino Acid	

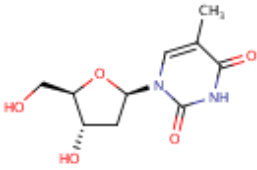
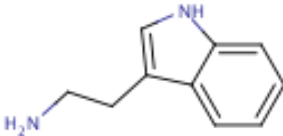
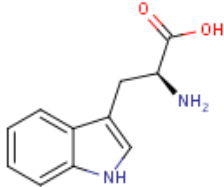
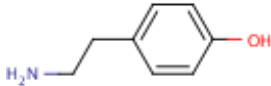
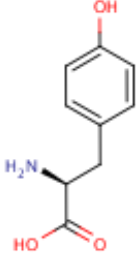
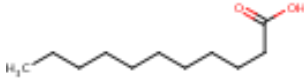
Methylsuccinic Acid	132.042 C ₅ H ₈ O ₄	3.5	Organic Acid	
N-Acetyl-Aspartic Acid	175.048 C ₆ H ₉ NO ₅	8.1	N-Acyl-Amino Acid	
N-Acetyl-Glutamic Acid	189.064 C ₇ H ₁₁ NO ₅	8.3	N-Acyl-Amino Acid	
N-Acetyl-Leucine	173.105 C ₈ H ₁₅ NO ₃	8.4	N-Acyl-Amino Acid	
N-Acetyl-Leukotriene E ₄	481.250 C ₂₅ H ₃₉ NO ₆ S	8.3	Cystienyl-leukotriene	

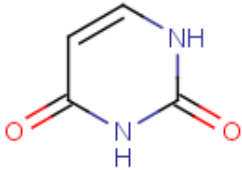
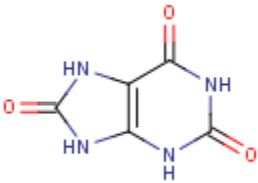
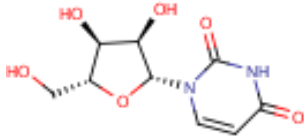
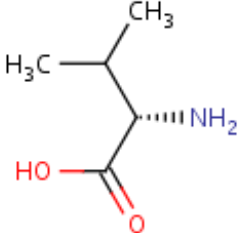
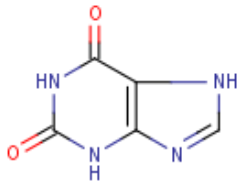
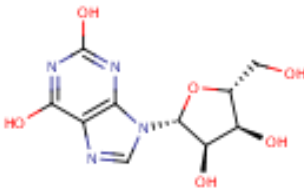
N-Acetyl-Phenylalanine	207.089 C ₁₁ H ₁₃ NO ₃	8.1	N-Acyl-Amino Acid	
Norepinephrine	169.074 C ₈ H ₁₁ NO ₃	8.4	Catechol	
Nicotinamide	122.048 C ₆ H ₆ N ₂ O	2.0	Pyridine	
Nicotinic Acid	123.032 C ₆ H ₅ NO ₂	4.1	Pyridine	
Norleucine	131.095 C ₆ H ₁₃ NO ₂	8.2	Amino Acid	
Norvaline	117.079 C ₅ H ₁₁ NO ₂	8.4	Amino Acid	

O-Phosphoserine	185.009 C ₃ H ₈ NO ₆ P	11.1	Amino Acid	
Ornithine	132.090 C ₅ H ₁₂ N ₂ O ₂	12.7	Amino Acid	
Oxaloacetic Acid	132.006 C ₄ H ₄ O ₅	2.1	Organic Acid	
Oxoglutaric Acid	146.022 C ₅ H ₆ O ₅	6.5	Organic Acid	
Palmitic Acid	256.240 C ₁₆ H ₃₂ O ₂	2.9	Fatty Acid	
Palmitoylcarnitine	399.335 C ₂₃ H ₄₅ NO ₄	5.3	Acyl Carnitine	
Pentadecanoic Acid	242.225 C ₁₅ H ₃₀ O ₂	3.0	Fatty Acid	

Phenylalanine	165.079 C ₉ H ₁₁ NO ₂	8.9	Amino Acid	
2-Phenylglycine	151.063 C ₈ H ₉ NO ₂	8.1	Amino Acid	
Phenylpyruvic acid	164.047 C ₉ H ₈ O ₃	4.0	Organic acid	
Proline	115.063 C ₅ H ₉ NO ₂	8.4	Amino Acid	
Pyridoxine	169.074 C ₈ H ₁₁ NO ₃	7.0	Pyridine	
Ribose-1-Phosphate	230.019 C ₅ H ₁₁ O ₈ P	2.8	Sugar Phosphate	

Sarcosine	89.048 C ₃ H ₇ NO ₂	9.3	Amino Acid	
Serine	105.093 C ₃ H ₇ NO ₃	9.8	Amino Acid	
Serotonin	176.095 C ₁₀ H ₁₂ N ₂ O	11.7	Biogenic Amine	
Shikimic Acid	174.053 C ₇ H ₁₀ O ₅	6.4	Organic Acid	
Taurine	125.014 C ₂ H ₇ NO ₃ S	9.2	Sulfonic Acid	
Threonine	119.058 C ₄ H ₉ NO ₃	9.4	Amino Acid	

Thymidine	242.090 $C_{10}H_{14}N_2O_5$	2.0	Nucleoside	
Tryptamine	160.100 $C_{10}H_{12}N_2$	13.4	Biogenic Amine	
Tryptophan	204.090 $C_{11}H_{12}N_2O_2$	9.5	Amino Acid	
4-Tyramine	137.084 $C_8H_{11}NO$	12.4	Biogenic Amine	
Tyrosine	181.074 $C_9H_{11}NO_3$	8.6	Amino Acid	
Undecanoic Acid	186.162 $C_{11}H_{22}O_2$	2.4	Fatty Acid	

Uracil	112.027 C ₄ H ₄ N ₂ O ₂	2.1	Purine	
Uric Acid	168.028 C ₅ H ₄ N ₄ O ₃	8.0	Purine	
Uridine	244.070 C ₉ H ₁₂ N ₂ O ₆	4.9	Nucleoside	
Valine	117.079 C ₅ H ₁₁ NO ₂	8.6	Amino Acid	
Xanthine	152.033 C ₅ H ₄ N ₄ O ₂	4.0	Purine	
Xanthosine	284.076 C ₁₀ H ₁₂ N ₄ O ₆	7.1	Nucleoside	

Appendix 2. XCMS and CAMERA Operational Parameters

```
sleep=0.0001
```

```
family="s", plotype="m"
```

```
bw = 30, minfrac = 0.5, minsamp= 1, mzwid = 0.25, max = 5, sleep = 0
```

```
xsa <- xsAnnotate(xset3)
```

```
groupFWHM(xsa, perfwHM=0.6)
```

```
xsaFI <- findIsotopes(xsaF, mzabs=0.01, maxcharge=3, maxiso=3, ppm=5)
```

```
xsaC <- groupCorr(xsaFI, cor_eic_th=0.75, polarity="")
```

Appendix 3. Metabolites Exhibiting statistically significant changes 20 minutes post challenge and beyond in mouse serum. Metabolites *identified unambiguously by comparison to authentic chemical standards are listed as 1°*; Metabolites *identified based on matches between their mass spectra and mass spectra found in databases are listed as 2°*; metabolites where chemical formulae were assigned based on accurate mass and isotope ratio measurements are listed as 3°; True unknown metabolites are listed as 4°.

m/z	Identification	Retention time (min)	p Value	Identification Confidence
(-)92.024	Aniline	3.9	<0.001	1°
(-)102.054	GABA	3.1	0.007	1°
(-)108.021	Hypotaurine	3.9	<0.001	1°
(-)110.025	Cytosine	4.1	<0.001	1°
(+)110.044	Hypotaurine	3.9	<0.001	1°
(-)111.018	Uracil	4	0.001	1°
(+)112.051	Cytosine	5.2	0.004	1°
(-)112.053	Creatinine	6.7	0.001	1°
(+)112.087	Histamine	13.1	0.004	1°
(+)113.035	Uracil	4	<0.001	1°
(+)132.102	Isoleucine	7.9	0.001	1°
(-)134.069	Methylcysteine	2.9	0.009	1°
(+)136.051	Methylcysteine	8.4	0.001	1°
(+)136.064	Adenine	3.3	0.008	1°
(+)150.059	Methionine	8.3	0.008	1°
(+)153.042	Xanthine	3.9	0.003	1°
(-)155.011	Orotic acid	7.6	0.003	1°
(+)156.077	Histidine	11.8	<0.001	1°
(-)167.022	Uric acid	8	<0.001	1°
(+)170.093	1-Methylhistidine	11.9	0.007	1°
(-)174.041	Acetyl-asp	7.6	0.005	1°
(-)174.080	Argininic acid	3.7	0.005	1°
(+)175.002	Aconitic acid	3.9	0.004	1°
(-)175.025	Ascorbic acid	8.2	0.001	1°
(-)266.091	Adenosine	3.4	0.006	1°
(-)267.073	Inosine	6.6	0.003	1°
(+)268.108	Adenosine	3.4	0.009	1°
(+)283.082	Xanthosine	5.7	0.006	1°
(+)487.179	Cytidine (2M+H)	7.5	0.01	1°
(+)86.096	Pyrrrolidinone	7.9	0.001	2°
(+)108.008	Diketogulonic acid	9.2	0.006	2°
(+)126.102	Methylhistamine	12.6	0.001	2°

(+)139.052	Urocanic acid	3.3	0.009	2°
(+)168.035	Thioguanine	6.2	0.003	2°
(-)176.040	Formyl-met	0	0.006	2°
(+)177.103	Allantoic acid	8.2	0.001	2°
(+)188.175	N-acetylspermidine	13.3	<0.001	2°
(-)191.996	5,6-Dihydroxyindole-2-carboxylic acid	9.3	0.006	2°
(+)202.181	Capryloylglycine	7.6	0.008	2°
(+)226.084	Murrayanine	5.2	0.005	2°
(+)232.059	N2-Succinyl-L-glutamic acid 5-semialdehyde	13.2	<0.001	2°
(-)232.059	Deoxyribose phosphate (NH ₄ ⁺ adduct)	13.2	<0.001	2°
(-)243.064	Uridine	4	0.005	2°
(+)244.093	C ₁₀ H ₁₀ N ₇ O	7.5	0.006	2°
(+)298.351	Isoprostane	4.5	0.001	2°
(+)329.270	MG(16:0)	4	0.005	2°
(+)418.156	Met-met-his	8.5	0.002	2°
(+)423.278	DHAP(18:0)	4	0.009	2°
(+)441.217	Tyr-lys-met	8.9	0.007	2°
(-)452.279	lysoPE(16:0)	7.3	0.009	2°
(-)476.278	lysoPE(18:2)	7.1	0.003	2°
(+)478.294	lysoPE(18:2)	7.1	0.001	2°
(+)478.294	lysoPE(18:2)	7.3	0.006	2°
(-)480.309	lysoPE(18:0)	7.9	0.002	2°
(+)502.296	lysoPE (20:4)	7	0.002	2°
(-)506.319	PE (20:1)	8.1	0.003	2°
(-)508.341	PE (20:0)	8.5	<0.001	2°
(-)520.410	lysoPC(18:1)	26.5	0.001	2°
(-)524.278	lysoPE(22:6)	7	<0.001	2°
(-)526.313	PE (22:5)	8	0.008	2°
(+)538.386	PE (22:0)	8.7	<0.001	2°
(+)540.331	PC (20:5)	8.1	0.002	2°
(+)542.324	LysoPC (20:5)	7.9	0.003	2°
(-)544.317	PC (20:3)	0	0.001	2°
(-)553.411	TG (30:0)	4.6	0.009	2°
(+)717.448	PG (32:2)	4	0.007	2°
(+)744.547	PC(33:2)	28.6	0.007	2°
(-)762.510	PC(36:4)	22.9	0.001	2°
(-)766.542	PC(35:4)	29	0.007	2°
(+)768.097	Coenzyme A	7	0.002	2°
(+)770.561	PE (38:3)	28.4	0.008	2°
(-)788.567	PE (38 :5)	4.5	0.01	2°
(+)801.431	PGP (32:1)	2.3	0.002	2°

(+)804.548	PC(38:7)	23.7	<0.001	2°
(+)190.053	Acetyl-met	2.3	0.001	2°
(-)85.029	C ₄ H ₅ O ₂	5.4	<0.001	3°
(-)88.040	C ₃ H ₆ NO ₂	5	0.001	3°
(-)88.041	C ₃ H ₆ NO ₂	9.5	0.007	3°
(+)88.076	C ₄ H ₁₀ NO	8.2	0.007	3°
(-)99.009	C ₄ H ₃ O ₃	8.2	0.009	3°
(-)99.045	C ₅ H ₇ O ₂	4.2	0.006	3°
(-)101.024	C ₄ H ₅ O ₃	2.2	0.009	3°
(+)104.107	C ₄ H ₉ NO ₂	8.3	0.008	3°
(-)107.037	C ₆ H ₅ NO	8.6	0.001	3°
(+)109.076	C ₆ H ₉ N ₂	12.6	0.009	3°
(-)110.072	C ₅ H ₈ N ₃	11.9	0.001	3°
(+)112.051	C ₄ H ₆ N ₃ O	7.5	0.005	3°
(-)114.032	C ₅ H ₆ O ₃	7.6	0.001	3°
(+)114.067	C ₆ H ₈ N ₃ O	6.6	0.001	3°
(-)114.093	C ₆ H ₁₂ NO	2.1	0.002	3°
(-)115.040	C ₅ H ₇ O ₃	3.5	0.002	3°
(-)116.035	C ₄ H ₆ NO ₃	6	<0.001	3°
(-)116.048	C ₅ H ₈ O ₃	7.9	<0.001	3°
(+)116.071	C ₅ H ₁₀ NO ₂	8.9	0.004	3°
(-)119.034	C ₄ H ₇ O ₄	4.1	<0.001	3°
(+)121.013	C ₃ H ₅ O ₅	2.1	<0.001	3°
(+)122.020	C ₃ H ₆ O ₅	2.7	0.002	3°
(+)126.069	C ₇ H ₁₂ O ₂	5.7	<0.001	3°
(+)128.019	C ₂ H ₂ N ₅ O ₂	9.2	0.002	3°
(-)128.036	C ₅ H ₆ NO ₃	8	0.006	3°
(+)128.131	C ₇ H ₁₆ N ₂	7.6	0.003	3°
(+)130.088	C ₆ H ₁₂ NO ₂	12	0.001	3°
(-)130.088	C ₆ H ₁₃ NO ₂	7.8	0.003	3°
(-)131.047	C ₄ H ₇ N ₂ O ₃	5	0.001	3°
(+)132.077	C ₄ H ₁₀ N ₃ O ₂	9.5	<0.001	3°
(+)133.033	C ₂ H ₅ N ₄ O ₃	8.3	0.006	3°
(+)133.062	C ₄ H ₉ N ₂ O ₃	5	<0.001	3°
(-)136.016	C ₇ H ₄ O ₃	20.7	0.001	3°
(+)136.048	C ₃ H ₈ N ₂ O ₄	9.6	0.003	3°
(+)139.039	C ₅ H ₅ N ₃ O ₂	20.7	<0.001	3°
(+)140.069	C ₅ H ₈ N ₄ O	8.9	0.001	3°
(-)145.063	C ₅ H ₉ N ₂ O ₃	9.7	0.004	3°
(-)145.099	C ₆ H ₁₃ N ₂ O ₂	12.1	<0.001	3°
(+)146.061	C ₉ H ₈ NO	7.9	0.003	3°
(-)147.053	C ₅ H ₉ NO ₄	8.5	<0.001	3°
(+)147.113	C ₆ H ₁₅ N ₂ O ₂	12.1	0.002	3°

(+)149.023	C ₈ H ₅ O ₃	21.2	0.001	3°
(+)150.013	C ₂ H ₄ N ₃ O ₅	9.8	0.001	3°
(-)153.029	C ₆ H ₅ N ₂ O ₃	7.1	<0.001	3°
(+)154.059	C ₄ H ₆ N ₆ O	9.6	<0.001	3°
(+)155.044	C ₄ H ₅ N ₅ O ₂	5	<0.001	3°
(-)156.067	C ₇ H ₁₀ NO ₃	2.2	<0.001	3°
(-)157.038	C ₆ H ₇ NO ₄	7.6	<0.001	3°
(+)159.026	C ₄ H ₅ N ₃ O ₄	3.9	<0.001	3°
(-)160.062	C ₆ H ₁₀ NO ₄	3.6	<0.001	3°
(+)160.134	C ₈ H ₁₈ NO ₂	9.5	0.001	3°
(+)162.113	C ₇ H ₁₆ NO ₃	10	0.001	3°
(+)163.063	C ₉ H ₉ NO ₂	2	<0.001	3°
(-)164.073	C ₉ H ₁₀ NO ₂	7.6	<0.001	3°
(+)167.000	C ₄ H ₇ O ₅ S	9.5	0.001	3°
(-)168.014	C ₃ H ₆ NO ₇	6.2	<0.001	3°
(-)170.082	C ₈ H ₁₂ NO ₃	2	0.001	3°
(+)173.131	C ₈ H ₁₇ N ₂ O ₂	7.6	<0.001	3°
(+)174.006	C ₈ H ₂ N ₂ O ₃	13.2	<0.001	3°
(+)174.137	C ₈ H ₁₈ N ₂ O ₂	7.6	<0.001	3°
(-)178.051	C ₉ H ₈ NO ₃	2.3	0.001	3°
(+)181.161	C ₁₂ H ₂₁ O	2.1	<0.001	3°
(+)187.059	C ₆ H ₉ N ₃ O ₄	6.1	0.002	3°
(-)187.073	C ₇ H ₁₁ N ₂ O ₄	8.1	0.004	3°
(-)188.058	C ₁₀ H ₈ N ₂ O ₂	8	<0.001	3°
(+)189.160	C ₉ H ₂₁ N ₂ O ₂	12.6	<0.001	3°
(+)191.056	C ₈ H ₇ N ₄ O ₂	2.3	0.001	3°
(+)191.091	C ₆ H ₁₃ N ₃ O ₄	7.9	<0.001	3°
(+)192.096	C ₄ H ₁₂ N ₆ O ₃	7.9	<0.001	3°
(+)192.159	C ₉ H ₂₂ NO ₃	6.8	<0.001	3°
(-)193.014	C ₉ H ₅ O ₅	7.6	0.001	3°
(-)195.010	C ₆ H ₁₁ O ₇	7.6	0.001	3°
(-)201.039	C ₆ H ₇ N ₃ O ₅	9.4	<0.001	3°
(-)201.089	C ₈ H ₁₃ N ₂ O ₄	8.4	0.01	3°
(+)203.053	C ₆ H ₉ N ₃ O ₅	8.6	0.008	3°
(-)204.067	C ₁₁ H ₁₀ NO ₃	3.6	0.002	3°
(+)204.124	C ₉ H ₁₈ NO ₄	9.2	0.009	3°
(-)206.081	C ₁₁ H ₁₂ NO ₃	2.1	0.004	3°
(+)209.105	C ₁₁ H ₁₅ NO ₃	3.6	0.001	3°
(-)210.042	C ₁₀ H ₄ N ₅ O	6.6	<0.001	3°
(-)213.087	C ₇ H ₁₁ N ₅ O ₃	12.1	0.006	3°
(+)215.081	C ₁₂ H ₁₁ N ₂ O ₂	8	0.003	3°
(-)222.077	C ₁₁ H ₁₂ NO ₄	3.4	0.001	3°
(-)225.063	C ₈ H ₉ N ₄ O ₄	8.6	0.009	3°

(-)226.085	C ₁₁ H ₁₄ O ₅	6.6	0.003	3°
(+)226.105	C ₇ H ₁₂ N ₇ O ₂	9.6	0.005	3°
(+)228.099	C ₉ H ₁₄ N ₃ O ₄	6.6	0.002	3°
(+)229.159	C ₁₆ H ₂₁ O	9.6	0.002	3°
(-)230.103	C ₁₀ H ₁₆ NO ₅	2.7	<0.001	3°
(+)231.087	C ₁₁ H ₁₁ N ₄ O ₂	3.6	0.001	3°
(+)231.097	C ₇ H ₁₃ N ₅ O ₄	8.1	0.001	3°
(+)231.137	C ₁₃ H ₁₇ N ₃ O	5.4	0.001	3°
(+)231.142	C ₅ H ₁₅ N ₁₀ O	6.8	<0.001	3°
(+)232.155	C ₁₁ H ₂₂ NO ₄	8.2	0.001	3°
(+)233.106	C ₉ H ₁₆ N ₂ O ₅	2.9	<0.001	3°
(+)235.084	C ₁₂ H ₁₃ NO ₄	7.3	0.009	3°
(+)235.166	C ₁₀ H ₂₃ N ₂ O ₄	8.8	0.001	3°
(-)242.080	C ₁₂ H ₁₀ N ₄ O ₂	7.5	0.004	3°
(+)243.048	C ₈ H ₉ N ₃ O ₆	8	0.002	3°
(-)246.154	C ₇ H ₁₈ N ₈ O ₂	6.8	0.001	3°
(+)246.171	C ₁₂ H ₂₄ NO ₄	7.9	<0.001	3°
(+)250.040	C ₃ H ₆ N ₈ O ₆	4.1	0.002	3°
(-)252.030	C ₁₂ H ₄ N ₄ O ₃	11.8	0.005	3°
(+)259.028	C ₄ H ₉ N ₃ O ₁₀	9.6	0.007	3°
(+)260.186	C ₁₃ H ₂₆ NO ₄	7.6	<0.001	3°
(+)262.165	C ₁₂ H ₂₄ NO ₅	9	<0.001	3°
(-)268.054	C ₇ H ₁₂ N ₂ O ₉	2.9	<0.001	3°
(-)269.055	C ₁₂ H ₇ N ₅ O ₃	7.6	<0.001	3°
(-)274.085	C ₁₅ H ₁₄ O ₅	6.6	<0.001	3°
(+)275.112	C ₁₁ H ₁₃ N ₇ O ₂	3.6	<0.001	3°
(-)276.123	C ₁₃ H ₁₆ N ₄ O ₃	7.8	0.001	3°
(+)282.121	C ₁₃ H ₁₈ N ₂ O ₅	8.6	0.002	3°
(-)284.133	C ₈ H ₂₀ N ₄ O ₇	7.6	<0.001	3°
(+)288.214	C ₁₀ H ₃₀ N ₃ O ₆	7.4	<0.001	3°
(+)288.292	C ₁₇ H ₃₈ NO ₂	3.8	<0.001	3°
(-)293.092	C ₁₅ H ₁₁ N ₅ O ₂	4.7	0.008	3°
(+)296.066	C ₁₅ H ₁₀ N ₃ O ₄	10.5	<0.001	3°
(+)297.157	C ₁₅ H ₂₃ NO ₅	3.9	0.003	3°
(+)304.043	C ₁₂ H ₈ N ₄ O ₆	6.7	<0.001	3°
(+)305.264	C ₁₁ H ₃₁ N ₉ O	21.2	<0.001	3°
(-)307.264	C ₂₀ H ₃₅ O ₂	2.8	<0.001	3°
(+)314.234	C ₁₃ H ₃₅ N ₂ O ₄ P	7.3	0.001	3°
(-)332.240	C ₁₂ H ₃₄ N ₃ O ₇	2.1	<0.001	3°
(-)333.094	C ₁₂ H ₁₇ N ₂ O ₉	4.1	0.002	3°
(-)334.031	C ₈ H ₁₅ O ₁₂ P	9.6	0.009	3°
(+)336.307	C ₁₅ H ₄₄ O ₇	21.5	0.001	3°
(+)338.051	C ₉ H ₉ N ₉ O ₄ P	8.3	0.001	3°

(+)340.043	C ₁₀ H ₁₅ NO ₁₀ P	8.3	<0.001	3°
(+)359.092	C ₈ H ₁₇ N ₅ O ₁₁	9.6	0.001	3°
(+)362.226	C ₁₃ H ₃₄ N ₂ O ₉	3.2	0.002	3°
(+)364.054	C ₁₀ H ₉ N ₁₀ O ₄ P	10.5	<0.001	3°
(-)367.284	C ₁₆ H ₄₀ N ₄ O ₃ P	2.9	0.002	3°
(+)368.327	C ₂₁ H ₄₂ N ₃ O ₂	22.9	0.004	3°
(-)369.069	C ₂₃ H ₁₄ O ₃ P	11.9	0.007	3°
(-)375.173	C ₉ H ₂₅ N ₇ O ₉	8.9	<0.001	3°
(+)377.082	C ₁₁ H ₁₅ N ₅ O ₁₀	9.2	0.001	3°
(-)378.036	C ₁₃ H ₁₅ O ₁₁ P	7.6	0.001	3°
(-)381.173	C ₁₁ H ₂₉ N ₂ O ₁₂	2.7	<0.001	3°
(-)383.189	C ₁₅ H ₂₈ O ₇ P ₂	4	0.005	3°
(+)394.296	C ₁₉ H ₄₃ N ₂ O ₄ P	7.2	0.009	3°
(+)396.312	C ₁₉ H ₄₅ N ₂ O ₄ P	7.2	0.002	3°
(+)397.084	C ₁₁ H ₁₇ N ₄ O ₁₂	9	<0.001	3°
(-)401.157	C ₁₃ H ₂₈ N ₃ O ₉ P	8.5	0.002	3°
(+)416.073	C ₁₈ H ₁₄ N ₃ O ₉	10.4	<0.001	3°
(-)417.014	C ₉ H ₁₁ N ₃ O ₁₆	9.6	0.003	3°
(-)418.004	C ₁₁ H ₉ N ₅ O ₁₁ P	9.2	0.003	3°
(+)424.343	C ₂₅ H ₄₆ NO ₄	7.3	<0.001	3°
(+)430.377	C ₂₄ H ₅₀ N ₂ O ₄	24.1	<0.001	3°
(+)438.306	C ₂₁ H ₄₄ NO ₈	7.3	0.001	3°
(+)442.356	C ₂₈ H ₄₆ N ₂ O ₂	7.6	0.009	3°
(-)445.330	C ₂₄ H ₄₁ N ₆ O ₂	2.3	<0.001	3°
(+)447.059	C ₂₃ H ₁₃ NO ₉	11.3	0.005	3°
(+)448.325	C ₁₈ H ₄₆ N ₃ O ₉	22.3	<0.001	3°
(-)449.363	C ₂₇ H ₄₆ O ₅	3.6	0.004	3°
(-)658.542	C ₄₀ H ₇₃ N ₃ O ₄	4	0.002	3°
(-)688.352	C ₃₆ H ₅₁ NO ₁₂	8	0.002	3°
(+)94.221	Unknown	9.7	0.001	4°
(-)97.005	Unknown	7.6	<0.001	4°
(-)101.029	Unknown	4.2	0.001	4°
(-)118.654	Unknown	3.1	0.006	4°
(+)120.003	Unknown	9.7	0.007	4°
(+)123.448	Unknown	7.7	0.01	4°
(+)124.034	Unknown	14.9	<0.001	4°
(+)125.019	Unknown	10	<0.001	4°
(-)125.074	Unknown	8.2	0.009	4°
(+)127.125	Unknown	7.7	0.005	4°
(-)131.839	Unknown	8	0.007	4°
(+)140.002	Unknown	15.6	<0.001	4°
(+)143.998	Unknown	15.6	0.005	4°
(+)151.215	Unknown	12.1	0.001	4°

(+)153.069	Unknown	2.1	<0.001	4°
(-)155.238	Unknown	4	0.001	4°
(+)158.097	Unknown	2.2	0.01	4°
(+)158.997	Unknown	15.6	<0.001	4°
(+)179.614	Unknown	12	0.006	4°
(-)180.975	Unknown	9.6	<0.001	4°
(+)184.075	Unknown	8	0.003	4°
(-)187.043	Unknown	3.8	<0.001	4°
(-)188.950	Unknown	3.6	<0.001	4°
(-)194.084	Unknown	2.2	0.002	4°
(-)194.928	Unknown	11.7	<0.001	4°
(-)196.030	Unknown	6.4	0.001	4°
(+)197.009	Unknown	7.6	0.001	4°
(+)200.073	Unknown	10	0.004	4°
(-)203.084	Unknown	7.9	0.006	4°
(-)209.095	Unknown	5.6	<0.001	4°
(-)221.015	Unknown	9.3	0.007	4°
(+)226.125	Unknown	2.6	0.002	4°
(+)233.106	Unknown	2.9	0.005	4°
(-)236.022	Unknown	9.3	<0.001	4°
(-)241.000	Unknown	11.9	0.001	4°
(+)244.265	Unknown	4.2	0.009	4°
(+)246.176	Unknown	12.3	<0.001	4°
(-)248.073	Unknown	2.7	0.005	4°
(-)248.962	Unknown	9.6	<0.001	4°
(+)251.669	Unknown	2	<0.001	4°
(-)260.400	Unknown	3.2	0.005	4°
(+)261.004	Unknown	4.2	0.008	4°
(+)262.886	Unknown	11.7	<0.001	4°
(-)269.253	Unknown	6.4	0.009	4°
(+)269.995	Unknown	9.7	0.002	4°
(+)270.317	Unknown	4	0.001	4°
(-)270.317	Unknown	4	0.006	4°
(-)271.607	Unknown	3.5	0.002	4°
(-)271.607	Unknown	3.5	<0.001	4°
(+)271.683	Unknown	2.1	0.003	4°
(+)273.665	Unknown	3.3	0.001	4°
(+)273.682	Unknown	2	<0.001	4°
(+)279.039	Unknown	4	<0.001	4°
(+)282.283	Unknown	2.1	0.001	4°
(-)292.988	Unknown	9.7	0.004	4°
(-)294.091	Unknown	9.6	0.003	4°
(+)295.695	Unknown	2	0.002	4°

(+)296.694	Unknown	2	<0.001	4°
(+)303.307	Unknown	3.4	0.003	4°
(+)312.548	Unknown	8.3	0.002	4°
(+)316.323	Unknown	3.8	0.009	4°
(+)324.330	Unknown	2.9	0.009	4°
(+)352.524	Unknown	6.8	<0.001	4°
(+)355.579	Unknown	21.1	0.005	4°
(-)360.975	Unknown	9.7	0.006	4°
(+)366.663	Unknown	8.9	<0.001	4°
(+)379.084	Unknown	9.2	0.004	4°
(-)381.074	Unknown	9.3	0.002	4°
(-)381.486	Unknown	8.3	<0.001	4°
(+)386.967	Unknown	21.4	0.006	4°
(-)388.684	Unknown	8.9	<0.001	4°
(+)403.860	Unknown	8.9	<0.001	4°
(+)404.973	Unknown	9.6	0.009	4°
(+)410.690	Unknown	9	<0.001	4°
(+)411.094	Unknown	8.1	0.003	4°
(+)419.203	Unknown	9	<0.001	4°
(+)419.203	Unknown	9	<0.001	4°
(-)419.554	Unknown	8.3	0.007	4°
(+)425.079	Unknown	11.3	0.003	4°
(+)425.378	Unknown	4	0.007	4°
(+)426.771	Unknown	2.4	<0.001	4°
(-)427.786	Unknown	9.7	0.005	4°
(-)432.708	Unknown	9	<0.001	4°
(+)435.788	Unknown	2.4	0.006	4°
(+)438.783	Unknown	3.8	0.008	4°
(+)441.217	Unknown	8.9	0.001	4°
(-)447.059	Unknown	11.3	0.009	4°
(+)451.361	Unknown	21.3	0.002	4°
(+)452.132	Unknown	8.7	0.003	4°
(-)452.923	Unknown	9.6	<0.001	4°
(+)454.200	Unknown	6.4	0.003	4°
(-)458.260	Unknown	8.7	0.001	4°
(+)458.638	Unknown	7.5	0.006	4°
(-)459.811	Unknown	2.6	0.002	4°
(-)461.786	Unknown	9.7	0.001	4°
(+)462.172	Unknown	4	0.004	4°
(+)463.229	Unknown	9	0.001	4°
(+)466.532	Unknown	4.5	0.003	4°
(-)466.938	Unknown	9.6	0.004	4°
(-)467.984	Unknown	4.1	0.008	4°

(+)468.309	Unknown	8	0.002	4°
(-)468.897	Unknown	9.6	<0.001	4°
(+)468.973	Unknown	7.1	0.005	4°
(-)470.343	Unknown	7.4	<0.001	4°
(+)470.568	Unknown	8.3	<0.001	4°
(+)471.054	Unknown	11.3	0.001	4°
(+)471.343	Unknown	2.4	0.007	4°
(+)471.562	Unknown	8.3	0.004	4°
(-)472.556	Unknown	8.3	0.004	4°
(-)473.280	Unknown	2	<0.001	4°
(+)473.362	Unknown	2.9	0.005	4°
(+)475.391	Unknown	6.8	<0.001	4°
(-)475.380	Unknown	3.6	0.004	4°
(+)475.380	Unknown	3.6	0.006	4°
(-)476.721	Unknown	9	0.003	4°
(-)477.395	Unknown	5.2	0.005	4°
(+)478.976	Unknown	7.8	0.002	4°
(+)480.310	Unknown	7.2	0.003	4°
(-)482.314	Unknown	4.7	0.007	4°
(+)482.324	Unknown	8.1	0.002	4°
(+)482.653	Unknown	5.6	0.009	4°
(-)485.001	Unknown	9.6	0.001	4°
(+)485.243	Unknown	9	0.004	4°
(-)485.619	Unknown	7.2	0.002	4°
(+)487.648	Unknown	6.5	0.009	4°
(+)488.428	Unknown	24.1	0.002	4°
(+)488.981	Unknown	7.8	0.006	4°
(-)492.359	Unknown	9.6	0.004	4°
(+)495.773	Unknown	9.7	<0.001	4°
(+)496.195	Unknown	6.6	<0.001	4°
(-)496.272	Unknown	2	0.006	4°
(+)496.341	Unknown	8.1	0.002	4°
(+)496.830	Unknown	3.5	<0.001	4°
(-)498.262	Unknown	7	0.006	4°
(+)498.324	Unknown	7.4	0.004	4°
(+)498.901	Unknown	9.6	<0.001	4°
(+)501.056	Unknown	8.3	<0.001	4°
(-)501.394	Unknown	3.6	0.004	4°
(+)501.394	Unknown	3.6	0.007	4°
(+)502.830	Unknown	2.6	0.009	4°
(+)504.825	Unknown	5.4	0.003	4°
(-)505.392	Unknown	2.3	0.001	4°
(+)506.375	Unknown	22.3	0.002	4°

(+)507.256	Unknown	9	0.008	4°
(-)507.273	Unknown	4.5	0.001	4°
(+)508.354	unknown	8	0.002	4°
(+)508.341	Unknown	8.5	0.004	4°
(+)510.357	Unknown	8.3	<0.001	4°
(+)512.337	Unknown	8	0.005	4°
(+)512.918	Unknown	9.6	<0.001	4°
(-)512.967	Unknown	3	0.003	4°
(+)513.635	Unknown	3	0.005	4°
(+)514.389	Unknown	20.6	0.004	4°
(-)516.282	Unknown	8.1	0.001	4°
(+)516.999	Unknown	7	0.006	4°
(+)517.673	Unknown	6.9	0.005	4°
(+)518.342	Unknown	3.9	0.002	4°
(-)519.852	Unknown	2.1	<0.001	4°
(+)520.341	Unknown	8	0.001	4°
(-)521.040	Unknown	9.2	<0.001	4°
(+)521.344	Unknown	8	0.001	4°
(+)521.662	Unknown	8.5	0.002	4°
(+)524.340	Unknown	8.1	0.006	4°
(+)524.370	Unknown	2.6	0.005	4°
(+)524.372	Unknown	8.5	0.001	4°
(+)524.829	Unknown	6.5	<0.001	4°
(-)527.332	Unknown	4	0.006	4°
(+)527.332	Unknown	4	<0.001	4°
(-)527.407	Unknown	2.7	0.002	4°
(+)527.676	Unknown	7.6	0.005	4°
(+)528.381	Unknown	20.7	0.001	4°
(+)529.057	Unknown	2.4	0.001	4°
(-)529.423	Unknown	4	0.001	4°
(+)529.426	Unknown	5.8	0.009	4°
(-)530.302	Unknown	8.1	0.008	4°
(-)530.839	Unknown	8.5	<0.001	4°
(+)531.349	Unknown	3	0.006	4°
(+)531.474	Unknown	29.7	<0.001	4°
(-)531.681	Unknown	7.1	0.007	4°
(+)533.638	Unknown	2.5	0.003	4°
(+)534.297	Unknown	9.4	0.001	4°
(-)536.118	Unknown	2.7	<0.001	4°
(-)537.487	Unknown	2.8	0.003	4°
(+)537.642	Unknown	2.7	0.007	4°
(-)538.315	Unknown	7.9	<0.001	4°
(+)538.357	Unknown	2.2	<0.001	4°

(+)538.386	Unknown	8.7	<0.001	4°
(+)538.161	Unknown	27.6	0.006	4°
(+)540.367	Unknown	8.2	0.006	4°
(+)540.949	Unknown	9.6	<0.001	4°
(+)541.016	Unknown	6.5	0.005	4°
(+)543.574	unknown	7.3	0.001	4°
(-)544.149	Unknown	2	<0.001	4°
(+)544.317	Unknown	8.3	0.006	4°
(+)544.342	Unknown	7.9	0.001	4°
(+)546.015	Unknown	4.3	<0.001	4°
(-)546.353	Unknown	8.7	<0.001	4°
(+)546.355	Unknown	2.9	0.001	4°
(-)547.297	Unknown	2.2	0.001	4°
(+)547.355	Unknown	7.9	0.009	4°
(+)547.526	Unknown	3.8	0.004	4°
(+)547.645	Unknown	2.6	0.004	4°
(+)548.499	Unknown	29.7	0.002	4°
(+)548.851	Unknown	6.3	<0.001	4°
(+)551.537	Unknown	4.1	0.001	4°
(+)552.071	Unknown	8.3	0.004	4°
(-)552.318	Unknown	3	0.006	4°
(-)552.306	Unknown	7.9	<0.001	4°
(+)552.395	Unknown	9.3	0.006	4°
(+)553.361	Unknown	3.3	0.001	4°
(+)553.411	Unknown	4.6	0.004	4°
(-)554.301	Unknown	8	0.002	4°
(+)554.392	Unknown	8.1	0.003	4°
(+)555.356	Unknown	6.8	0.001	4°
(+)555.441	Unknown	6.1	0.008	4°
(-)556.055	Unknown	8.3	0.004	4°
(-)557.458	Unknown	23.9	0.006	4°
(+)557.664	Unknown	3.4	0.003	4°
(-)558.063	Unknown	11.1	<0.001	4°
(+)558.297	Unknown	7.9	0.002	4°
(-)558.331	Unknown	8.4	0.001	4°
(-)559.469	Unknown	2.2	0.002	4°
(+)560.327	Unknown	9.4	0.004	4°
(+)560.703	Unknown	5.2	0.001	4°
(-)562.009	Unknown	3.7	0.001	4°
(+)562.081	Unknown	7.2	0.006	4°
(-)562.315	Unknown	7.9	0.007	4°
(+)562.867	Unknown	5	<0.001	4°
(-)563.501	Unknown	2.7	0.001	4°

(+)564.334	Unknown	8.6	0.005	4°
(-)567.534	Unknown	4	0.002	4°
(-)568.264	Unknown	7.5	<0.001	4°
(+)568.366	Unknown	3.1	0.003	4°
(+)568.301	Unknown	8.6	0.006	4°
(+)569.428	Unknown	29.7	0.004	4°
(+)569.578	Unknown	7	0.009	4°
(+)570.361	Unknown	6.7	0.002	4°
(+)571.030	Unknown	7	0.006	4°
(-)571.580	Unknown	2.7	0.004	4°
(-)571.668	Unknown	4.2	0.006	4°
(+)572.341	Unknown	3.1	0.006	4°
(+)572.364	Unknown	8	0.005	4°
(-)572.481	Unknown	27.6	0.001	4°
(-)573.438	Unknown	3.5	0.005	4°
(+)575.201	Unknown	6.5	0.004	4°
(-)575.462	Unknown	4.1	0.003	4°
(+)575.462	Unknown	4.1	0.004	4°
(+)575.484	Unknown	28.8	0.007	4°
(-)576.352	Unknown	8.7	0.003	4°
(+)576.350	Unknown	4.1	0.003	4°
(-)588.332	Unknown	7.8	0.007	4°
(+)589.525	Unknown	29.7	<0.001	4°
(-)589.717	Unknown	6.2	0.003	4°
(+)590.380	Unknown	3.5	0.009	4°
(+)590.557	Unknown	8.5	0.003	4°
(+)591.024	Unknown	4.6	<0.001	4°
(-)591.319	Unknown	2.3	0.009	4°
(+)591.549	Unknown	8.5	<0.001	4°
(+)591.594	Unknown	7.2	0.002	4°
(+)591.670	Unknown	2.9	0.008	4°
(+)592.367	Unknown	6.9	0.003	4°
(-)593.436	Unknown	23.8	0.009	4°
(+)594.920	Unknown	9.6	0.001	4°
(+)595.349	Unknown	7.4	0.002	4°
(+)595.508	Unknown	2.3	0.001	4°
(+)598.320	Unknown	8	0.003	4°
(+)600.331	Unknown	8	0.006	4°
(+)601.339	Unknown	7.4	0.002	4°
(+)601.352	Unknown	5.4	0.001	4°
(+)601.357	Unknown	3.8	0.007	4°
(+)602.002	Unknown	3	0.002	4°
(+)602.349	Unknown	8.5	0.005	4°

(+)603.067	Unknown	8.3	0.003	4°
(+)604.725	Unknown	6.5	0.008	4°
(+)604.899	Unknown	2.7	0.007	4°
(-)605.404	Unknown	3.5	0.002	4°
(+)606.301	Unknown	7.8	0.004	4°
(+)606.679	Unknown	3	0.006	4°
(+)606.892	Unknown	6.1	0.002	4°
(+)607.325	Unknown	3.8	<0.001	4°
(-)608.357	Unknown	7.9	0.009	4°
(+)608.936	Unknown	9.6	<0.001	4°
(+)610.907	Unknown	9.6	<0.001	4°
(+)611.056	Unknown	8.3	0.003	4°
(+)611.148	Unknown	11.3	0.003	4°
(+)611.688	Unknown	3.3	0.008	4°
(-)612.390	Unknown	3.9	0.009	4°
(+)613.056	Unknown	8.3	0.007	4°
(+)613.605	Unknown	7.3	0.001	4°
(+)614.330	Unknown	2.8	0.003	4°
(+)614.343	Unknown	9.6	<0.001	4°
(-)616.457	Unknown	5	0.002	4°
(-)616.650	Unknown	7.9	0.008	4°
(+)616.680	Unknown	3.1	0.006	4°
(+)617.111	Unknown	7.5	<0.001	4°
(+)619.901	Unknown	4.7	0.002	4°
(+)621.022	Unknown	3.2	0.003	4°
(+)624.613	Unknown	7.3	<0.001	4°
(-)625.320	Unknown	2.4	0.004	4°
(+)626.409	Unknown	3	0.007	4°
(-)627.785	Unknown	7.1	0.002	4°
(+)629.323	Unknown	3.7	0.008	4°
(+)630.322	Unknown	9.5	0.001	4°
(+)630.702	Unknown	6.3	0.005	4°
(+)631.354	Unknown	3.1	<0.001	4°
(-)632.353	Unknown	7.8	0.001	4°
(+)634.537	Unknown	25.2	<0.001	4°
(+)634.536	Unknown	23.9	0.003	4°
(+)634.877	Unknown	9.6	0.006	4°
(-)635.347	Unknown	2.5	0.003	4°
(+)635.621	Unknown	7.4	<0.001	4°
(+)635.698	Unknown	2.9	0.007	4°
(+)636.901	Unknown	7.3	<0.001	4°
(+)638.577	Unknown	3.6	0.007	4°
(-)638.937	Unknown	2.9	0.003	4°

(+)641.353	Unknown	2.7	0.007	4°
(+)642.019	Unknown	2.7	0.004	4°
(+)643.028	Unknown	25.2	0.001	4°
(+)643.018	Unknown	23.9	0.003	4°
(+)644.833	Unknown	5.4	0.002	4°
(+)645.188	Unknown	28.8	0.008	4°
(+)645.377	Unknown	6.5	0.009	4°
(+)646.320	Unknown	7.8	0.003	4°
(+)646.695	Unknown	3.1	0.002	4°
(-)647.373	Unknown	7.9	0.003	4°
(+)648.304	Unknown	7.9	0.005	4°
(-)649.419	Unknown	7.9	0.004	4°
(-)650.278	Unknown	7	0.003	4°
(+)651.040	Unknown	3.1	0.009	4°
(-)652.390	Unknown	5.2	0.003	4°
(+)655.050	Unknown	3.9	<0.001	4°
(-)656.353	Unknown	7.8	0.004	4°
(-)656.523	Unknown	2.8	0.007	4°
(-)656.883	Unknown	9.6	0.004	4°
(+)656.924	Unknown	5.9	0.006	4°
(+)657.881	Unknown	7.5	0.006	4°
(+)658.544	Unknown	6.4	0.001	4°
(+)660.053	Unknown	6.8	0.002	4°
(+)660.066	Unknown	8.3	0.002	4°
(+)660.369	Unknown	2.8	<0.001	4°
(+)661.177	Unknown	8.2	0.008	4°
(-)662.352	Unknown	8	0.004	4°
(-)663.430	Unknown	2.7	0.002	4°
(+)665.049	Unknown	3.3	0.01	4°
(+)665.414	Unknown	7.6	0.006	4°
(+)665.705	Unknown	3.3	0.004	4°
(-)666.030	Unknown	2.4	0.005	4°
(+)668.170	Unknown	7.8	0.01	4°
(-)669.348	Unknown	2.7	0.002	4°
(+)669.726	Unknown	4.3	0.003	4°
(+)670.056	Unknown	6.3	0.002	4°
(+)670.428	Unknown	4.4	<0.001	4°
(+)670.719	Unknown	6.4	0.004	4°
(+)671.036	Unknown	2.8	0.003	4°
(+)672.433	Unknown	7	0.007	4°
(+)672.712	Unknown	8.3	0.007	4°
(+)673.129	Unknown	7	0.008	4°
(+)673.351	Unknown	3.6	0.002	4°

(+)674.730	Unknown	6.9	0.002	4°
(+)677.578	Unknown	28.8	<0.001	4°
(+)678.429	Unknown	5.6	0.003	4°
(-)679.373	Unknown	2.7	<0.001	4°
(-)680.351	Unknown	7.8	0.001	4°
(+)680.705	Unknown	3.2	0.006	4°
(+)682.327	Unknown	9.6	0.004	4°
(+)682.327	Unknown	9.6	0.001	4°
(-)683.399	Unknown	7.9	0.003	4°
(+)683.642	Unknown	7.1	0.004	4°
(+)684.728	Unknown	6.6	0.002	4°
(+)685.048	Unknown	3.7	0.001	4°
(+)685.401	Unknown	6.6	0.004	4°
(-)685.523	Unknown	6.4	0.004	4°
(-)686.354	Unknown	7.9	<0.001	4°
(+)687.205	Unknown	8.4	0.01	4°
(-)687.519	Unknown	26.7	0.002	4°
(+)688.344	Unknown	5.2	0.002	4°
(+)689.406	Unknown	7	0.003	4°
(+)689.720	Unknown	3.2	0.003	4°
(+)690.074	Unknown	7	0.001	4°
(+)690.384	Unknown	3.2	0.009	4°
(+)691.346	Unknown	5.3	0.003	4°
(+)692.447	Unknown	5	0.002	4°
(+)692.953	Unknown	4.1	0.01	4°
(+)694.399	Unknown	2.4	0.001	4°
(+)695.052	Unknown	3.2	0.003	4°
(+)695.864	Unknown	3.5	0.008	4°
(+)696.031	Unknown	8.3	0.003	4°
(-)698.481	Unknown	7.9	0.002	4°
(+)699.403	Unknown	6.7	0.004	4°
(+)699.410	Unknown	5.3	0.009	4°
(+)699.712	Unknown	3.2	0.002	4°
(+)700.053	Unknown	3.1	0.004	4°
(+)700.072	Unknown	6.7	0.003	4°
(+)700.390	Unknown	2	0.006	4°
(-)700.364	Unknown	7.8	<0.001	4°
(+)703.319	Unknown	2	0.004	4°
(+)702.868	Unknown	9.6	0.002	4°
(+)704.082	Unknown	7.2	0.007	4°
(+)708.747	Unknown	6.7	0.006	4°
(+)709.076	Unknown	4.4	0.002	4°
(-)709.500	Unknown	5.3	0.001	4°

(+)709.720	Unknown	3.2	0.003	4°
(+)709.735	Unknown	4.4	0.005	4°
(+)710.368	Unknown	5.1	0.002	4°
(-)710.360	Unknown	8.3	0.003	4°
(+)710.727	Unknown	4.4	0.003	4°
(+)711.048	Unknown	2.4	0.005	4°
(+)711.074	Unknown	8.3	0.007	4°
(+)711.365	Unknown	5.1	0.001	4°
(+)711.366	Unknown	3.2	0.004	4°
(+)712.364	Unknown	5.1	0.003	4°
(+)713.067	Unknown	8.3	0.009	4°
(-)713.363	Unknown	2.8	0.007	4°
(+)714.084	Unknown	6.9	0.002	4°
(+)714.396	Unknown	3.3	0.003	4°
(-)714.457	Unknown	4.6	0.01	4°
(-)714.509	Unknown	25.8	0.01	4°
(+)714.743	Unknown	6.9	0.004	4°
(+)715.062	Unknown	3.3	0.004	4°
(+)715.064	Unknown	8.3	0.008	4°
(+)716.523	Unknown	25.8	0.007	4°
(+)718.757	Unknown	7.3	0.004	4°
(+)720.384	Unknown	2.9	0.001	4°
(-)722.412	Unknown	7.9	0.001	4°
(+)724.085	Unknown	4.8	0.003	4°
(-)724.376	Unknown	7.8	<0.001	4°
(+)724.726	Unknown	3.3	0.001	4°
(+)725.559	Unknown	9.6	0.006	4°
(+)726.855	Unknown	4.5	0.001	4°
(-)727.447	Unknown	7.9	<0.001	4°
(+)728.757	Unknown	7	0.003	4°
(+)729.074	Unknown	3.4	0.004	4°
(+)729.423	Unknown	7	0.007	4°
(+)730.898	Unknown	9.6	0.007	4°
(+)732.409	Unknown	2.3	0.008	4°
(+)732.875	Unknown	4.9	0.002	4°
(+)733.841	Unknown	4.9	0.001	4°
(+)734.084	Unknown	4.1	0.003	4°
(-)734.390	Unknown	8.1	0.006	4°
(+)737.565	Unknown	8.3	0.001	4°
(-)738.379	Unknown	8.5	0.01	4°
(+)738.565	Unknown	8.3	0.006	4°
(+)738.754	Unknown	6.8	0.005	4°
(+)738.759	Unknown	5.4	0.004	4°

(+)739.074	Unknown	3.4	0.002	4°
(+)739.578	Unknown	8.3	0.007	4°
(+)739.738	Unknown	3.4	0.003	4°
(-)740.399	Unknown	8.5	0.005	4°
(+)740.568	Unknown	8.3	0.004	4°
(+)743.107	Unknown	6.5	0.007	4°
(+)743.433	Unknown	7.1	0.006	4°
(+)743.745	Unknown	3.7	<0.001	4°
(+)744.099	Unknown	7.2	0.004	4°
(+)744.907	Unknown	9.6	0.009	4°
(+)745.072	Unknown	3.8	0.003	4°
(+)745.201	Unknown	22.9	0.009	4°
(+)747.871	Unknown	4.4	0.001	4°
(+)748.108	Unknown	7.4	0.005	4°
(-)748.114	Unknown	9.6	0.002	4°
(+)748.753	Unknown	4.5	0.002	4°
(+)750.405	Unknown	2.9	0.005	4°
(-)751.450	Unknown	7.9	0.003	4°
(+)753.098	Unknown	6.9	0.005	4°
(-)754.081	Unknown	3.6	0.008	4°
(+)756.546	Unknown	25.7	0.008	4°
(-)758.377	Unknown	8	0.005	4°
(+)760.215	Unknown	24.2	<0.001	4°
(-)760.529	Unknown	4.3	0.002	4°
(+)760.583	Unknown	23.7	<0.001	4°
(+)761.429	Unknown	2.4	0.004	4°
(+)761.586	Unknown	23.8	<0.001	4°
(+)763.099	Unknown	5	0.003	4°
(+)763.417	Unknown	2.4	0.001	4°
(+)763.747	Unknown	3.8	0.004	4°
(+)763.600	Unknown	5	0.008	4°
(+)764.407	Unknown	2.8	0.003	4°
(+)765.074	Unknown	2.8	0.002	4°
(+)766.538	Unknown	23.7	<0.001	4°
(-)767.425	Unknown	3.3	0.003	4°
(+)767.775	Unknown	6.4	0.01	4°
(+)768.751	Unknown	3.8	0.006	4°
(+)768.920	Unknown	2.5	0.008	4°
(+)769.086	Unknown	3.8	0.005	4°
(+)769.884	Unknown	4.3	0.003	4°
(+)770.855	Unknown	9.6	0.001	4°
(+)772.012	Unknown	22.8	0.003	4°
(+)772.779	Unknown	7.3	0.008	4°

(+)773.099	Unknown	4.4	0.005	4°
(+)773.754	Unknown	4.4	0.002	4°
(+)774.418	Unknown	4.5	0.002	4°
(-)774.546	Unknown	29.8	<0.001	4°
(+)775.079	Unknown	4.5	0.003	4°
(+)776.910	Unknown	3.1	0.002	4°
(+)779.086	Unknown	3.9	0.004	4°
(+)779.750	Unknown	4	0.004	4°
(+)780.505	Unknown	2	0.005	4°
(+)781.151	Unknown	28.5	0.002	4°
(+)782.567	Unknown	28.5	<0.001	4°
(+)783.760	Unknown	4	0.007	4°
(+)784.524	Unknown	3.5	<0.001	4°
(+)788.105	Unknown	4.8	0.003	4°
(+)789.090	Unknown	4.6	0.002	4°
(+)790.081	Unknown	4.5	0.002	4°
(+)792.777	Unknown	6.1	0.007	4°
(-)792.856	Unknown	9.6	0.003	4°
(+)793.421	Unknown	4.1	0.002	4°
(+)793.427	Unknown	2.7	0.004	4°
(+)794.092	Unknown	4.1	0.002	4°
(+)796.529	Unknown	9.4	0.002	4°
(+)798.104	Unknown	4.3	0.002	4°
(+)798.766	Unknown	4.4	0.001	4°
(+)799.426	Unknown	3	0.002	4°
(+)800.414	Unknown	3	0.002	4°
(+)803.422	Unknown	4.6	0.001	4°
(+)803.559	Unknown	2.5	0.01	4°
(+)804.466	Unknown	2.7	0.006	4°
(+)804.772	Unknown	4.5	0.002	4°
(+)806.560	Unknown	26.6	0.006	4°
(+)808.102	Unknown	4.3	0.002	4°
(+)808.433	Unknown	2.7	0.005	4°
(+)808.765	Unknown	4.3	0.005	4°
(+)809.577	Unknown	26.5	<0.001	4°
(+)811.987	Unknown	3.3	0.008	4°
(+)812.947	Unknown	2.6	0.002	4°
(+)813.110	Unknown	4.7	0.003	4°
(+)813.910	Unknown	4.1	0.003	4°
(-)816.533	Unknown	28.6	0.003	4°
(+)818.430	Unknown	4.7	0.002	4°
(+)818.431	Unknown	3.4	0.009	4°
(+)819.098	Unknown	4.7	0.005	4°

(+)820.439	Unknown	2.8	<0.001	4°
(+)820.929	Unknown	2.9	0.009	4°
(+)820.929	Unknown	2.9	0.004	4°
(+)822.437	Unknown	4.5	0.004	4°
(+)823.445	Unknown	4.6	0.004	4°
(+)823.445	Unknown	4.6	0.002	4°
(+)826.808	Unknown	7.2	0.01	4°
(+)827.119	Unknown	5	0.004	4°
(+)828.434	Unknown	2.4	0.009	4°
(+)830.567	Unknown	24	<0.001	4°
(+)832.581	Unknown	26.4	<0.001	4°
(+)833.109	Unknown	4.8	0.005	4°
(+)834.612	Unknown	2.9	<0.001	4°
(+)835.581	Unknown	2.6	<0.001	4°
(+)835.921	Unknown	4	0.004	4°
(+)836.800	Unknown	7	0.007	4°
(+)837.781	Unknown	4.8	0.007	4°
(+)838.842	Unknown	9.6	0.003	4°
(+)841.149	Unknown	7.3	0.007	4°
(+)841.261	Unknown	24	0.003	4°
(+)841.816	Unknown	7.3	0.005	4°
(+)842.467	Unknown	2.8	0.002	4°
(-)842.532	Unknown	26.6	0.009	4°
(+)843.453	Unknown	2.8	0.004	4°
(+)843.600	Unknown	2.4	0.007	4°
(-)844.558	Unknown	8.2	0.004	4°
(+)847.777	Unknown	5	0.001	4°
(+)848.489	Unknown	3.1	0.006	4°
(+)848.563	Unknown	7.5	0.006	4°
(+)849.958	Unknown	2.2	<0.001	4°
(+)850.421	Unknown	5.6	0.005	4°
(+)850.563	Unknown	7.4	0.009	4°
(+)850.563	Unknown	7.4	<0.001	4°
(+)851.422	Unknown	5.6	0.002	4°
(+)852.858	Unknown	9.6	0.001	4°
(+)853.702	Unknown	23.8	0.003	4°
(+)854.560	Unknown	23.2	0.002	4°
(+)855.520	Unknown	4.1	0.002	4°
(+)864.409	Unknown	23.3	0.001	4°
(+)864.467	Unknown	2.8	0.008	4°
(+)864.467	Unknown	2.8	0.002	4°
(+)864.964	Unknown	3.4	0.002	4°
(+)866.159	Unknown	7.3	0.009	4°

(+)868.555	Unknown	2.2	0.002	4°
(+)871.012	Unknown	3.4	0.009	4°
(+)874.014	Unknown	8.3	0.007	4°
(-)874.561	Unknown	24	0.002	4°
(+)875.711	Unknown	23.7	0.001	4°
(-)876.573	Unknown	26.4	0.003	4°
(+)878.987	Unknown	2.8	0.002	4°
(+)880.954	Unknown	3.8	0.003	4°
(+)881.166	Unknown	7.4	0.008	4°
(+)883.581	Unknown	1.9	0.006	4°
(+)885.503	Unknown	3.1	0.008	4°
(-)886.008	Unknown	3.1	0.009	4°
(+)886.970	Unknown	3.3	0.006	4°
(+)889.410	Unknown	4.5	0.007	4°
(+)889.589	Unknown	7	0.003	4°
(+)892.590	Unknown	3.9	0.006	4°
(+)892.667	Unknown	3	0.01	4°
(-)893.016	Unknown	3.8	0.009	4°
(+)893.016	Unknown	3.8	0.002	4°
(+)893.482	Unknown	2.2	0.001	4°
(+)893.981	Unknown	2.9	0.009	4°
(+)893.981	Unknown	2.9	0.002	4°
(+)894.941	Unknown	5.3	0.002	4°
(+)901.000	Unknown	2.9	0.007	4°
(+)901.000	Unknown	2.9	0.001	4°
(+)901.967	Unknown	3.7	0.002	4°
(+)902.451	Unknown	3	0.005	4°
(+)906.829	Unknown	9.6	<0.001	4°
(+)908.028	Unknown	3.3	0.008	4°
(+)908.989	Unknown	2.7	0.002	4°
(+)911.857	Unknown	9.7	0.005	4°
(+)912.582	Unknown	2.3	0.005	4°
(+)916.001	Unknown	3	0.007	4°
(+)917.957	Unknown	5.3	<0.001	4°
(-)922.612	Unknown	3.7	0.003	4°
(+)924.979	Unknown	3.6	0.002	4°
(+)930.024	Unknown	3.6	0.006	4°
(+)930.990	Unknown	2.7	0.002	4°
(+)932.423	Unknown	4.3	0.002	4°
(+)933.836	Unknown	6.8	<0.001	4°
(+)934.724	Unknown	6.9	0.002	4°
(+)939.008	Unknown	3.1	0.006	4°
(+)938.463	Unknown	5.3	0.002	4°

(+)938.599	Unknown	7.6	0.004	4°
(+)945.030	Unknown	3.3	0.006	4°
(+)945.502	Unknown	3.4	0.007	4°
(+)946.456	Unknown	3	0.003	4°
(+)946.988	Unknown	3.5	0.009	4°
(+)956.605	Unknown	2.5	0.001	4°
(+)960.029	Unknown	3.3	0.002	4°
(+)960.976	Unknown	5.2	0.002	4°
(+)968.552	Unknown	9.6	0.006	4°
(+)969.508	Unknown	3.5	0.008	4°
(+)975.018	Unknown	2.6	0.004	4°
(+)976.448	Unknown	4.2	0.005	4°
(+)981.534	Unknown	3.4	0.005	4°
(+)982.035	Unknown	2.1	0.01	4°
(+)983.999	Unknown	5.2	0.001	4°
(+)986.185	Unknown	2	0.005	4°
(+)987.975	Unknown	4.2	<0.001	4°
(+)988.830	Unknown	9.6	0.004	4°
(+)989.535	Unknown	3.4	0.009	4°
(+)990.021	Unknown	4.2	0.002	4°
(+)990.485	Unknown	3	0.01	4°